이학박사학위논문

Biogeochemical characteristics of stream and river carbon in Asia investigated by multiscale approach

2019년 7월

서울대학교 환경대학원

환경계획학과

이 은 주

Abstract

Rivers link the lands with the oceans, the two large pools in the global carbon cycle. The riverine carbon load is about 1.0 Pg-C yr^{-1}, which is comparable to the net ecosystem production (NEP), and thus is essential to determine whether the terrestrial ecosystem is a carbon sink or a source. Many studies have been conducted to quantify the carbon load in streams and rivers, and to analyze the factors influencing the loads and biogeochemical properties of the carbon at different spatial scales.

Studies on small watersheds are suitable to analyze the effects of a single factor on the change of loads or characteristics of stream carbon, while the studies on meso- or macro-scale watersheds are appropriate to systemically examine the effects of several factors. In order to deeply understand on the amounts and biogeochemical characteristics of stream and river carbon in Asia, I analyzed the loads and properties of stream and riverine carbon at multiple scales of watersheds: a forest headwater stream, the five largest rivers of South Korea (the Han River, the Geum River, the Youngsan River, the Sumjin River, and the Nakdong River), and the rivers in Asia.

The concentration of stream carbon was measured for weekly collected samples and dual carbon isotopes ($\delta^{13}C$ and $\Delta^{14}C$) were analyzed seasonally from a

small forested watershed during January 2012–April 2015. Stream samples were also collected at 2–24 hour intervals during eight summer storms within the period. Annual total carbon (DIC (dissolved inorganic carbon), DOC (dissolved organic carbon), and POC (particulate organic carbon) combined) yield was 1.7 g-C m^{-2} yr^{-1}, of which 83% was released as DIC. More than a half of annual stream carbon load was transported during summer (June–August). The $\Delta^{14}C_{DOC}$ ranged from -81.5‰ to 45.5‰, whereas $\delta^{13}C_{DOC}$ ranged from -29.4‰ to -13.4‰, indicating the sources of stream organic carbon can be shifted from deep, ground water in dry period to surface organic matter during rainfall.

About 580 Gg-C yr^{-1} was released by the five largest rivers of South Korea in 2012–2013, corresponding to the total carbon yield of 10 g-C m^{-2} yr^{-1}, which was twice of global average. The DIC was the main component of riverine carbon, accounting for 80% of the total carbon yield. About 34-46% of the annual riverine carbon load was exported during summer. The $\Delta^{14}C_{DIC}$ ranged from -88.7 to 26.9‰, $\Delta^{14}C_{DOC}$ from -124.3 to 0.8‰, and $\Delta^{14}C_{POC}$ from -125.5 to 35.1‰. The most enriched $\Delta^{14}C$ was observed in summer regardless of carbon species, suggesting that relatively young carbon was released during summer while old carbon was transported in the other seasons.

A total of 241 Tg-C was newly estimated to be transported through the rivers in Asia, which is similar to the estimates of previous studies. The DIC was the dominant component of carbon in rivers, accounting for 57% of the total carbon load

followed by DOC (26%), POC (15%), and PIC (2%). However, the proportion of DIC load to the total carbon load was up to 19% higher, while the proportion of POC load was 11–19% lower than those of previous studies possibly because new relationships between carbon loads and Q were developed in this study with more data on rivers in Asia. Natural factors including water yields and slope have significant correlations with riverine carbon loads than anthropogenic factors such as %urban, %agriculture, and population density of watersheds. The results suggest that riverine carbon sources are dynamically changing depending on season, especially during summer monsoon. The amounts and biogeochemical properties of stream and river carbon in Asia could be dominantly affected by summer storms, impacting estuarine and oceanic ecosystems.

Keywords: Carbon, isotope, load, dissolved inorganic carbon, dissolved organic carbon, particulate inorganic carbon, particulate organic carbon, river, watershed, Asia

Student Number: 2013-30709

Table of Contents

CHAPTER THREE:

CHAPTER FOUR:

LIST OF TABLES

Appendix

LIST OF FIGURES

CHAPTER TWO:

Appendix

CHAPTER THREE:

CHAPTER FOUR:

Appendix

CHAPTER ONE
General Introduction

Rivers connect the lands and the oceans, the two largest carbon pools in the global carbon cycle. The riverine carbon load to the oceans is approximately 1.0 Pg-C yr^{-1} which is much smaller than the other carbon fluxes such as photosynthesis (120 Pg-C yr^{-1}), autotrophic respiration (60 Pg-C yr^{-1}), and heterotrophic respiration (60 Pg-C yr^{-1}) (Schlesinger and Bernhardt, 2013). However, the riverine carbon load is comparable with net ecosystem production (NEP) which determines whether an ecosystem is a carbon sink or a source (Mayorga *et al.*, 2005; Cole *et al.*, 2007). Concentrations and properties of carbon in streams and rivers are the results of a variety of physicochemical reactions within terrestrial and aquatic ecosystems, from short-term processes (seconds to decades) such as photosynthesis, respiration, air-water CO_2 exchange to long-term responses (centuries to millions of years) such as weathering (Cole *et al.*, 2007).

There are four species of carbon in streams and rivers, dissolved inorganic carbon (DIC), dissolved organic carbon (DOC), particulate organic carbon (POC), and particulate inorganic carbon (PIC). DIC is mainly associated with weathering process and respiration of biota, DOC is mainly derived from leaching of soil

organic matter and plants, POC is related to soil erosion and generation or inputs of microorganisms, and PIC is mostly caused by erosion of carbonates (Meybeck, 1993). The loads of DIC, DOC, POC, and PIC account for 39.5%, 22.0%, 21.0%, and 17.5% of riverine carbon exports globally, respectively (Meybeck and Vörösmarty, 1999).

Studies on quantity and quality of stream and riverine carbon have been actively conducted from first-order small streams to the large rivers which flow across several countries (Ludwig *et al.*, 1996; Cole *et al.*, 2007; Marwick *et al.*, 2015). The amount and characteristics of stream and riverine carbon can be governed by a variety of factors, such as climate, soil properties, and land use land cover (LULC) (Alvarez-Cobelas *et al.*, 2012; Butman *et al.*, 2012). The effects of each factor on stream and riverine carbon quality and quantity can be scale dependent. Research on a small stream or a study on paired watersheds is suitable to scrutinize the effect of a single factor, such as precipitation, LULC, or soil properties, on concentrations and properties of stream carbon (Shin *et al.*, 2011; Jung *et al.*, 2012; Lu *et al.*, 2014). In contrast, studies on major river systems could provide comprehensive analysis on the effects of the factors on loads and characteristics of riverine carbon (Butman *et al.*, 2012; Wang *et al.*, 2012; Wang *et al.*, 2016). For example, whereas the relationships between $\Delta^{14}C$ and the factors such as water discharge (Q), vegetation, and population density were not clear within each river watershed, clear relationships among them were observed across

15 large rivers in USA (Butman *et al.*, 2012). This suggests that the effects of those factors on the quality of riverine carbon can be identified by a study employing many watersheds over a continent (Dai *et al.*, 2012; Huang *et al.*, 2012; Patra *et al.*, 2013; Butman *et al.*, 2015).

The objective of this research is to broaden our understanding on both the quantity and quality of stream and riverine carbon on multiple spatial scales, from a small mountainous headwater stream to the five largest rivers in South Korea, and to rivers in Asia. For this, concentrations, loads, and biogeochemical properties of streams and rivers including dual carbon isotopes ($\delta^{13}C$ and $\Delta^{14}C$) were investigated and the factors governing them were systematically examined.

In Chapter two, the concentrations of each stream carbon species (*i.e.*, DIC, DOC, and POC) and optical properties of DOM were measured for weekly collected samples from January 2012 to April 2015 and for storm samples during the summer of 2012–2014. The dual carbon isotopes for DOC and POC were analyzed on a seasonal basis for the first time in South Korea.

In Chapter three, loads and biogeochemical properties of riverine DIC, DOC, and POC were analyzed for seasonally collected samples and the dual carbon isotopes were measured in the five largest rivers (the Han River, the Geum River, the Youngsan River, the Sumjin River, and the Nakdong River) of South Korea for the first time. The effects of soil types, LULC, and hydrological characteristics on loads and ^{14}C-ages of riverine carbon were investigated.

In Chapter four, a total of 128 papers were collected to build a database and to estimate riverine carbon loads in Asia. Asian carbon yield maps were provided, and correlations between watershed carbon yields and a variety of factors including climate, slope, rock types, and population density were analyzed. Despite that carbon loads of the rivers in Asia were estimated to contribute to ~50% of global riverine carbon loads, only data on <30 rivers in Asia have been used to estimate global riverine carbon loads, accounting for 24–35% of the number of global rivers used for estimation. I provided new, improved estimates on riverine carbon load of Asia.

This multiscale study from a headwater stream in South Korea to the major rivers in Asia would help us to better understand stream and riverine carbon dynamics. The results could be used to develop and implement water management policies.

CHAPTER TWO

Dynamics of Stream Carbon Species in a Small Forested Watershed under Asian Monsoon Climates

1. Introduction

Stream carbon works as energy sources for aquatic biota (Jaffé *et al.*, 2004), transfers pollutants (Jaffé *et al.*, 2004), and can generate carcinogenic byproducts during water purification process (Chow *et al.*, 2005; Hur *et al.*, 2014; Jung *et al.*, 2014). Thus, many studies have been conducted to investigate concentration, load and properties of stream carbon over the world (Hood *et al.*, 2006; Fellman *et al.*, 2009; Jung *et al.*, 2014; Sanderman *et al.*, 2009).

Stream discharge (Q) is one of the most dominant factors on stream carbon loads. The other factors include soil type, land use/land cover, and human activities in watersheds of the 1st–2nd order streams (Hood *et al.*, 2006; Fellman *et al.*, 2009; Raymond and Saiers, 2010; Jeong *et al.*, 2012). DIC concentration ([DIC]) decreases as PPT increases due to dilution effects by rapid increase of surface runoff while DOC concentration ([DOC]) and POC concentration ([POC]) increase because of flushing

effect and erosion of soils as PPT increases in small forested streams (Hood *et al.*, 2006; Jeong *et al.*, 2012; Dhillon and Inamdar, 2013, 2014). Stream carbon loads drastically increased during extreme rainfall events such that 48–50 % of annual DOC load and 80–84% of annual POC load were discharged from a couple of forested streams in monsoonal storm events (Kim *et al.*, 2010; Jeong *et al.*, 2012).

Isotope ratios ($\delta^{13}C$ and $\Delta^{14}C$) of stream DOC can change during intensive storm events in monsoon period (Sanderman *et al.*, 2009). The $\Delta^{14}C_{DOC}$ increased and $\delta^{13}C_{DOC}$ decreased by rising PPT and Q in a small forested watershed in USA, suggesting that relatively fresh dissolved organic matter (DOM) from shallow soils flowed into the stream in monsoon period, whereas aged DOM of deep soil water was the main source at the baseflow (Sanderman *et al.*, 2009; Jin *et al.*, 2018).

Studies to examine carbon properties in headwater streams using dual carbon isotopes have received little attention than large river systems, although the 1st and 2nd streams account for 77% of the total stream length of the earth (Downing *et al.*, 2012). More than 70 studies have been conducted on carbon isotopes of small streams. However, dual carbon isotopes have been measured only in 16 studies among them since 1990 (Schiff *et al.*, 1990; Schiff *et al.*, 1997; Neff *et al.*, 2006; Sanderman *et al.*, 2009). In general, modern DOC was released by forested streams due to fresh OM inputs derived from top soils and plants. However, low $\Delta^{14}C_{DOC}$ down to -125‰ was observed in mountainous streams, corresponding to the ^{14}C age of ~1,000 years BP, due to contribution of groundwater or old soil OM (organic matter) in deep soil

horizons (Sanderman *et al.*, 2009). Only one study reported dual carbon isotopes in South Korea to determine the sources of river carbon (Jin *et al.*, 2018). River samples were collected and analyzed for dual carbon isotopes in July, 2014 and May, 2015 at 15 sites from upper reaches to lower reaches the Han River (HR) of South Korea in which $\Delta^{14}C_{DOC}$ was higher in forested headwater stream than lower reach and decreased down to -129‰ in downstream of the HR because of the contribution of WWTP effluents (Jin *et al.*, 2018).

Forests account for 64% of land area of South Korea, and it is important to quantify the carbon that is released by forest streams and to identify its characteristics to understand the stream carbon dynamics in South Korea. The objective of this research is to assess the effects of hydrological events on the amounts and properties of stream carbon and to track the dominant sources of carbon in a small mountainous watershed of South Korea under monsoon climate. For this aim, concentration of stream carbon was measured during January 2012 – April 2014, and annual stream carbon loads of stream carbon species (DIC, DOC, and POC) were estimated. Dual carbon isotopes were also analyzed for seasonal samples. This study can expand our understanding on biogeochemical change of stream carbon in a forested watershed under monsoon climates.

2. Methods

2.1. Study site

This study was conducted in the Bukmoongol watershed (henceforth BW) of Mt. Baekwoon, within the Seoul National University Forest in Gwangyang, South Korea (35°01'30"N – 35°03'00"N, 127°36'00"E – 127°37'30"E) (Figure 1). Annual mean temperature was 12.8^{o}C and annual mean PPT was 1,583 mm during January 2012 – April 2015. The BW is under monsoon climate zone where 50% of annual PPT fell in summer (June – August) during the three study years. The area of the BW is 0.33 km^2 and the altitude ranged from 120 to 341 m with mean slope of 29%, where the dominant rock types are granite and gneiss, and the soil structure is mostly sandy loam and silt loam (Choi, 2001). Seventy percent of the BW area is covered with coniferous trees (e.g. *Cryptomeria japonica*, *Pinus densiflora*, *Pinus rigida*, *Pinus thunbergii*, *Pinus koraiensis*), and the remaining 30% with deciduous trees (e.g. *Castanea crenata*, *Quercus acutissima*).

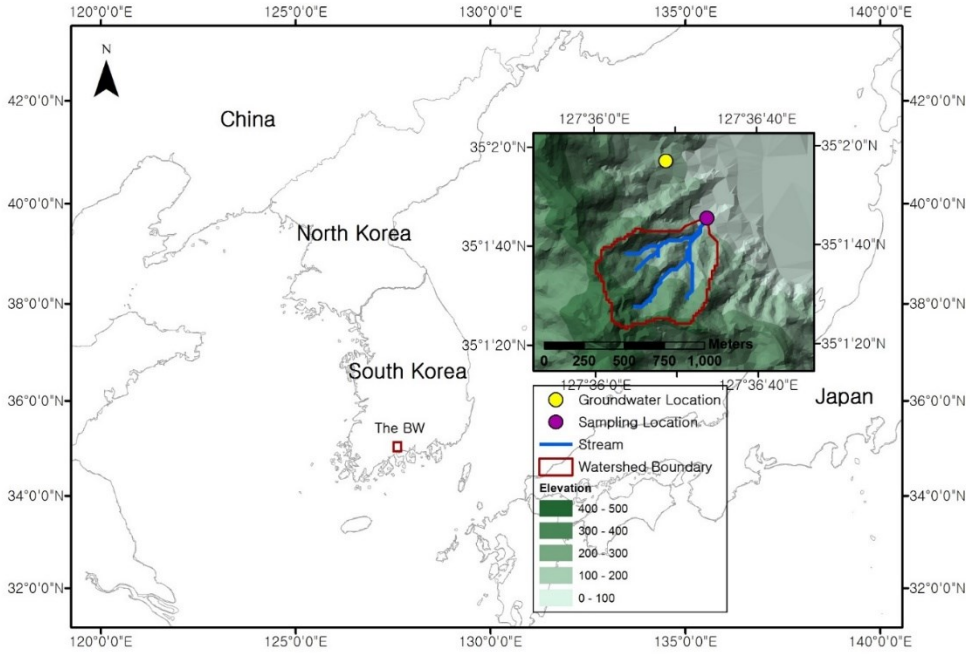

Figure 1. The location of the study site (red square), the Bukmoongol watershed in Mt. Baekwoon of South Korea. The small box is an enlargement of red square. Purple and yellow circles are the sampling points of stream water and groundwater, respectively. The blue lines are streams.

2.2. Sampling scheme and analysis

About one liter of stream water was sampled weekly in a ponding basin in front of a U-shaped weir during January 2012 – April 2015. The water sample was transferred to the laboratory in a polycarbonate (PC) bottle and filtered with Whatman glass fiber filter (GF/F filter of 0.7 μm pore size). The filter was subsequently frozen for [POC] and $\Delta^{14}C_{POC}$ analysis. About 600 mL of filtered water was also frozen in a PC bottle for $\Delta^{14}C_{DOC}$ analysis. The remaining filtered water was stored in polyethylene (PE) bottle to analyze pH, [DIC], [DOC], [POC], and optical properties. The pH was measured by Metrohm 827 pH meter (Metrohm AG., Herisau, Switzerland). Alkalinity was calculated by ion balance method (Cho *et al.*, 2009; Cho *et al.*, 2010; Cho *et al.*, 2012) using the concentrations of major cations (Na^+, NH_4^+, K^+, Mg^{2+}, Ca^{2+}) and anions (Cl^-, NO_2^-, NO_3^-, PO_4^{3-}, SO_4^{2-}) (Dionex ICS-1600 ion chromatography, Dionex, Sunnyvale, CA, USA). The [DIC] was determined by pH and alkalinity of filtered water using CO2SYS program (CO2SYS Version.2.1, http://cdiac.ess-dive.lbl.gov/ftp/co2sys/). The [DOC] was analyzed using TOC-V_{CPH} instrument (Shimadzu Corporation, Japan) and [POC] was measured by SSM instrument (Shimadzu Corporation, Japan). The ultraviolet-visible (UV-VIS) absorbance was measured by UV-VIS spectrophotometer (Agilent Technologies, Santa Clara, California, USA) and fluorescence characteristics of DOC were determined using fluorescence spectrometer (Cary Eclipse Fluorescence

Spectrophotometer, Agilent Technologies, USA). About 200–250 mL of the weekly water samples were composited to make seasonal samples and frozen in PC bottle until the $\Delta^{14}C_{DOC}$ analysis.

Stream water was sampled intensively during eight storm events during 2012–2014 (Table 1). The water samples were collected in two-hour intervals until the water discharge reached its peak, and at 4- to 24-hour intervals for the remaining period. All samples were filtered using GF/F filter and put into PC bottle for $\Delta^{14}C_{DOC}$ analysis and PE bottle for [DOC] analysis. Samples in PC and PE bottles and the filters were frozen on the spot before moving them to the laboratory. The [DIC],[DOC], and [POC] were estimated in the same way as described above.

Table 1. Information on the storms in which stream samples were collected.

Storm No.	Duration	Total PPT (mm)	Max PPT intensity (mm day^{-1})	Mean PPT intensity (mm day^{-1})	Note
Storm 1	29 June – 1 July 2012	24.1	18.5	8.0	
Storm 2	05–06 July 2012	48.0	29.5	16.0	
Storm 3	10–15 July 2012	200.5	102.5	33.4	Two consecutive storm events
Storm 4	17–18 October 2012	33.1	33.0	16.6	
Storm 5	10–11 November 2012	14.5	9.0	7.3	
Storm 6	23–24 April 2013	58.0	57.5	29.0	
Storm 7	03–08 July 2013	122.6	55.1	20.4	Three consecutive storm events
Storm 8	02–09 August 2014	240.0	170.0	30.0	Typhoon NAKRI

About 300 mL of stream water was filtered using GF/F filter and 100 μL of saturated $HgCl_2$ solution was added to prevent respiration of microbes in pre-burned biological oxygen demand (BOD) bottle for $\Delta^{14}C_{DIC}$ analysis in March 2014.

Groundwater was collected monthly from November 2016 to October 2018 and filtered using GF/F filter. About 200 mL was refrigerated in a PE bottle to measure concentrations of DOC and major ions. About 10 L of groundwater was sampled in October 2018 and March 2019, filtered by GF/F filter, and kept frozen in PC bottle until $\Delta^{14}C_{DOC}$ analysis (Table 2).

Water depth of the BW was measured every hour on a U-weir by the Forest Engineering Lab in Seoul National University, and used to calculate daily Q using Francis's equation, $Q=1.84 \times H^{(3/2)}$ (Horton and Murphy, 1906). Daily stream carbon loads (= concentration x Q) were estimated for May 2012 – April 2013, using the log-linear relationship between measured carbon loads (DIC, DOC, and POC) and daily Q (model 1) of the LOADEST (load estimator) program developed by US Geological Survey (Runkel *et al*., 2004).

Table 2. The number of samples used for each analysis

Analysis	Duration	Number of samples
Stream carbon concentration		
DIC	January 2012 – April 2015	226
DOC	January 2012 – April 2015	330
POC	January 2012 – April 2015	175
Optical Properties	May 2012 – April 2015	211
Dual carbon isotopes		
Stream DOC	January 2012 – April 2015 (Seasonal)	17
Stream POC	Storm 7 (July 2013)	2
Groundwater DOC	October 2018 and March 2019	2

2.3. Optical properties

Optical properties of dissolved organic matter (DOM) were analyzed using UV-VIS absorbance and fluorescence intensities of the water samples. Each sample was set at the room temperature before measurement. The UV-VIS absorbance was measured between 250 nm and 750 nm using 1.0 cm quartz cell. Deionized water (DI) was used for blank. Specific UV absorbance at 254 nm ($SUVA_{254}$) which represents aromaticity, was calculated by the UV absorbance at 254 nm divided by [DOC]. One mole of HCl was added to decrease the pH by 2–3, to reduce the fluorescence interference effects due to the combination metal compound and DOM (Westerhoff *et al.*, 2001) until November 2014. Samples were not acidified after December 2014. The optical properties of DOM can change by acidification (Spencer *et al.*, 2007) and freezing of samples (Spencer *et al.*, 2007; Fellman *et al.*, 2008). Thus, the optical data should be interpreted with caution. Parallel factor analysis (PARAFAC) was used to identify DOM components by DOMFluor Toolbox of MATLAB program (The MathWorks Inc. version 8.1) (Stedmon and Bro, 2008). Three components (C1–C3) were selected: C1 is terrestrial humic materials, C2 is terrestrial fulvic substances, and C3 is protein-like matter (Table 3). The detailed process for PARAFAC analysis is explained in Shin *et al.* (2016).

Table 3. The three DOM components of streamwater by PARAFAC analysis

Component	Excitation maximum wavelength	Emission maximum wavelength	Origin	Fluorophore Group	Components classified in previous study Stedmon and Markager (2005)
C1	<250	436	Terrestrial	Terrestrial, Humic acid fluorophore group	3
C2	<250	490	Terrestrial	Terrestrial/Autochthonous, Fulvic acid fluorophore group	2
C3	<250	340	Autochthonous	Autochthonous, Protein-like (Tryptophan-like) fluorescence	7

2.4. Dual carbon isotopes analysis

A total of 14 samples were examined for dual carbon isotopes of DOC: 4 seasonal samples (spring, summer, fall, and winter) and 2 samples during a storm in 2013, 7 composited samples (one composite sample for each season) during 2014–2015, and one sample during Storm 8 (Table 2 and A1). For $\Delta^{14}C_{DOC}$ analysis, each sample was acidified using 40% of H_3PO_4 solution to eliminate DIC. Then, samples were oxidized to CO_2 with ultrahigh purity O_2 gas using UV lamp for at least for four hours (Raymond and Bauer, 2001). The CO_2 was extracted using liquid nitrogen in vacuum line, and sealed in pre-combusted pyrex tube.

The $\Delta^{14}C_{POC}$ was analyzed for residues on GF/F filter in summer and storm events of 2014. The concentration of POC in the other seasons was too low to conduct dual carbon isotope analysis. Each filter was fumigated by concentrated HCl and dried at 60 ^{o}C. The dried filter was sealed in a pre-combusted quartz tube with silver wire and CuO, and oxidized to CO_2 at 850^{o}C in a furnace (Druffel *et al.*, 1992). The released CO_2 was sealed in a pre-burned pyrex tube in the vacuum line after cryogenic separation. The sealed CO_2 samples were sent to the NOSAMS (National Ocean Sciences Accelerator Mass Spectrometry) facility and analyzed for $\delta^{13}C$ and $\Delta^{14}C$. More specific preparation process is illustrated in detail in Raymond and Bauer (2001).

3. Results

3.1. Stream carbon concentrations and loads

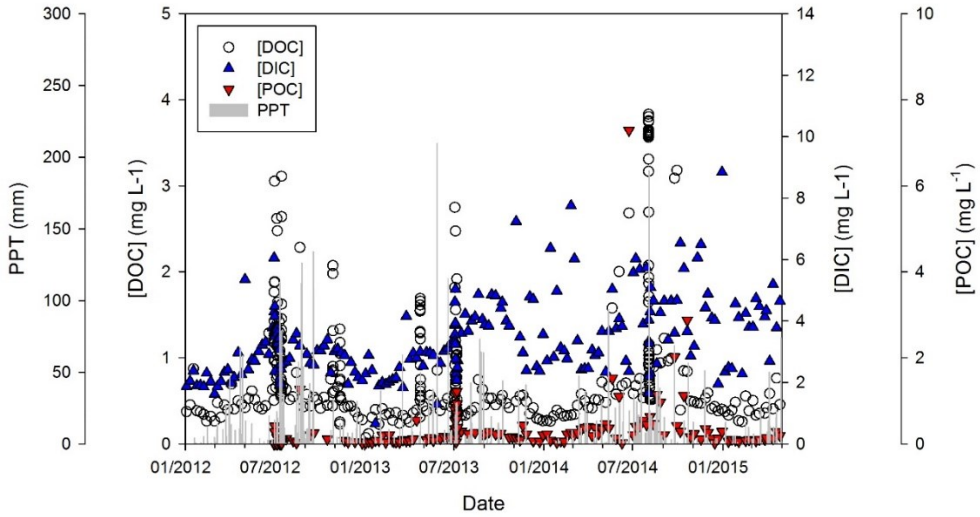

Figure 2. Concentrations of stream carbon during January 2012 – April 2015. [POC] was analyzed from July 2012.

The annual mean concentrations of each carbon species in the BW during 2012–2015 were 3.4 ± 0.1 mg L^{-1} (mean ± s.e.) for DIC, 0.9 ± 0.0 mg L^{-1} for DOC, and 0.4 ± 0.1 mg L^{-1} for POC (Figure 2). The annual mean concentration of total stream carbon ([TC]: concentrations of DIC, DOC, and POC combined, not including

PIC) was 4.7 mg L^{-1}. The [OC] was the highest during summer, 1.3 mg L^{-1} for DOC and 0.6 mg L^{-1} for POC. The [DIC] increased up to 3.9 mg L^{-1} in autumn.

The mean [DIC], [DOC], and [POC] of the 8 storm events (Table 1) were 3.3 ± 0.1 mg L^{-1}, 1.3 ± 0.1 mg L^{-1}, 0.5 ± 0.3 mg L^{-1}, respectively. The [DIC] slightly decreased while [DOC] and [POC] increased during the storms. The mean [DOC] of storm events was 2.4 times higher than that of weekly samples ($p < 0.01$). The increase of [DOC] and the dilution of [DIC] was conspicuous in Storm 8 which was a typhoon storm with the highest PPT.

A total of 1,006 kg of carbon was released from the BW during May 2012 – April 2013, of which DIC accounted for 738 kg-C yr^{-1}, followed by 200 kg-C yr^{-1} of DOC, and 67 kg-C yr^{-1} of POC. This is equal to 1.21 g-C m^{-2} yr^{-1} of DIC, 0.38 g-C m^{-2} yr^{-1} of DOC, and 0.12 g-C m^{-2} yr^{-1} of POC. The DIC was the dominant component form of stream carbon based on loads in 2012, accounting for about 73% of TC loads, followed by DOC (20% of TC), and POC (7% of TC). The precipitation during June–August 2012 was 947 mm, which corresponds to 53% of the annual PPT in 2012. About 54% of annual DIC, 62% of annual DOC, and 58% of annual POC loads were released from the watershed.

3.2. Properties of stream DOC

3.2.1. Optical properties of stream DOC

The mean $SUVA_{254}$ during 2012–2015 was 3.5 ± 0.1 L m^{-1} mg-C^{-1} with the highest being in winter (3.8 ± 0.2 m^{-1} L mg-C^{-1}) and lowest being in summer (3.4 ± 0.1 L m^{-1} mg-C^{-1}) (Figure A1). The dominant component of stream DOM during 2012–2015 was terrestrial humic material (C1) accounting for 53.1% of DOM, followed by 29.3% of terrestrial fulvic material (C2), and 17.6% of protein-like matter (C3) (Figure A1). The proportion of terrestrial materials (%C1 + %C2) of DOM was highest in summer (85.2%) and lowest in winter (74.2%), while the proportion of protein-like matter (%C3) in winter was 25.8%, which was higher than those of the other seasons (14.8–18.0%) (Figure A1).

The analysis for DOM components in Storm 7 and Storm 8 showed that C1 accounted for 55.6% of DOM, followed by C2 (30.6%) and C3 (13.8%) (Figure A2). The percentage of C3 temporarily increased up to 34.0% during Storm 7 and up to 37.7% during Storm 8, and subsequently declined by decreasing Q.

3.2.2. Stream $\delta^{13}C_{DOC}$ and $\Delta^{14}C_{DOC}$

The stream $\delta^{13}C_{DOC}$ ranged from -29.4‰ to -13.4‰ and $\Delta^{14}C_{DOC}$ ranged from -81.5‰ to 45.5‰ during 2013–2015 (Figure 3 and Table A1). The $\delta^{13}C_{DOC}$ and $\Delta^{14}C_{DOC}$ varied seasonally. The $\delta^{13}C_{DOC}$ was high in winter (December–February) with the mean of -19.2‰ and low in summer (June–August) with the mean of -26.0‰. Relatively high $\Delta^{14}C_{DOC}$ of -3.4 ± 13.5‰ was observed in summer and down to -58.1 ± 10‰ in winter, except for the sample of February 2013. The sample with the lowest $\delta^{13}C_{DOC}$ and the largest $\Delta^{14}C_{DOC}$ was observed during a storm in summer (Figure 3). The $\delta^{13}C_{DOC}$ increased while $\Delta^{14}C_{DOC}$ decreased in the other seasons. Relatively young carbon with $\Delta^{14}C_{DOC}$ ranging from -6.2‰ to 45.5‰ was observed at the peak of intense rain events (Figure 3 and Table A1). Only two POC samples were analyzed for $\Delta^{14}C_{POC.}$ The $\Delta^{14}C_{POC}$ was 24.8‰ during a storm event and -17.8‰ for summer (Figure 3).

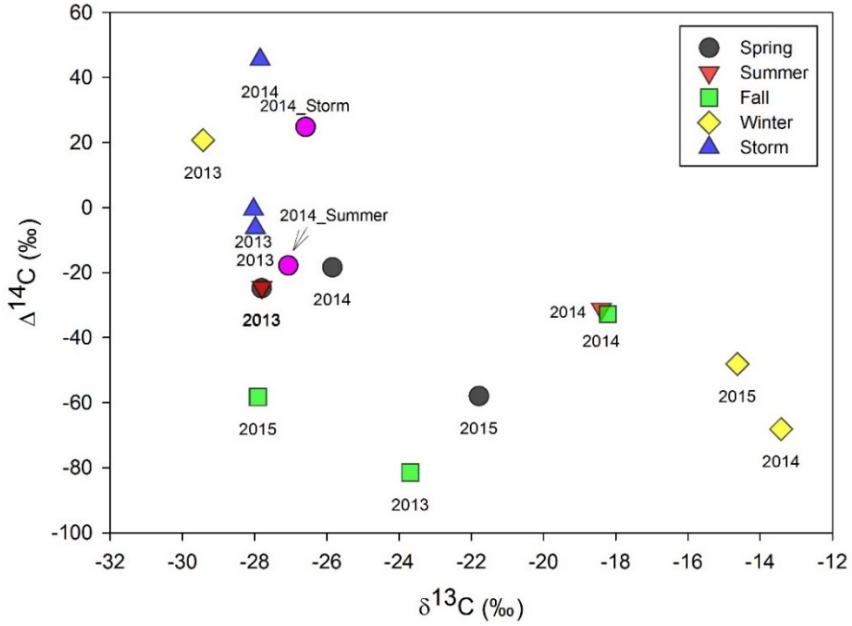

Figure 3. The $\delta^{13}C$ and $\Delta^{14}C$ of organic carbon in the forest stream during 2013–2015. POC in pink and DOC in the other colors. Spring is March–May, summer is June–August, fall is September–November, and winter is December–February.

4. Discussion

4.1. Stream carbon dynamics

4.1.1. Concentrations of stream carbon in weekly samples

Stream [DIC] accounted for 81% of [TC], followed by DOC (15%), and POC (6%) over the three years. The [DIC] of the BW ranged 0.7–8.8 mg L^{-1}, which was comparable with those of the other forest streams (3–8 mg L^{-1}) that have low carbonate bedrock area (Table 4; Shibata *et al.*, 2001; Lu *et al.*, 2014). Bicarbonate was the dominant component of stream DIC, accounting for 78% of [DIC] because water pH was ~7.0. [HCO_3^-] was positively correlated with [Ca^{2+}+Mg^{2+}] (R^2=0.61; $p<0.01$), suggesting that weathering be the main process to produce DIC.

The [DOC] of BW where there is no wetland, was lower than those of the other forest streams which ranged from 1.2 to 12.3 mg L^{-1} globally (Table 4). However, less than 1 mg L^{-1} of [DOC] during baseflow was not uncommon in several mountainous head streams in South Korea (Kim *et al.*, 2010; Jeong *et al.*, 2012; Yang *et al.*, 2015a; Yang *et al.*, 2015b).

The SOC and organic-rich clay content can positively be correlated with stream [DOC] (Hope *et al.*, 1994; Aitkenhead and McDowell, 2000; Alvarez-Cobelas *et al.*, 2012) because DOC is derived from solubilization of soil organic matter (Deb

and Shukla, 2011). The SOC can be hard to be accumulated in forest with steep slopes of South Korea. The BW is also a watershed with steep slope with the mean of 29% (Choi, 2001). The [SOC] in BW ranged from 3.4% at 0–10 cm to 2.7% at 10–30 cm soil depth. The SOC content was estimated to be 4.05 kg m^{-2} within 1 m deep soils in forests of South Korea (Hong *et al.*, 2010), which was ~4 times lower than that of global temperate forests (14.5 to 17.4 kg m^{-2}) (Jobbágy and Jackson, 2000). Clay content is also low in BW soils and the predominant soil texture is sandy loam (Combalicer *et al.*, 2008). These suggest that the low [DOC] in BW and the other forest watersheds of South Korea could be due to relatively low SOC content and low clay content.

The [POC] in BW was comparable with or lower than those of the other forested watersheds (Table 4), which also might be caused by low SOC content in BW because stream POC is generated by erosion of SOC. More than 1 mg L^{-1} of [POC] were observed in only 11 samples during 2012–2015, the [POC] down to 0.01 mg L^{-1} during baseflow.

Table 4. Concentrations of stream carbon in small forested watersheds which have less than 100 ha of watershed area. The units are in parenthesis. The units of concentration are mg L^{-1}.

Location	Area (ha)	Soil or rock types	Land use or plants species	PPT (mm)	[DIC]	[DOC]	[POC]	Year	Reference
BW, South Korea	33	Granite and gneiss	Mixed forest (70% coniferous and 30% deciduous)		3.4 ± 0.1	0.9 ± 0.0	0.4 ± 0.1	2012–2015	this study

Location	Area (ha)	Soil or rock types	Land use or plants species	PPT (mm)	[DIC]	[DOC]	[POC]	Year	Reference
Haean Basin, South Korea	38	Biotite granite (basin bottom) metamorphic rocks (mountain ridges)	Mixed deciduous forests	1,068		1.1 (total) 0.7 (baseflow)	0.7 (total) 0.2 (baseflow)	2009–2010	Jeong et al. (2012)
Gwangnueng catchment, South Korea	22	Weathered gneiss				<1.0 (baseflow)	<1.0 (baseflow)	2005	Kim et al. (2010)

Location	Area (ha)	Soil or rock types	Land use or plants species	PPT (mm)	[DIC]	[DOC]	[POC]	Year	Reference
Ehwa Brook, South Korea	22.7		Broadleaf forests (65%) mixed forests (27%) grasslands (8%)	1,100		0.9-2.0	~0.1 (baseflow) up to 13.6 (peak flow)	2 storms on August, 2013	Yang et al. (2015a)
						1.2-9.5		4 storms in 2014	Yang et al. (2015b)
first-order streams in sub-watersheds of		Quaternary and upper Tertiary sedimentary	83% forest (F1)		3.7	4.7	0.3	2008–2009	Lu et al. (2014)
			100% forest (F2)		8.6	7.1	1.2	2008–2009	

Location	Area (ha)	Soil or rock types	Land use or plants species	PPT (mm)	[DIC]	[DOC]	[POC]	Year	Reference
Pamunkey, Mattaponi and James Rivers, USA		deposits	100% forest (F3)		3.4	7.4	1.0	2008–2009	
Piedmont region of Maryland forested watershed, USA	12		Deciduous forest with pasture	1,231		1.7 (baseflow)		2008–2009	Inamdar et al. (2011)
						22.3		2 Storm events (1) 6–9 Sep.	Fellman et al. (2009)

Location	Area (ha)	Soil or rock types	Land use or plants species	PPT (mm)	[DIC]	[DOC]	[POC]	Year	Reference
Mineral forest, USA	23	Spodozol, igneous intrusive material	T. heterophylla, Vaccinium spp.			5.3–10.1 (baseflow) 10.3–12.3 (Storm flow)		2006, (2) 9–14 Jul. 2007	
W30, USA	49-340	Ultisols,	74% forest	1,215		1.0±0.7		summer,1998 – fall, 2002	Molinero et al. (2009)
W47, USA	49-340	Ultisols	74.5% forest	1,215		0.8±0.4			
W71, USA	49-340	Ultisols	77% forest	1,215		1.2±1.1			

Location	Area (ha)	Soil or rock types	Land use or plants species	PPT (mm)	[DIC]	[DOC]	[POC]	Year	Reference
Johzankei Experimental Watershed, Japan	2.0	Quartz porphyry, no calcareous materials	Mixed deciduous and coniferous forest	1,249	2.1	3.6	2.3	Dec.1995–Nov. 1996	Sakamoto et al. (1999)
1st-order subwatershed in Tennessee Valley, USA	3.9	Typic Haplustolls	Coastal prairie vegetative community	1,150		5.4±0.3		2004	Sanderman et al. (2009)

Location	Area (ha)	Soil or rock types	Land use or plants species	PPT (mm)	[DIC]	[DOC]	[POC]	Year	Reference
Hubbard Brook (Bear Brook), USA		Spodosols				3.1		1978–1979	McDowell et al. (1988)
Hubbard Brook (W6), USA	13.2		Spruce–fir–birch (20%) hardwood (80%)	1,400		2.1 (growing season) 1.9 (non-growing season)		1992–2003	Dittman et al. (2007)

4.1.2. Change of stream carbon concentrations during storm events

There was no significant relationship between [DIC] and daily PPT in the BW on a weekly basis sampling (R^2=0.04, p = 0.12) (Figure 4a), whereas [DIC] significantly decreased during storm events (R^2=0.12, p=0.02) (Figure 4d). Dilution effects of [DIC] were conspicuous during storm events with high PPT (> 100 mm), such as Storm 3, Storm 7, and Storm 8.

The [DOC] increased as the PPT increased for weekly samples as well as in storms (R^2: 0.05–0.06, p: 0.00–0.09) (Figure 4b and 4e), which might be due to labile allochthonous OM inputs from surface soil and plants, erosion of soil, and resuspended sediments during rainfall events (Jeong *et al.*, 2012; Jung *et al.*, 2012). Clockwise hysteresis between [DOC] and relative water depth (RWD = instant water depth – baseflow water depth) was observed during storms (Figure A3b), which suggested that OM was mobilized quickly from shallow soils at the beginning of hydrological events, and became limited during continuous storms.

The [POC] had no significant relationships with daily PPT when weekly collected samples were used for the analysis (Figure 4c), and was not related with the PPT per sampling intervals during storms (Figure 4f). The [POC] was below detection limit in general over the study period, and measurable only during storms. An outlier of 19.1 mg L^{-1} of POC was measured during the first rainfall event of Storm 7, which was >40 times the average [POC]. The [POC] increases with increasing PPT intensity

(Hope *et al.*, 1994; Jeong *et al.*, 2012; Jung *et al.*, 2014), however; there was no significant relationship between [POC] and PPT intensity in BW (Figure 5).

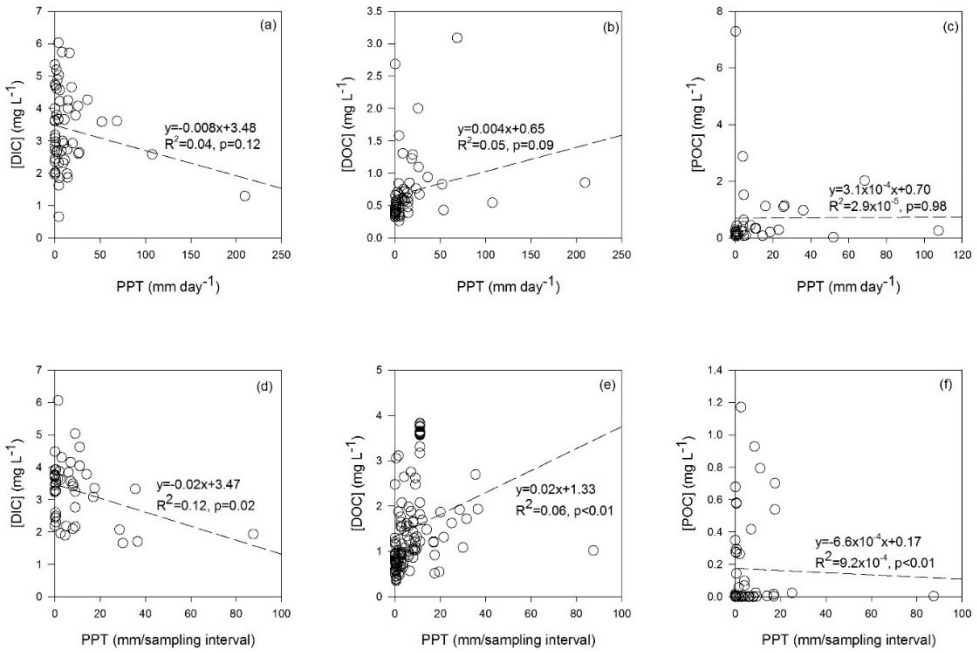

Figure 4. Relationships between daily PPT and (a) [DIC], (b) [DOC], and (c) [POC] of weekly collected samples during May 2012 –April 2015, and between PPT per sampling interval (2 – 24 hrs) and (d) [DIC], (e) [DOC], and (f) [POC] during eight storm events. Abnormal data with high [POC] of 19 mg L^{-1} on 7 July 2013 was excluded from the analysis.

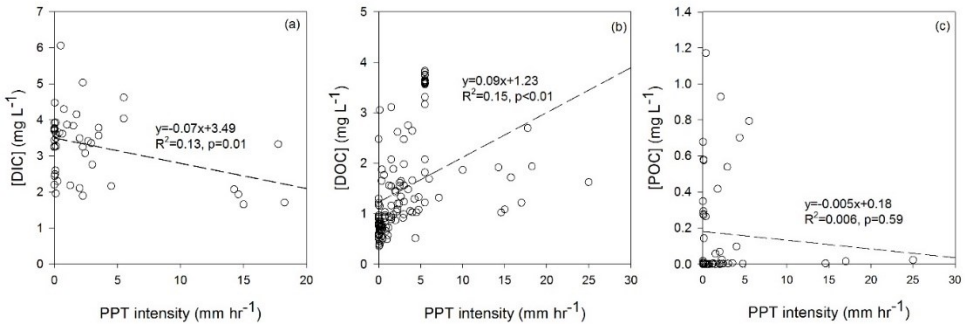

Figure 5. Relationships between PPT intensity and (a) [DIC], (b) [DOC], and (c) [POC] during eight storm events during May 2012 – April 2015. Abnormal data with high [POC] of 19 mg L^{-1} on 7 July 2013 was excluded.

4.2. Sources of stream organic carbon

There was a significant negative correlation between $\delta^{13}C_{DOC}$ and $\Delta^{14}C_{DOC}$ (R^2=0.32, p-value<0.05) (Figure 3). The $\delta^{13}C_{DOC}$ was the highest and $\Delta^{14}C_{DOC}$ was the lowest in winter, except in 2013, and conversely $\delta^{13}C_{DOC}$ decreased and $\Delta^{14}C_{DOC}$ increased in summer. The seasonal variation of carbon isotopes of DOC of BW stream, especially $\delta^{13}C_{DOC}$, was greater than that of the other streams and rivers of the world (Figure 6), suggesting that the dominant sources of DOC in BW can quickly change depending on season.

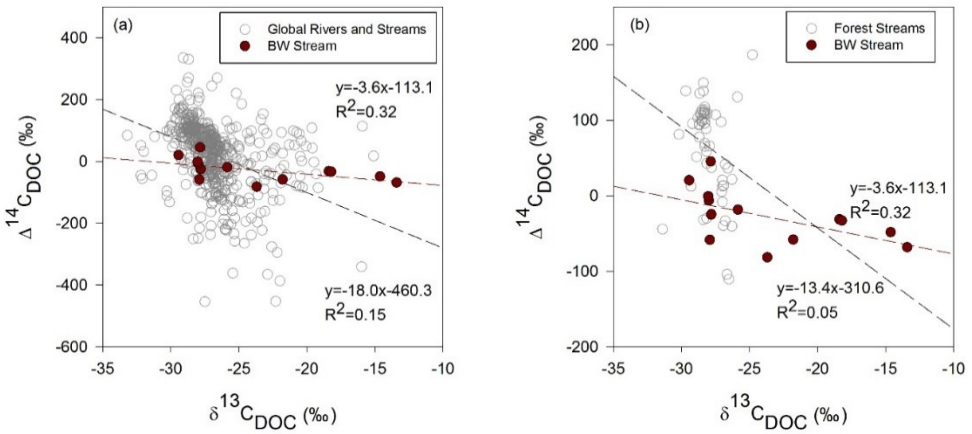

Figure 6. The $\delta^{13}C_{DOC}$ and $\Delta^{14}C_{DOC}$ of (a) rivers and streams of the world and the BW stream, and (b) the other forested streams and the BW stream. Open grey circles are from Marwick *et al.* (2015) and Qu *et al.* (2017).

The $\delta^{13}C_{DOC}$ decreased to -26.0‰ in summer, which was similar to $\delta^{13}C_{SOC}$ of -25.8‰ at 0–10 cm soils collected within the watershed (Table 5). The $\Delta^{14}C_{DOC}$ in summer and storms was up to 70‰ higher than in winter (Figure 3), suggesting that relatively young OM derived from C3 plants can be a main source of stream DOC in summer, especially during storm events, like other forest streams or rivers in monsoon climate regions (Schiff *et al.*, 1997; Wang *et al.*, 2012; Martin *et al.*, 2013; Lu *et al.*, 2014; Ishikawa *et al.*, 2016). There was a difference in $\Delta^{14}C_{DOC}$ among stream water samples collected during storms (Table A1), which may be due to the difference in PPT intensities. The $\Delta^{14}C_{DOC}$ increased with increasing the amount of cumulated PPT in storms, although only three data points were available in this study (Figure A4).

Enriched $\Delta^{14}C_{DOC}$ due to fresh OM inputs from vegetation and surface soils has been reported in many studies on mountain watersheds (Schiff *et al.*, 1990; Schiff *et al.*, 1997; Neff *et al.*, 2006; Lu *et al.*, 2014). However, the $\Delta^{14}C_{DOC}$ of BW stream was lower than most of the other forest streams (Figure 6b), indicating that relatively old carbon can be also a main source of stream DOC in BW during baseflow. Similarly, old DOC (less than -50‰, which is the average $\Delta^{14}C_{DOC}$ of stream water in BW in the seasons except summer) was reported in the other two forest streams because of old OM input from deep soil layer and groundwater (Schiff *et al.*, 1990; Schiff *et al.*, 1997; Sanderman *et al.*, 2009).

Stream $\Delta^{14}C_{DOC}$ less than -100‰ was observed in a coastal forest watershed in USA due to old soil organic matter (SOM), and highly recalcitrant humified OM was dominant in deep soil solution with low $\Delta^{14}C_{SOM}$ and $\Delta^{14}C_{DOC}$ (Sanderman *et al.*, 2008; Sanderman *et al.*, 2009). The $\Delta^{14}C_{DOC}$ of groundwater can be as low as -400‰ in other forest watersheds due to OC recycling in the soil layer during translocation (Schiff *et al.*, 1990; Schiff *et al.*, 1997). For example, the $\Delta^{14}C_{DOC}$ was observed to be -170‰ in the upper catchment of Harp Lake basin, Canada (Schiff *et al.*, 1990; Schiff *et al.*, 1997). There was a significant positive relationship between the ratio of [DOC] to [sum of base cations] and $\Delta^{14}C_{DOC}$ in BW (R^2=0.31; p=0.05), suggesting that depleted $\Delta^{14}C_{DOC}$ in baseflow condition could be due to old OM from deep soils or groundwater (Barnes *et al.*, 2018). The $\Delta^{14}C_{DOC}$ of groundwater of the BW ranged from -494.9‰ to -344.2‰ (Table 5), and the contribution of groundwater to annual stream flow in BW was estimated to be in the range of 26% to 75% (Combalicer *et*

al., 2008). The relatively low $\Delta^{14}C_{DOC}$ of the BW stream could be due to relatively high contribution of groundwater considering that the first-order streams could retain groundwater characteristics compared to higher-order streams (Johnson *et al.*, 2008).

Enriched $\delta^{13}C_{DOC}$ was observed in BW during dry seasons, increasing up to -13.4‰ in winter, except in 2013, which might be due to groundwater input considering that the $\delta^{13}C_{DOC}$ of groundwater in BW was -14.3‰ in October 2018 and -13.5‰ in March 2019. Annual mean [DOC] of groundwater was 0.2 mg L^{-1}, which was about a fifth of [DOC] of stream water. The ratio of Na^+ concentration ([Na^+]) to Ca^{2+} concentration ([Ca^{2+}]) of the groundwater was 6.4, which was 6 times higher than that of stream water (1.0). This suggests that groundwater might be diluted about five to six times in the stream. The $\delta^{13}C_{DOC}$ increased up to -13.4‰ in winter, which was similar to the $\delta^{13}C_{DOC}$ of groundwater.

The OM derived from C4 plants can also increase $\delta^{13}C_{DOC}$ in streamwater in winter. If there are C4-derived OM in soils, high $\delta^{13}C_{DOC}$ and low $\Delta^{14}C_{DOC}$ of streamwater can be observed. However, $\delta^{13}C_{SOC}$ at 0–70 cm soil depth in BW was similar to the $\delta^{13}C$ of C3 plants, and up to 12.4‰ lower than stream $\delta^{13}C_{DOC}$ in dry period (the seasons except summer) (Table 5), thus, SOC cannot be a main source of stream DOC in dry period. Sediments and freshwater plants in the BW stream also had lower $\delta^{13}C_{OC}$ than stream $\delta^{13}C_{DOC}$ in non-summer seasons (Table 5). Groundwater could be a main contributor of enriched $\delta^{13}C_{DOC}$ in streamwater in BW through the year except summer.

There was no significant relationships between $SUVA_{254}$ and $\Delta^{14}C_{DOC}$ (R^2<0.10, p>0.09) (Figure 7a). A weak positive relationship between %C1 and $\Delta^{14}C_{DOC}$ and a weak negative correlation between %C1 and $\delta^{13}C_{DOC}$ were observed, which was not statistically significant (R^2=0.17–0.24, p-value: 0.11–0.19) (Figure 7b). Thus, stream carbon isotopes may not be related to aromatic and terrestrial humic substances, which are the main components of OM in mountain watersheds. Other components of DOM (%C2 and %C3) also had no significant correlation with $\delta^{13}C_{DOC}$ or $\Delta^{14}C_{DOC}$ (R^2:0.01–0.13, p>0.1) (Figure 7c and 7d).

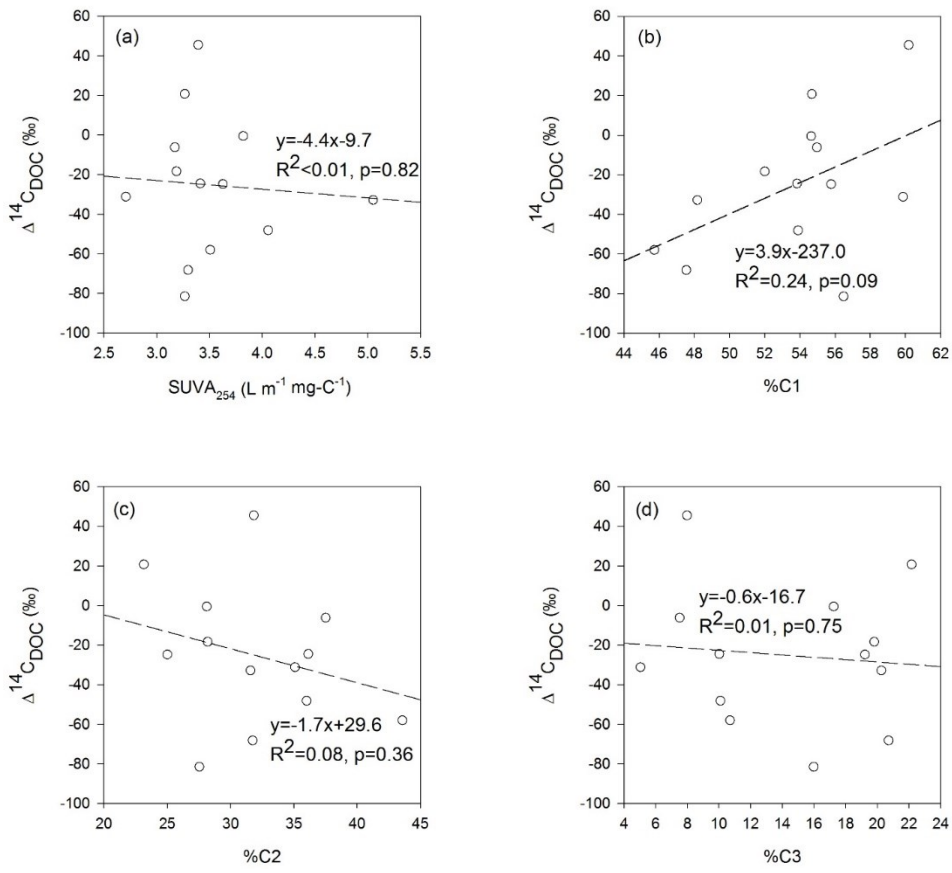

Figure 7. Relationships between $\Delta^{14}C_{DOC}$ and (a) $SUVA_{254}$, (b) %C1, (c)%C2, and (d) %C3.

The ^{14}C-enriched and ^{13}C-depleted stream DOC was observed in the winter of 2013 (Figure 3 and Table A1), which may be due to young OM inputs during high PPT in winter of 2013 than the other winters. Higher PPT (98 mm) was observed over a month (21 January – 19 February 2013) than the other winter months (a total of 32–68 mm PPT over 3 months (November – February) during 2013–2015).

Table 5. The OC concentration, $\delta^{13}C$, and $\Delta^{14}C$ of various OC sources in the BW.

Sample	OC (%)	$\delta^{13}C$ (‰)	$\Delta^{14}C$ (‰)
Riparian soil OC – 10cm	3.1	-25.8	
30cm	2.3	-24.8	
50cm	1.6	-24.6	
70cm	0.9	-24.7	
Sediment – Bukmoongol	3.4	-29.7	
Sediment – upper Bukmoongol	2.9	-28.4	
Freshwater plants (*Miscanthus sinensis var. purpurascens*)	41.2	-31.6	
Groundwater DOC			
October 2018	0.16*	-14.3	-344.2
March 2019	0.13*	-13.5	-494.9

* [DOC]: mg L^{-1}

Stream $\delta^{13}C_{POC}$ in summer and storm ranged from -27.1‰ to -26.6‰ which was similar to $\delta^{13}C_{OC}$ of 0–30 cm depth soils in BW where C3 plants (*Cryptomeria japonica*, *Carpinus laxiflora*, and *Pinus koraiensis*) were dominant. The $\Delta^{14}C_{POC}$ was modern in a storm event (Table A1), suggesting that stream POC were resulted from allochthonous OM inputs during increasing Q in summer.

5. Conclusions and Implications

The DIC, DOC, and POC concentrations and properties were analyzed during 2012–2015 in a small forest stream in South Korea. The DIC accounted for about 73% of stream carbon load in 2012, and about 81% of TC was released in the form of DIC based on concentration during 2012–2015. More than half of annual TC load was released in summer. The [DIC] decreased and [DOC] and [POC] increased during storm events. The $\delta^{13}C_{DOC}$ ranged from -28.0‰ to -13.4‰, and $\Delta^{14}C_{DOC}$ ranged from -81.8‰ to 45.5‰. Relatively old DOC (mean $\Delta^{14}C_{DOC}$ of -44.6‰) was released from the BW during 2012–2015 except storm periods. There was seasonal variation of dual carbon isotopes of the stream DOC. Low $\delta^{13}C_{DOC}$ and high $\Delta^{14}C_{DOC}$ was observed in spring and summer; and $\delta^{13}C_{DOC}$ increased and $\Delta^{14}C_{DOC}$ decreased in fall and winter. Recently photosynthesized C3 plant-derived OM can be a main source of stream DOC during storms, whereas groundwater can be a dominant source of stream DOC over non-summer seasons. This suggests that the change of hydrological path by rainfall can be a major factor affecting stream carbon concentration and biogeochemical characteristics. Under climate change, the amount of PPT and the number of days with heavy rainfall (>80 mm per day) are predicted to increase by 16–18% and 30% in South Korea during the 21st century, respectively (KMA, 2012). Stream carbon loads can increase, and the source of stream OC can be shifted to young terrestrial OM, with increasing frequency of intense precipitation under climate change.

Appendix

Table A1. Streamwater sample information and results for carbon isotopes analysis

Sampling Date	Season	$\delta^{13}C$	$\Delta^{14}C$	Note
2013-05-20	Spring	-27.81	-24.80	
2013-07-03	Summer	-27.80	-24.49	before Storm 7
2013-11-26	Fall	-23.69	-81.48	
2013-02-26	Winter	-29.43	20.72	
2014-01 2014-02	Winter	-13.42	-68.14	composite sample
2014-05	Spring	-25.85	-18.34	composite sample
2014-08	Summer	-18.40	-31.19	composite sample
2014-11	Fall	-18.22	-32.78	composite sample
2015-02	Winter	-14.63	-48.10	composite sample
2015-04	Spring	-21.79	-57.97	composite sample
2015-11	Fall	-27.91	-58.26	composite sample
2013-07-03	Storm	-27.98	-6.23	the first peak of the three peaks in [DOC] during Storm 7 (Table 1)
2013-07-07	Storm	-28.03	-0.53	the third peak of the three peaks in [DOC] during Storm 7 (Table 1)
2013-08-02	Storm	-27.85	45.54	The highest [DOC] during Storm 8 (Typhoon NAKRI) (Table 1)

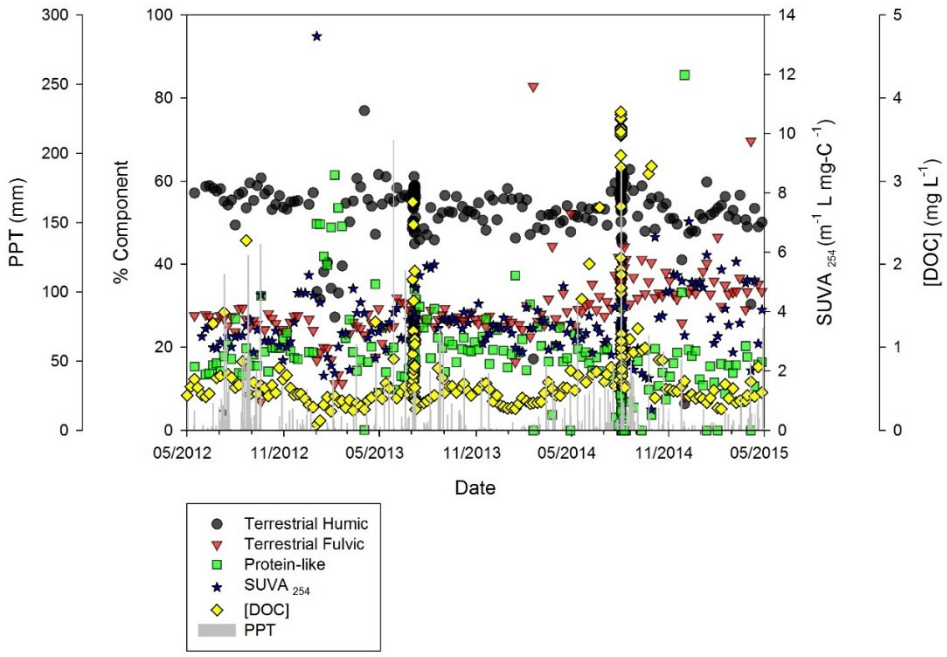

Figure A1. The three components of DOM, $SUVA_{254}$, and [DOC] concentration of the forest stream for May. 2012–Apr. 2015. The grey bar is daily precipitation.

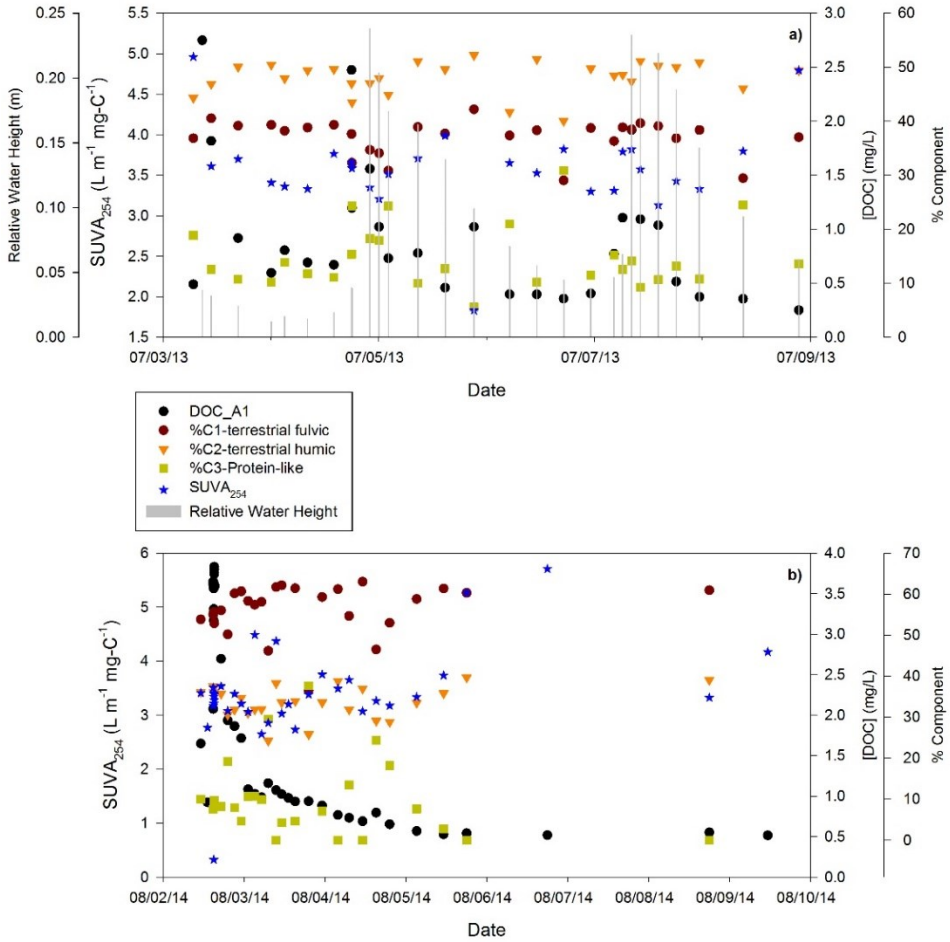

Figure A2. The three components of DOM, $SUVA_{254}$, and [DOC] of the forest stream (a) during Storm 7 and (b) during Storm 8.

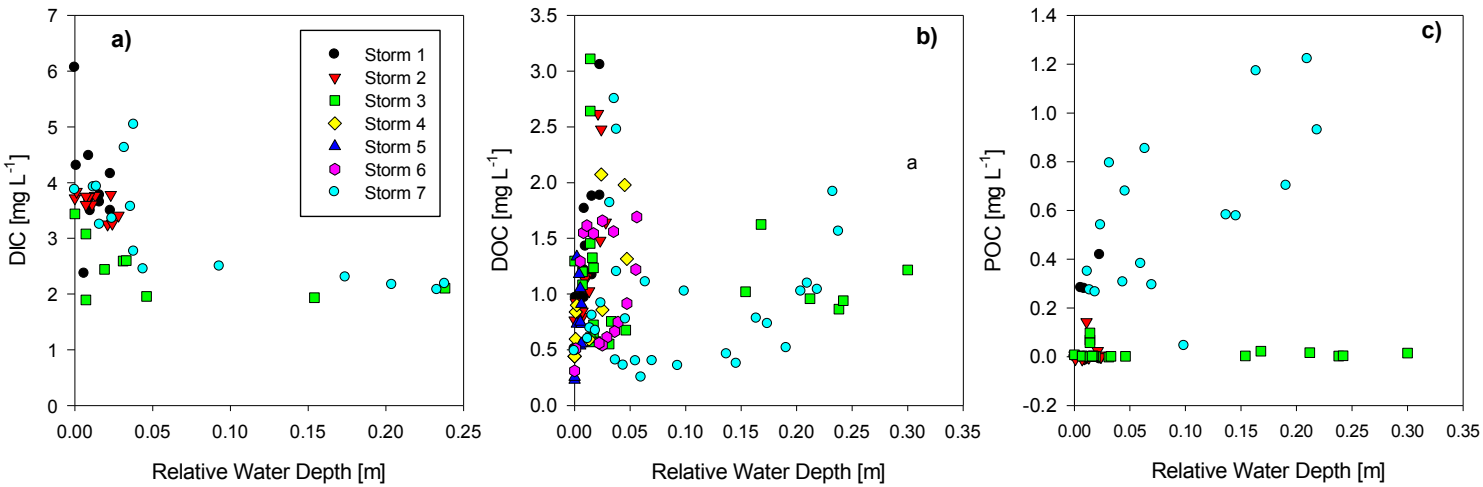

Figure A3. Relationships between a) DIC, b) DOC, and c) POC concentrations and the relative water depth (RWD) during storm events (RWD = instant water depth – baseflow water depth).

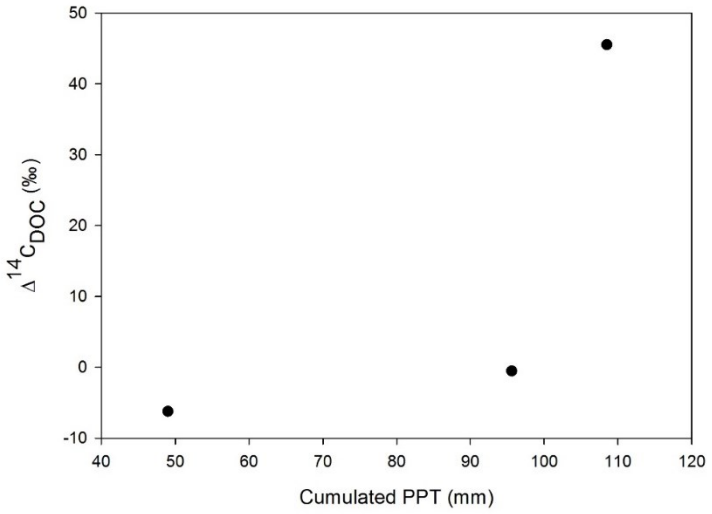

Figure A4. A relationship between cumulated PPT during sampling intervals and $\Delta^{14}C_{DOC}$ in storm events.

CHAPTER THREE

Loads and Ages of Carbon from the Five Largest Rivers in South Korea under Asian Monsoon Climates

1 Introduction

Riverine carbon export is a key component of the global carbon cycle, connecting terrestrial and oceanic ecosystems. The three species of riverine carbon, *i.e.*, dissolved inorganic carbon (DIC), dissolved organic carbon (DOC), and particulate organic carbon (POC) account for >80% of the total riverine carbon loads, and have been studied extensively (Ludwig *et al.*, 1998; Meybeck, 2003; Huang *et al.*, 2012). The number of studies on particulate inorganic carbon (PIC) is relatively small because physical transfer of PIC from lands to the oceans does not significantly alter carbon sinks or sources in the global carbon cycle (Meybeck, 2003). Since riverine carbon species can influence the concentrations of pollutants by precipitation, adsorption, and complexation, the ratio among the carbon species can be directly linked with the fate of pollutants in rivers (Jaffé *et al.*, 2004). The

ratio among the carbon species are regulated by a variety of biogeochemical reactions and processes such as photosynthesis, respiration, sedimentation, and CO_2 evasion (Meybeck, 1993; Raymond and Bauer, 2001; Raymond *et al.*, 2013).

Concentrations of DIC ([DIC]) in rivers are mainly controlled by carbonic acid weathering of soils and rocks of the corresponding watershed (Oh and Raymond, 2006; Shin *et al.*, 2011b) while [DOC] and [POC] are determined by the dynamic changes of inputs and outputs of organic matter (OM). Inputs of OM include autochthonous production as well as allochthonous contributions from watersheds including soil organic matter (SOM), geologic deposits of organic materials (eg. coal and chert), and wastewater treatment plants (Aitkenhead and McDowell, 2000; Griffith *et al.*, 2009; Wei *et al.*, 2010), whereas outputs include burial of organic matter to the bottom of lakes and rivers (Tranvik *et al.*, 2009), and respiration followed by CO_2 evasion (Raymond *et al.*, 2013).

The concentrations and loads of riverine carbon are strongly dependent on precipitation (PPT) and watershed hydrology. Riverine carbon load is calculated by multiplying [carbon] and discharge (Q), thus, an increase in PPT can raise the riverine carbon load even though carbon concentrations are diluted (Raymond and Oh, 2007; Li and Bush, 2015). Consequently, riverine carbon export during summer monsoon can account for a large portion of annual carbon loads in Asia such that ~40% of annual DOC and ~79% of annual POC were transported by the Huanghe river and the Yangtze river, respectively, to the Yellow Sea during only 2–3 summer months in 2009 (Wang *et al.*, 2012). Furthermore, anthropogenic impacts

by dams and reservoirs can change hydrology by controlling inflow and releases. The rivers that have many artificial dams and reservoirs differ from natural river systems in that they can have large seasonal variation of hydrological residence time (HRT) (Park *et al.*, 2009) and possibly carbon loads.

The increased PPT during summer monsoon can not only increase riverine carbon loads but also change the biogeochemical properties of river water by shifting the major sources of carbon (Wang *et al.*, 2012). Dual carbon isotopes (^{13}C and ^{14}C) have been used to determine the sources of riverine carbon (Raymond and Bauer, 2001; Mayorga *et al.*, 2005; Marwick *et al.*, 2015). Whereas $\delta^{13}C$ overlays in a relatively narrow range from about -40 to 0‰, $\Delta^{14}C$ covers a wide range from -1,000 to ~200‰ in rivers, and thus the dual carbon isotope analysis has merits to identify the sources of carbon compared to a single carbon isotope analysis (Butman *et al.*, 2015; Marwick *et al.*, 2015). Although studies have been conducted using the dual carbon isotope analysis for the major rivers of the world, the studies examined one or two species of carbon in general, typically DOC or POC (Butman *et al.*, 2015; Marwick *et al.*, 2015), with less than 10% of the analyses conducted for all three species of carbon, *i.e.*, DIC, DOC, and POC (Marwick *et al.*, 2015). Dual carbon isotopes have been used for rivers in Asia including the Yellow River, the Changjiang River, the Mekong River, and rivers in Japan and Taiwan (Kao and Liu, 1997; Alam *et al.*, 2007; Wang *et al.*, 2012; Martin *et al.*, 2013; Wang *et al.*, 2016). However, no rivers in Asia has been analyzed for all three species of carbon using dual carbon isotopes (Marwick *et al.*, 2015).

Riverine carbon with the ^{14}C ages of modern to >10,000 ybp (years before present) was reported worldwide, and the rivers in Asia also showed similar ranges in the ^{14}C ages (Marwick *et al.*, 2015). Rivers in Korea can share the characteristics of the rivers in Asia such as changing hydrology under monsoon climates and anthropogenic perturbations of natural systems by many dams and reservoirs. Although many studies have been conducted for streams and a few large river systems in Korea (Shin *et al.*, 2011a; Kim *et al.*, 2013; Lee *et al.*, 2013; Shin *et al.*, 2015), there has been no study on the annual carbon loads and the ^{14}C ages for the major river systems in the Republic of Korea (South Korea). Here we report estimates of annual riverine carbon loads (DIC, DOC, and POC) and dual carbon isotope results for the five largest river systems in South Korea for the first time, which will deepen our understanding on river biogeochemistry under Asian monsoon climates.

2 Methods

2.1 Study sites

Korea is under temperate monsoon climates, with mean annual temperature of 10–15oC (Korea meteorological administration: www.kma.go.kr). Annual mean PPT is between 1,000 mm and 1,900 mm and 50–60% of PPT falls during summer (June-August) for 1981-2010. The Han River (HR), the Geum River (GR), the Youngsan River (YR), the Sumjin River (SR), and the Nakdong River (NR) are the five largest rivers in South Korea, draining ~70% of land area (Figure 1) and providing water for ~33 million people (Water management information system (WAMIS): www.wamis.go.kr). Precambrian gneisses and Mesozoic granites are dominant rock materials of the basins except NR and south HR basins (Chough *et al*., 2000). Mesozoic clastic sedimentary and volcanic rocks are distributed across NR basin, and Paleozoic carbonate and clastic sedimentary rocks in south HR basin (Shin *et al*., 2011b).

The HR has the largest basin area where forest is the dominant land use/land cover (~75%), followed by agricultural land (14.6%) and urban area (3.2%) (Table 1). The GR and the YR flow to the Yellow Sea through croplands downstream. The proportion of agricultural land use is 25.9% and 31.8% in the GR and YR basins, respectively, the largest among the five river basins (Table 1). The proportion of urban land use is also the largest in the two river basins. The SR is the

second smallest river in terms of basin area or mainstream length and about 2/3 of the basin is covered by forest (Table 1). The NR is the longest river in South Korea and the water flow is the slowest (Lee *et al*., 2003).

The mean slope of the five river basins ranged from 26.6 to 37.3% (Shin *et al*., 2016), and the proportion of wetland was less than 3% of total basin area (Table 1). Due to the extreme range in flow conditions, anthopogenic structures including 1,213 dams and ~18,000 reservoirs have been used to manage water resources (Park *et al*., 2005; http://www.kwater.or.kr). Thus, the water chemistry and discharge of the river systems reflect not only natural but also anthropogenic settings within the basins.

Table 1. Sampling locations and characteristics of the five river basins. Basin area and the land use/land cover of each river basin was calculated using data downloaded from WAMIS and the Ministry of Environment of South Korea.

River	Sampling location	Mainstream length (km)	Basin area (km^2)	Slope (%)	Forest (%)	Agriculture (%)	Urban (%)	Wetland (%)
Han River (HR)	127.11°E 37.54°N	483	2.42×10^4	37.3	75.2	14.6	3.2	1.8
Geum River (GR)	127.01°E 36.15°N	388	9.38×10^3	29.6	61.0	25.9	6.0	2.5
Youngsan River (YR)	126.71°E 36.00°N	135	2.15×10^3	26.6	51.6	31.8	8.8	2.6
Sumjin River (SR)	127.62°E 35.19°N	222	4.34×10^3	33.7	67.7	22.9	2.7	2.6
Nakdong River (NR)	128.52°E 35.39°N	511	2.07×10^4	32.9	68.0	22.6	4.2	1.6

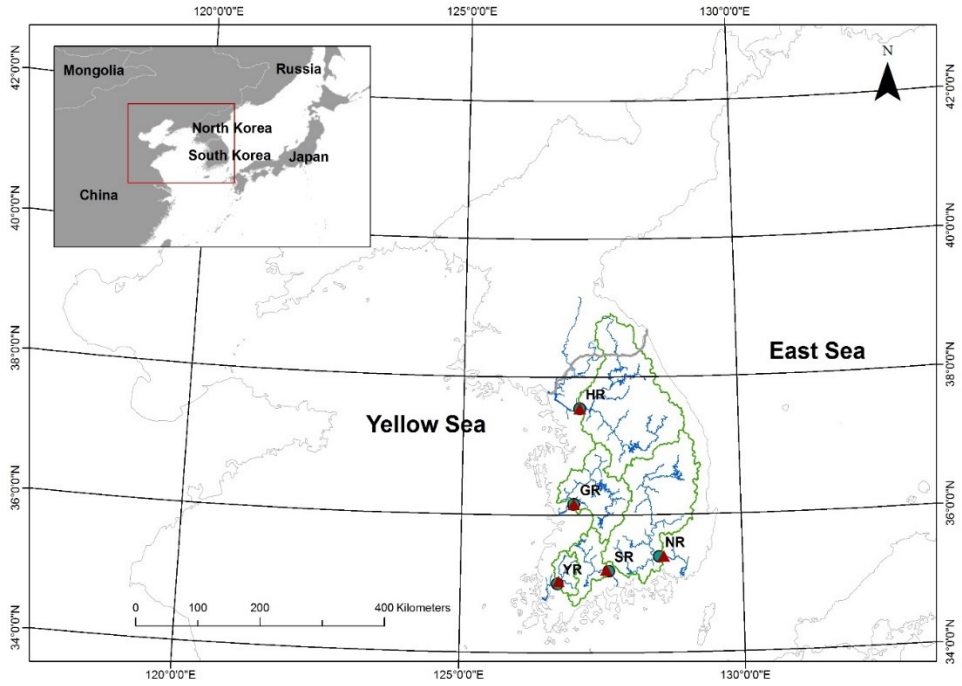

Figure 1. Sampling locations (green dots) and discharge gauging stations (red triangles) of the five largest rivers in South Korea. The blue lines are rivers and green polygons are boundaries of the river basins.

2.2 Chemical properties and loads of riverine carbon

Water samples were collected on seasonal basis from February, 2012 to November, 2013 at the middle of the bridge that is located on the lower reach of the five rivers to prevent the influence of tidal seawater (Figure 1). 10–11 of water sampling was conducted in each river, water samples were filtered in a field using

pre-combusted Whatman GF/F glass fiber filter of 0.7 μm pore size during Feb.–May in 2012 and were transported to the laboratory on ice, and were filtered within two days in Jul.2012 – Nov.2013. About 300 mL of filtered water was refrigerated below 4^{o}C after 100 μL of saturated $HgCl_2$ was added to prevent microbial respiration in pre-combusted BOD bottle for $\Delta^{14}C_{DIC}$ analysis. About 1 L of filtered water was transferred to a polycarbonate bottle and was frozen for $\Delta^{14}C_{DOC}$, and the residue on filter was frozen for $\Delta^{14}C_{POC}$ analysis.

Alkalinity was determined by ion balance using concentrations of cations (Na^+, NH_4^+, K^+, Mg^{2+}, Ca^{2+}) and anions (Cl^-, NO_2^-, NO_3^-, PO_4^{3-}, SO_4^{2-}). Major ions of the filtered water samples were quantified by Dionex ICS-1600 ion chromatography (Dionex, Sunnyvale, CA, USA). Water pH and temperature were measured before filtering in a field, and also measured in laboratory for filtered samples using Metrohm 827 pH meter (Metrohm AG., Herisau, Switzerland). Riverine [DIC] was calculated from the filtered water pH and alkalinity using CO2SYS program (CO2SYS Version.2.1, http://cdiac.ess-dive.lbl.gov/ftp/co2sys/). Riverine [DOC] was analyzed using Shimadzu TOC-V_{CPH} (Shimadzu Corporation, Japan) for filtered samples. Before POC analysis, each filter was fumigated using concentrated HCl vapor for ~6 hours, and dried at 80^{o}C for ~24 hours (Hedges and Stern, 1984; Komada *et al.*, 2008). [POC] was measured by Shimadzu SSM-5000A (Shimadzu Corporation, Japan).

The LOADEST (load estimator) program by US Geological Survey (Runkel *et al.*, 2004) was used to quantify riverine carbon loads which used a

relationship between intermittently measured loads (= concentration x Q) and continuously measured daily Q. The daily Q data for each site or the nearest gauging station were downloaded from WAMIS for 2012–2013. A log-linear relationship between loads and Q was used to estimate daily DIC, DOC, and POC loads that were summed to estimate annual carbon loads in 2012–2013 (model 1 of LOADEST). The calculated POC load bias exceeded -25% after a typhoon hit in the NR in 2012, and thus the POC load was estimated by the LOADEST (model 1) for the two separate periods, the period of high Q (> mean + 3 standard deviation) and the period of normal Q to prevent overestimation. A total of 11 days of the NR was categorized as the high Q period ($Q > 0.16$ km^3 day^{-1}). The POC loads of the two periods were combined to provide the annual POC load.

2.3 Dual carbon isotope analysis

Dual carbon isotope (^{14}C and ^{13}C) analysis was conducted for river water samples collected seasonally in 2013. For ^{14}C-DIC analysis, filtered water samples were acidified using 40% H_3PO_4 solution to convert DIC to CO_2, then the released CO_2 was extracted cryogenically in a vacuum line and sealed in a pre-baked pyrex tube (Raymond and Bauer, 2001). For ^{14}C-DOC analysis, each filtered water sample was also acidified with 40% H_3PO_4 solution and sparged with helium gas to remove DIC. Then, the sample was oxidized with ultrahigh purity O_2 gas using UV lamp for 4 hours (Raymond and Bauer, 2001). The oxidized CO_2 was purified cryogenically

in a vacuum line and sealed in a combusted pyrex tube. For ^{14}C-POC analysis, each filter was fumigated with concentrated HCl vapor, dried, sealed in a pre-burned quartz tube with CuO and a few strands of silver, and oxidized at 850^{o}C (Druffel *et al.*, 1992). The generated CO_2 from this step was collected in a pre-combusted pyrex tube in the same manner as DIC and DOC.

Dual carbon isotopes (δ^{13}C and Δ^{14}C) were measured at the NOSAMS (national ocean sciences accelerator mass spectrometry) facility at the Woods Hole Oceanographic Institution (http://www.whoi.edu/nosams/) in US. The CO_2 samples in the sealed pyrex tubes were converted to graphite targets for ^{14}C measurement. The ^{14}C pre-treatment and analysis are explained in detail in a review (Raymond and Bauer, 2001). The dual carbon isotope analyses for DIC and DOC were conducted for the water samples collected over the four seasons while the analysis for POC for summer and winter only.

3 Results

3.1 Loads and yields of riverine carbon

Annual mean [DIC], [DOC], and [POC] of the five rivers ranged from 7.1 to 14.1 mg L^{-1}, 1.4 to 3.7 mg L^{-1}, and 0.5 to 2.4 mg L^{-1}, respectively, that were comparable with the results of previous studies on some of the rivers (Lee *et al.*, 2007; Shin *et al.*, 2011a; Shin *et al.*, 2011b; Kim *et al.*, 2013; Shin *et al.*, 2015). Annual flow-weighted mean DIC, DOC, and POC concentrations ($[DIC]_f$, $[DOC]_f$, and $[POC]_f$, respectively) ranged from 5.2 to 11.2 mg L^{-1}, 1.4 to 3.6 mg L^{-1}, and 0.5 to 3.0 mg L^{-1}, respectively. The lower $[DIC]_f$ than [DIC] was due to the negative correlation between [DIC] and river discharge (Q), suggesting that DIC was diluted by increased Q although [DIC] was higher than what dilution accounted for. In contrast, [DOC] was not dependent on Q ($p>0.05$) and [POC] increased as Q increased, resulting in the similar or slightly higher flow weighted mean concentrations than the simple averages.

A total of 601.1 and 560.1 Gg-C yr^{-1} of riverine carbon were transported by the five rivers in 2012 and 2013, corresponding to the carbon yields (i.e., riverine carbon loads/basin area) of 10.3 and 9.6 g-C m^{-2} yr^{-1}, respectively (Table 2). The YR showed the largest riverine carbon yields of 17.1 g-C m^{-2} yr^{-1} and the SR the lowest carbon yields of 4.7 g-C m^{-2} yr^{-1} (Table 2). DIC was the dominant form of

riverine carbon, accounting for 80% of the total carbon loads with ~14% by DOC and ~6% by POC in the five rivers.

The annual PPT was 1,479 and 1,163 mm in 2012 and 2013, respectively, which corresponds to 113% and 89% of the mean PPT for the years 1981–2010, respectively. About 36–51% of annual PPT rained during summer. The riverine carbon yields of the basins ranged from 2.4 to 6.2 g-C m^{-2} $season^{-1}$ during summer which corresponds to 34–46% of the annual carbon yields including DIC, DOC, and POC. The contribution of summer carbon yields to the annual carbon yields were 34–45% for DIC, 37–50 % for DOC, and 33–48% for POC (Figure 2).

Table 2. Annual flow-weighted mean concentrations, loads, and yields of the riverine carbon from the five basins during 2012-2013.

River	Discharge (km^3 yr^{-1})		$[DIC]_f$ (mg L^{-1})		$[DOC]_f$ (mg L^{-1})		$[POC]_f$ (mg L^{-1})		DIC loads (Gg yr^{-1})		DOC loads (Gg yr^{-1})		POC loads (Gg yr^{-1})		TC[a] loads (Gg yr^{-1})		DIC yield (g m^{-2} yr^{-1})		DOC yield (g m^{-2} yr^{-1})		POC yield (g m^{-2} yr^{-1})		TC yield (g m^{-2} yr^{-1})	
	2012	2013	2012	2013	2012	2013	2012	2013	2012	2013	2012	2013	2012	2013	2012	2013	2012	2013	2012	2013	2012	2013	2012	2013
HR	20.0	23.9	11.1	11.7	1.4	1.6	0.6	0.5	224.6	255.3	28.7	34.6	9.4	9.9	262.7	299.8	10.3	11.7	1.3	1.6	0.4	0.5	12.0	13.8
GR	6.1	4.1	9.6	10.5	2.2	2.5	1.4	0.7	64.8	50.8	14.5	10.7	7.5	5.4	86.8	66.9	6.9	5.4	1.5	1.1	0.8	0.6	9.2	7.1
YR	2.4	1.9	10.3	7.9	2.7	3.6	1.3	1.8	25.2	22.2	7.5	6.2	4.1	3.6	36.8	32.0	11.7	10.3	3.5	2.9	1.9	1.7	17.1	14.9
SR	3.3	2.5	5.2	6.4	1.6	1.9	0.5	0.8	18.0	14.7	5.6	4.3	1.8	1.4	25.4	20.4	4.2	3.4	1.3	1.0	0.4	0.3	5.9	4.7
NR	12.9	9.0	8.8	10.9	2.9	2.4	3.0	0.8	138.3	109.3	34.5	22.8	16.7	8.8	189.5	140.9	6.7	5.3	1.7	1.1	0.8	0.4	9.2	6.8
Total	49.2	46.6	9.5	10.4	2.3	1.8	2.1	0.8	470.9	452.4	90.7	78.6	39.5	29.1	601.1	560.1	8.1	7.8	1.6	1.3	0.7	0.5	10.3	9.6

a TC (total carbon): DIC, DOC, and POC combined (PIC was excluded)

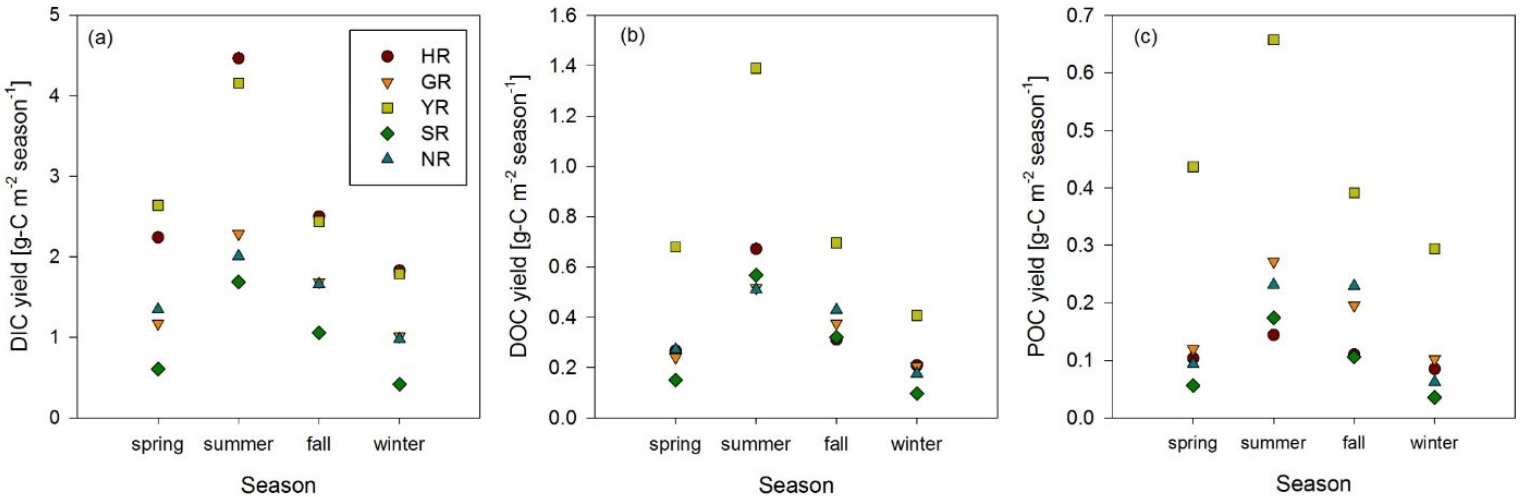

Figure 2. Seasonal mean (a) DIC (b) DOC, and (c) POC yields of the five river basins in 2012 and 2013 (spring: March–May, summer: June–August, fall: September–November, and winter: December–February).

3.2 δ ^{13}C and Δ^{14}C of the five rivers

The $\delta^{13}C_{DIC}$ of the five rivers ranged from -14.4 to -4.3‰, with the most depleted $\delta^{13}C_{DIC}$ in the YR and the most enriched in the HR (Figure 3a). The $\delta^{13}C_{DIC}$ of each river was the lowest in summer (Figure 3a). Flow-weighted mean $\delta^{13}C_{DIC}$ ($\delta^{13}C_{DIC, f}$) of the YR was the lowest (-12.1‰), followed by the SR (-11.6‰), the NR (-10.2‰), the HR (-9.4‰), and the GR (-9.0‰). The $\Delta^{14}C_{DIC}$ of the five rivers ranged from -89 to 27‰ (Figure 3a) which corresponded to the ^{14}C ages of 685 ybp to modern, respectively. In contrast to $\delta^{13}C_{DIC}$, the $\Delta^{14}C_{DIC}$ was the highest in summer resulting in a negative correlation between $\delta^{13}C_{DIC}$ and the $\Delta^{14}C_{DIC}$ (Figure 3a). The most depleted $\Delta^{14}C_{DIC}$ was observed in the HR and the most enriched in the SR. The flow-weighted mean $\Delta^{14}C_{DIC}$ ($\Delta^{14}C_{DIC, f}$) was the highest in the SR (15.8‰), followed by the YR (-22.1‰), the GR (-30.1‰), the NR (-44.6‰), and the HR (-55.7‰) in 2013.

The riverine $\delta^{13}C_{DOC}$ ranged from -27.7 to -21.9‰, and depleted $\delta^{13}C_{DOC}$ was observed in summer (Figure 3b). Flow-weighted mean $\delta^{13}C_{DOC}$ ($\delta^{13}C_{DOC, f}$) of the NR was the highest (-19.6‰), followed by the SR (-22.7‰), the YR (-26.5‰), the HR (-27.0‰), and the GR (-27.2‰). The $\Delta^{14}C_{DOC}$ ranged from -124.3 to 0.8‰ which corresponded to the ^{14}C ages of 1,000 ybp to modern, respectively (Figure 3b). The lowest $\Delta^{14}C_{DOC}$ was observed in the GR and the NR, and the highest in the HR and the SR. The most enriched $\Delta^{14}C_{DOC}$ in each river was observed in summer

(Figure 3b). Flow-weighted mean $\Delta^{14}C_{DOC}$ ($\Delta^{14}C_{DOC, f}$) of GR was the lowest (-100.1‰), followed by the NR (-63.2‰), the YR (-56.3‰), the SR (-22.3‰), and the HR (-20.2‰).

The $\delta^{13}C_{POC}$ ranged from -29.9 to -21.2‰ (Figure 3c). The $\Delta^{14}C_{POC}$ was higher in summer than winter, ranging from -125.5 to 35.1‰ which corresponded to the ^{14}C ages of 1,020 ybp to modern, respectively (Figure 3c). Despite of the oldest POC in the HR in summer, relatively young POC was released during summer in general (Figure 3c).

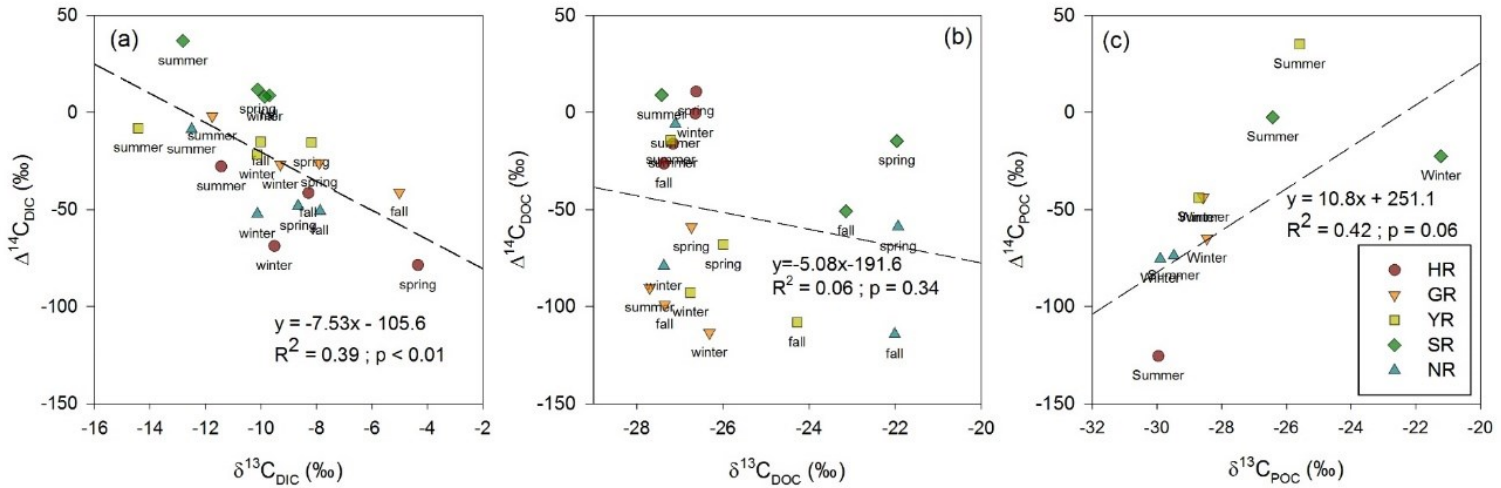

Figure 3. Relationships between $\delta^{13}C$ and $\Delta^{14}C$ of (a) DIC, (b) DOC, and (c) POC in the five largest rivers in South Korea during 2013. The dashed lines are linear regression lines. The analysis for DIC, and DOC were conducted for the water samples collected over the four seasons while the analysis for POC for summer and winter only. The winter HR sample for $\Delta^{14}C_{POC}$ was lost during the analysis, unfortunately.

4 Discussion

4.1 Concentrations, loads, and yields of riverine carbon

The mean $[DIC]_f$ of the five rivers in South Korea was 7.4 mg L^{-1} which was comparable with the global average $[DIC]_f$ of the 35 major rivers, 8.6 mg L^{-1} (Ludwig *et al.*, 1998; Huang *et al.*, 2012). However, the DIC yields of the five river basins ranged from 3.4 to 11.7 g-C m^{-2} yr^{-1} with the mean of 7.9 g-C m^{-2} yr^{-1} which were higher than the mean DIC yield of the 60 major global river basins, 2.6 g-C m^{-2} yr^{-1} (Gaillardet *et al.*, 1999; Huang *et al.*, 2012).

Lithology is one of the strongest factors that can influence riverine [DIC] and possibly also DIC yield of a basin. For example, a large annual DIC yield of 38.3 g-C m^{-2} yr^{-1} was observed in a carbonate dominant catchment of the South HR (Shin *et al.*, 2011a), one of the two major tributaries of the HR, which suggests that carbonate bedrocks can raise the DIC yield of the HR basin downstream. However, the dominant bedrock composition across these river basins includes granites and granitic gneiss (Chough *et al.*, 2000), suggesting that factors other than lithology can raise the DIC yield of the basins.

The DIC yield of a watershed can be boosted by increased PPT and subsequently Q because weathering products stored in a watershed can be released by increased water flow despite a decrease in [DIC] due to dilution (Li and Bush, 2015). About 38% of annual DIC was released from the five river basins during summer while only ~16% in winter (Figure 2a). In contrast to many other temperate

systems where temperature and biological activities peak in low flow season, the high flow period here occurs during the summer, releasing the increased weathering products (HCO_3^-) due to enhanced biological activities.

Annual water yields (i.e., annual Q/basin area) of the five river basins ranged 0.5–1.0 m yr^{-1}, two to four times larger than the global mean water yield of 0.25 m yr^{-1} (Global Runoff Data Center; http://www.bafg.de/GRDC/). The ratio of DIC yield of each river basin to the global mean DIC yield ranged from 2.1 to 4.0, which was close to that of water yield ranging from 2.3 to 4.3, suggesting that the difference of DIC yields among the five river basins can be mainly explained by the hydrological difference. Since the annual PPT of 2012 and 2013 were 1,479 and 1,163 mm, which was 13% larger and 11% lower than the 30-year (1981–2010) mean annual PPT of 1,307 mm, respectively, the estimated DIC yields may be close to the DIC yield over a long term not overestimating or underestimating it.

The [DOC] of the five rivers were relatively low (1.1–5.5 mg L^{-1}) compared to that of the 48 global major rivers which ranged from 0.3 to 70.8 mg L^{-1}(Marwick *et al.*, 2015). The mean $[DOC]_f$ of the five rivers was 2.0 mg L^{-1} which was also lower than that of the global mean of 118 rivers, 5.3 mg L^{-1} (Dai *et al.*, 2012). However, the DOC yield was similar to the global average DOC yield of ~1.4 g-C m^{-2} yr^{-1} due to high water yields of the five river basins (Ludwig *et al.*, 1996; Huang *et al.*, 2012).

Considering that riverine [DOC] can increase as OC (organic carbon) content or C:N ratio of a watershed increases and that [DOC] can be positively

correlated with the proportion of wetlands in a watershed (Aitkenhead and McDowell, 2000; Alvarez-Cobelas *et al.*, 2012), it is not surprising to find low [DOC] in the five rivers in South Korea because the area covered by wetland is <1%, and because >80% of land area is mapped as entisols or inceptisols with low OM content (Jeong *et al.*, 2003). Furthermore, areas with slope ≥30% cover 30–60% of the five river basins (Ji *et al.*, 2012), which can reduce the contact time between water and SOM, and thus possibly reducing riverine [DOC].

Riverine DOC load was also mainly controlled by riverine discharge such that ~43% of annual DOC load was released during summer while only ~13% in winter (Figure 2b). Other river systems in Asia demonstrated that ~40–90% of annual DOC load was transported during summer monsoon period, indicating the strong role of hydrology on riverine DOC loads under monsoon climates (Bird *et al.*, 2008; Wang *et al.*, 2012).

The [POC] was relatively low (0.5–2.4 mg L^{-1}) in the five rivers compared to that of the 36 major global rivers which ranged from ~0.1 to 242 mg L^{-1} (Marwick *et al.*, 2015). The mean $[POC]_f$ of the five rivers was 1.0 mg L^{-1} which was lower than that of the 35 major rivers, 4.5 mg L^{-1} (Huang *et al.*, 2012). In addition, the POC yields during summer in the five river basins were about 2–10 times lower than the mean POC yield (1.3 g-C m^{-2} yr^{-1}) of 32 major rivers despite the high water yield of the five rivers (Ludwig *et al.*, 1996; Huang *et al.*, 2012) (Figure 2).

Dams and reservoirs can increase mean HRT, allowing particles to be settled down and trapped within the reservoir, thus [POC] and subsequently POC yields can decrease. Many dams and reservoirs have been used to manage water resources especially since 1960s (Kim *et al.*, 2001; http://www.kwater.or.kr), which could decrease [POC] of the dam effluent. For example, the [POC] of the Paldang Reservoir which is the major reservoir for water supply for Seoul, was less than a quarter of [POC] of the inlet water (Kim *et al.*, 2014), and [POC] in outflow were lower than that of inflow of other two large dams with $1 km^3\ yr^{-1}$ of reservoir capacity in the HR, and refractory [POC] decreased in effluent probably due to sedimentation (Shin *et al.*, 2013), suggesting that the POC yield at the lower reach of the river can decrease as the river passes through many dams and reservoirs.

4.2 $\delta^{13}C$ and $\Delta^{14}C$ of riverine carbon

4.2.1 DIC

The mean of $\delta^{13}C_{DIC}$ of the five rivers was -9.6‰ which was higher than the global mean $\delta^{13}C_{DIC}$ of -12.5‰ (p-value < 0.05), and the mean of $\Delta^{14}C_{DIC}$ of the five rivers was -33‰ which was comparable with the global mean $\Delta^{14}C_{DIC}$ of -32‰ (Figure 4a, Marwick *et al.*, 2015). While $\delta^{13}C_{DIC}$ ranged from -14.4 to -11.4‰ during summer across the five rivers that of the other seasons ranged from -10.1 to -4.3‰ (Figure 3a). This suggests that the relative contribution of respiration to riverine DIC increases in summer while that of carbonate weathering increases in the other seasons considering that carbonate weathering can raise the $\delta^{13}C$ of river water (Figure 3a). CO_2 exchange between atmosphere and the river can be one of DIC sources. However, $\Delta^{14}C_{DIC}$ was depleted in dry seasons, air-water CO_2 exchange cannot mainly influence on DIC of the five rivers of South Korea.

The shift of major sources of riverine DIC in summer is also reflected by the highest $\Delta^{14}C_{DIC}$ (Figure 3a) because respiration of biota can produce relatively modern $\Delta^{14}C_{DIC}$. In contrast, weathering of sedimentary rocks including carbonates can significantly lower the $\Delta^{14}C_{DIC}$ because there is no detectable ^{14}C in old (>60,000 years) rocks. Although pedogenic carbonates can contain modern ^{14}C, they tend to be formed in dry environment where annual PPT is lower than 500 mm yr^{-1} (Zamanian *et al.*, 2016), the annual PPT of South Korea is ~1300 mm yr^{-1}, and

thus, contribution of pedogenic carbonates to riverine DIC is unlikely. The $\Delta^{14}C_{DIC}$ was the lowest in the HR, which could be due to weathering of sedimentary carbonates within the HR basin.

Urban land-use can lower riverine $\Delta^{14}C_{DIC}$ by wastewater effluent or dissolution of building and road materials containing carbonates (Zeng and Masiello, 2010; Zeng *et al.*, 2011; Hossler and Bauer, 2013). Annual median dilution factor (=sewage Q/riverine Q) ranged from 0 to 1226 over the world, South Korea had ~40 of annual median dilution factor, thus, the effects of wastewater effluent on riverine carbon of South Korea can be higher than the other global rivers (Keller *et al.*, 2014). Agricultural practices such as liming (e.g., application of crushed carbonates) which is needed to optimize soil pH for crops (Oh and Raymond, 2006) can also potentially reduce riverine $\Delta^{14}C_{DIC}$. The largest proportion of urban and agricultural land use was observed in the YR and GR (Table 1). Thus, $\Delta^{14}C_{DIC}$ can be also low in the YR and GR although the lowest $\Delta^{14}C_{DIC}$ was observed in the HR (Figure 3) indicating the strong role of lithology of the basin.

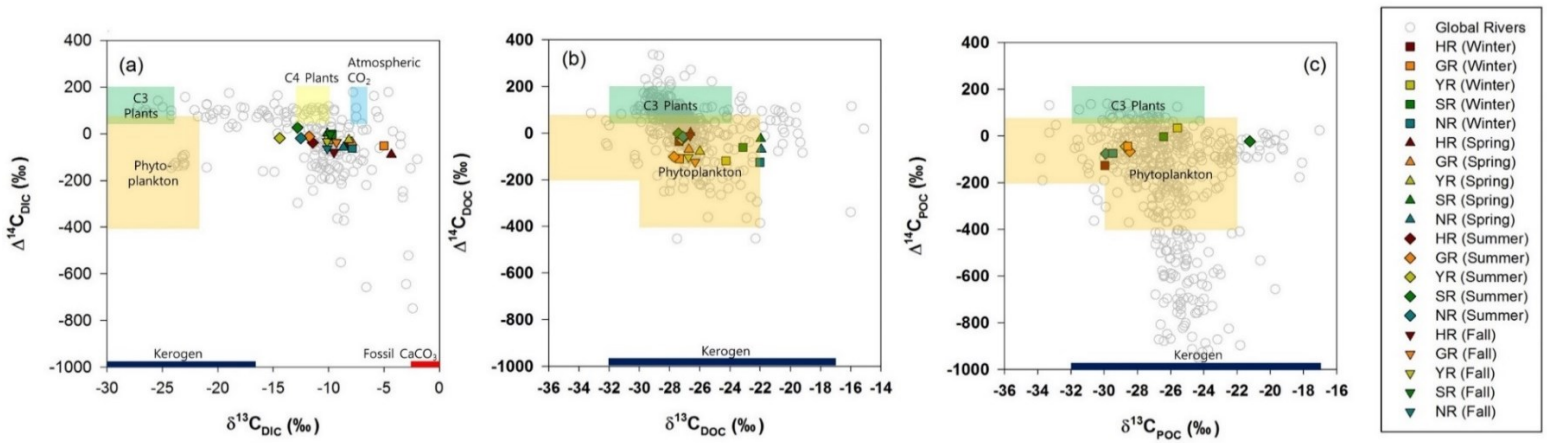

Figure 4. Dual carbon isotope values of (a) DIC, (b) DOC, and (c) POC in global major rivers and Korean rivers. Grey open circles are from Marwick et al. (2015) and colored symbols are from this study.

4.2.2 DOC

The mean $\delta^{13}C_{DOC}$ of the five rivers was -25.8‰ which was close to the mean of 60 world rivers (-26.9‰) whereas the mean $\Delta^{14}C_{DOC}$ of the five rivers was -60.3‰ which was significantly depleted than the mean of 70 world rivers, 22.5‰ ($p<0.05$) (Figure 4b). The depleted $\Delta^{14}C_{DOC}$ could be due to the release of aged soil DOC in deep soil horizons or groundwater DOC during base flow (Barnes *et al.*, 2018). However, the soils are mapped as entisols or inceptisols with relatively shallow depth, suggesting that there could be other sources of old DOC in the rivers.

The low $\Delta^{14}C_{DOC}$ can be due to petrochemical products processed in wastewater treatment plant (WWTP) or applied in agricultural fields (Griffith *et al.*, 2009; Sickman *et al.*, 2010; Butman *et al.*, 2012). For example, the average ^{14}C ages of WWTP effluent DOC can be as low as 2,650 ybp in the Hudson River and the Connecticut River (Griffith *et al.*, 2009) which corresponds to $\Delta^{14}C_{DOC}$ of -187‰. Similarly, $\Delta^{14}C_{DOC}$ of -254‰ was reported from drainage of agricultural fields (Sickman *et al.*, 2010), suggesting that urban and agricultural land use can lower the riverine $\Delta^{14}C_{DOC}$. This may explain the depleted $\Delta^{14}C_{DOC}$ in the GR and the YR (Figure 3) where the proportion of agricultural and urban areas are the largest among the five river basins (Table 1).

The WWTP effluent accounted for 4–49% of river discharge in the four rivers (the HR, the GR, the YR, and the NR) during the low flow period (Jan.–May, & Oct.–Dec.) in 2004–2008 (Moon *et al.*, 2010). The proportion increased up to 83–100% in the HR, GR, and YR when the discharge was the lowest (Moon *et al.*, 2010). The mean [DOC] of effluents from 110 WWTPs located over South Korea was 5.3 mg L^{-1} in 2014–2015 (Jeong *et al.*, 2016), which was larger than mean $[DOC]_f$ of the five rivers (2.0 mg L^{-1}), thus, WWTP effluent could be a main source of old DOC in the five rivers of South Korea when the river flow is relatively low.

4.2.3 POC

Since the number of measurements on $\Delta^{14}C_{POC}$ is only about a half of $\Delta^{14}C_{DOC}$, the isotope results should be interpreted with caution. Nonetheless, the $\Delta^{14}C_{POC}$ ranged from -125.5‰ to 35.1‰ in the five rivers with the mean of -46‰, which was significantly higher than that of 64 major world rivers of -204‰ ($p < 0.05$), suggesting that relatively young POC is released from the five rivers (Figure 4c; Marwick *et al.*, 2015). The riverine $\delta^{13}C_{POC}$ and $\Delta^{14}C_{POC}$ of summer was higher than winter in most rivers, and $\Delta^{14}C_{POC}$ increased significantly with [POC] across the five rivers ($R^2 = 0.60$, p-value = 0.02; except the SR in winter), possibly due to

increased allochthonous OC inputs by high PPT during summer (Kwon *et al.*, 2002; Kim *et al.*, 2013; Lee *et al.*, 2013).

Autochthonous OM inputs such as plankton- or algae-derived OM could also be a major source of young POC in the rivers, which could be increased by inputs of TN (total N) and TP (total P) released from WWTPs. High [TN] and [TP], 2.6–34.5 mg L^{-1} and 0.1–0.7 mg L^{-1}, respectively, were observed in the effluents of the four different types of WWTPs (Cho *et al.*, 2014), which suggests that plankton or algal growth could be facilitated by nutrient supply from WWTP effluents as well as by long HRT due to many dams and reservoirs in the rivers except summer high rainfall period.

In general, riverine $\Delta^{14}C_{DOC}$ tends to be higher than $\Delta^{14}C_{POC}$ in world rivers because solubilized DOC in soils tends to be younger than the POC from which it is derived (O'Brien, 1986; Trumbore *et al.*, 1992; Raymond and Bauer, 2001; Marwick *et al.*, 2015). Furthermore, higher $\Delta^{14}C_{DOC}$ than $\Delta^{14}C_{POC}$ can be observed if POC undergoes deposition/resuspension in river systems whereas DOC quickly exits through the rivers (Raymond and Bauer, 2001; Marwick *et al.*, 2015). However, $\Delta^{14}C_{DOC}$ was lower than $\Delta^{14}C_{POC}$ in the five rivers during winter (Figure 5) possibly due to the increased contribution of DOC from WWTP or agricultural petrochemicals to the rivers, whereas POC inputs from WWTP is minor (Kwon *et al.*, 2002; Lee *et al.*, 2013; Kim *et al.*, 2014).

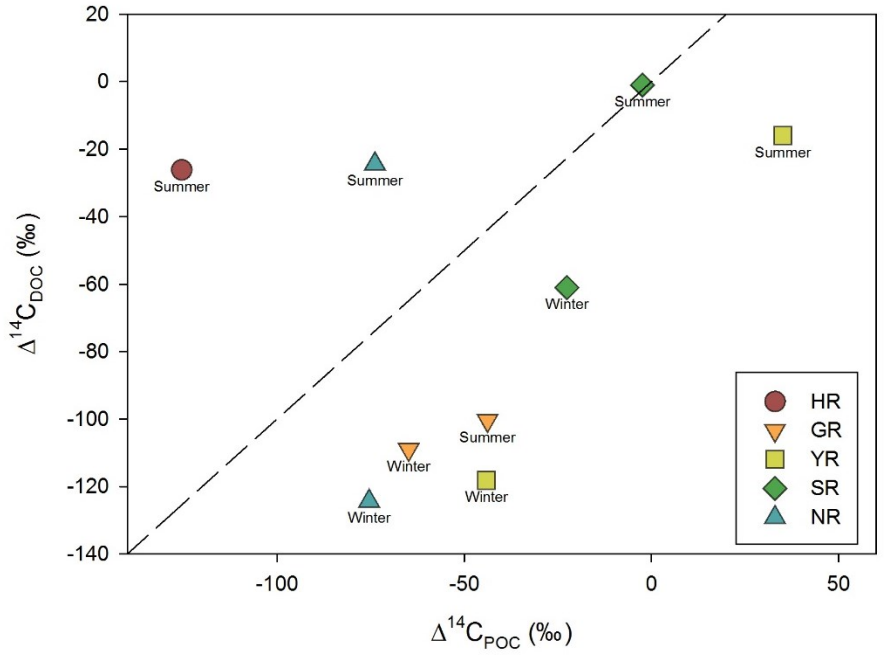

Figure 5. The relationship between Δ^{14}C-DOC and Δ^{14}C-POC in the five largest rivers of South Korea. The dashed line is 1: 1 line.

5 Conclusions

A total of ~581 Gg yr^{-1} of riverine carbon (DIC, DOC, and POC combined) was released by the five largest rivers in South Korea during 2012–2013, with 80% of it in the form of DIC. About 34–46% of total carbon was discharged throughout the rivers during summer, demonstrating the role of monsoons on riverine carbon loads. The ^{14}C ages of the riverine carbon varied from modern to 1,020 ybp, with higher $\Delta^{14}C_{DIC}$, $\Delta^{14}C_{DOC}$, and $\Delta^{14}C_{POC}$ in summer than the other seasons across the five rivers, indicating the shift of the carbon sources. The riverine $\Delta^{14}C_{DIC}$ was mainly controlled by natural factors such as weathering of soils and rocks within a basin, while $\Delta^{14}C_{DOC}$ and $\Delta^{14}C_{POC}$ could have been influenced by anthropogenic factors such as dams and WWTPs in South Korea, in particular during low flow season. If the frequency and intensity of precipitation increases with climate change, the seasonal changes of riverine carbon sources could be amplified. This would result in higher riverine carbon loads from the five major rivers, leading to more CO_2 exchange between atmosphere and oceans through mineralization process in estuaries. The impact that sudden increases of organic and inorganic carbon fluxes to estuarine and ocean environments in the context of the cycling of carbon is not yet known.

CHAPTER FOUR

Riverine Carbon Exports in Asia

1. Introduction

Asia is the largest continent with ~30% of global land area under a variety of climates from tropical to polar regions over a wide range of latitude and longitude. About 4.5 billion people, ~60% of world's population live in Asia with the highest population density among the continents. And thus, the pressure on environment such as urbanization and dam construction has increased which is coupled with rapid economic growth (Zarfl *et al.*, 2015; Maavara *et al.*, 2017). Subsequently, terrestrial ecosystem and hydrological cycle can be altered by anthropogenic impacts, affecting riverine carbon loads (Sun *et al.*, 2010; Xia and Zhang, 2011).

A total of ~1.0 Pg-C yr^{-1} is released from the rivers to the ocean globally, and organic carbon (OC: DOC and POC combined) is estimated to be 0.33–0.46 Pg-C yr^{-1} based on studies since 1990 (Table 1). The annual total carbon (TC: DIC, DOC, POC, and PIC combined) load through rivers in Asia accounts for 32–51% of global TC load (Table 1), even though the Asian land area covers ~30% of the global land area (Table 1). Annually 42% of global riverine OC is released from the rivers in Asia

because of high Q and peat soils with high organic carbon content in Southeast Asia (Schlünz and Schneider, 2000; Huang *et al.*, 2012). Dissolved inorganic carbon (DIC) load from the rivers of Asia at low latitudes, between 30°S and 30°N, accounts for 53% of global DIC loads at the same latitudes due to wide areas covered by carbonates (Huang *et al.*, 2012). The TC yield of the river basins in Southeast Asia is 9.5 g-C m^{-2} yr^{-1}, which is more than two times of the global mean of 4.1 g-C m^{-2} yr^{-1} (Battin *et al.*, 2009; Aufdenkampe *et al.*, 2011; Patra *et al.*, 2013).

Despite that Asia can have up to 50% of global riverine carbon loads (Ludwig *et al.*, 1996; Cole *et al.*, 2007; Cai, 2011; Alvarez-Cobelas *et al.*, 2012), data from the Asian rivers were not included or data measured in fewer rivers than in other continents were used in studies to estimate global riverine carbon loads. For example, Schlesinger and Melack (1981) estimated global TOC load of 0.37 Pg-C yr^{-1} using logarithmic regression between TOC load and Q of 12 major rivers of the world, however; the analysis did not include any river in Asia (Schlesinger and Melack, 1981). Since then, many studies have been conducted to estimate global riverine carbon loads, only less than 30 rivers in Asia were included among ~150 major rivers which were used to estimate the global riverine carbon load in most studies (Table 1). Data on concentrations and loads of riverine carbon in Asia are scattered and not well organized, thus, a synthesis on riverine carbon loads with new, updated data reflecting the inherent environmental characteristics in Asia is needed.

Studies estimating the riverine carbon loads in Asia have been conducted

mostly focused on OC and used measured data with low sampling frequency in a year. First, less than 20 studies have been conducted on concentrations or loads of inorganic carbon (IC: DIC and PIC combined) where PIC was mostly excluded. In contrast, there have been more than 100 studies on riverine OC loads in Asia since 1975. Furthermore, it is erroneous to estimate riverine carbon loads based on data collected with low sampling frequency (less than seasonally) only from a part of a year, dry or wet seasons, because there is a large seasonal variation in precipitation and riverine discharge (Q) under monsoon climates. For example, annual POC load estimates of the Godavari River in India ranged 756Gg-C yr^{-1} to 2,810Gg-C yr^{-1} because only 2–3 measured data in less than year were used to calculate annual loads (Gupta *et al.*, 1997; Balakrishna and Probst, 2005). Thus, new estimates on riverine carbon loads in Asia are needed.

The objectives of this study are to provide improved riverine carbon load estimates in Asia and to quantitatively understand the major factors affecting them. To understand the spatial characteristics of carbon loads, carbon yield maps of Asian rivers are created using database including newly added field data of every carbon species (DIC, DOC, POC, and PIC) during wet and dry seasons. Correlations were investigated between riverine carbon loads and environmental factors such as climate, soil types, and land use land cover (LULC). The results of this study can help us understand spatiotemporal changes of riverine carbon loads in Asia.

Table 1. Riverine carbon loads of Asia and the globe. The units are in parenthesis. The units of carbon loads are Tg-C yr^{-1}, and the units of carbon yields are g-C m^{-2} yr^{-1}.

Reference	Component	Continent	Number of rivers used	Sum of area (10^6 km^2)	Sum of Q (km^3 yr^{-1})	DIC Load	DOC Load	POC Load	PIC Load	TC Load
Degens *et al.* (1991)	DIC, DOC, POC	Asia	18	45	12,205	158	94	128	NA	380 [a]
Dai *et al.* (2012)	DOC	Asia	26	NA	9,838	NA	52	NA	NA	NA
Li *et al.* (2017)	DIC, DOC, POC	Asia	NA[†]	NA	14,070	97	87	77	NA	261 [a]

Reference	Component	Continent	Number of rivers used	Sum of area (10^6 km^2)	Sum of Q (km^3 yr^{-1})	DIC Load	DOC Load	POC Load	PIC Load	TC Load
Harrison *et al.* (2005)	DOC	Asia (excluding Indonesia)	16	32	NA	NA	32	47	NA	79 [b]
Seitzinger *et al.* (2005)	DOC, POC									
Degens *et al.* (1991)	DIC, DOC, POC, PIC	Global	51	128	35,319	407	335[b]	NA	NA	407 [a]
Smith and Hollibaugh (1993)	DOC, POC	Global	NA	NA	NA	NA	204	204	NA	408 [b]
Meybeck and Vörösmarty (1999)	DIC, DOC, POC, PIC	Global	>40	150	37,400	385	215	205	170	975

Reference	Component	Continent	Number of rivers used	Sum of area (10^6 km^2)	Sum of Q (km^3 yr^{-1})	DIC Load	DOC Load	POC Load	PIC Load	TC Load
Ludwig *et al.* (1996)	DOC, POC	Global	60	106	38,170	NA	205	173	NA	378 [b]
Ludwig *et al.* (1998)	DIC, DOC, POC	Global	NA	NA	38,170	327	206	188	NA	721 [a]
Aitkenhead and McDowell (2000)	DOC	Global	164	NA	NA	NA	360	NA	NA	NA
Harrison *et al.* (2005)	DOC	Global	68	114	37,400	NA	170	197	NA	367 [b]
Seitzinger *et al.* (2005)	DOC, POC									

Reference	Component	Continent	Number of rivers used	Sum of area (10^6 km^2)	Sum of Q (km^3 yr^{-1})	DIC Load	DOC Load	POC Load	PIC Load	TC Load
Cai (2011)	DIC, DOC, POC, PIC	Global	NA	NA	NA	407	246	216	168	1037
Dai *et al.* (2012)	DOC	Global	118	NA	NA	NA	170	NA	NA	NA
Li *et al.* (2017)	DIC, DOC, POC	Global (excluding Oceania)	263	NA	37,910	366	233	228	NA	827 [a]

[a] DIC, DOC and POC combined

[b] TOC: DOC and POC combined

[†] NA: not available

2. Methods

2.1. The riverine carbon database of Asia

The riverine carbon database was constructed using the data from 128 published studies in Asia (Appendix Table A1–A4). The database contained watershed area, sampling location (latitude and longitude), Q, concentration of each carbon species (DIC, DOC, POC, and PIC), and loads. Graphic data were changed into numbers using getData Graph Digitalizer program (GetData Graph Digitizer 2.26; http://getdata-graph-digitizer.com) and appended into the database. The instant carbon loads were scanned or downloaded from published studies, or was calculated by multiplying concentration and Q. The COSCAT (The Coastal Segmentation and its related Catchment) watersheds were used as a unit to show riverine carbon loads separating the regions based on geological, climatological, and oceanographic characteristics (Meybeck *et al.*, 2006). Asia in this study was defined following the definition used in the COSCAT watersheds, including Russia and Southwest Asia (Meybeck *et al.*, 2006; Figure A1). The data on 18 rivers of Southeast Asia were newly added in this study, which was provided by Dr. Chen-Tung Arthur Chen (National Sun Yat-sen University, Taiwan).

A 30 m by 30 m resolution data of Advanced Spaceborne Thermal Emission and Reflection Radiometer (ASTER) Global Digital Elevation Model Version 2

(GDEM V2) files (NASA, 2011) were used to delineate the boundaries of the watersheds using ArcHydro tools in ArcGIS 10.1 program (Environmental Systems Research Institute (ESRI), USA). More than 6,000 image GDEM files were merged by mosaic method of ENVI program (Version 4.5, ITT Visual Information Solutions, Boulder, CO, USA). A total of 135 watersheds were delineated, which covers about 70% of Asia.

2.2. GIS data on environmental factors

GIS data on environmental factors were collected including climate, LULC, rock types, soil organic carbon (SOC) content (ton per hectare at 0–30cm depth), slope (0 to 0.5, 0.5 to 2, 2 to 5, 5 to 8, 8 to 16, 16 to 30, and 30 to 45 degree), population density (0, 0 to 2, 2 to 10, 10 to 50, 50 to 250, and above 250 persons km^{-2}), the proportion of trapped sediment within the watershed (%TS), and carbonate outcrop area, to analyze the effects of environmental variables on riverine C loads. Maps of climate, LULC, slope, and population density were downloaded from Land Degradation Assessment in Dryland (LADA) project Version 1.1 (http://www.fao.org/land-water/land/land-assessment/assessment-and-monitoring-impacts/en/) (Figure A3, A4, and A5). The carbonate outcrop map was downloaded from environmental school of the University of Auckland (http://web.env.auckland.ac.nz/our_research/

karst/). Global lithological map (GLiM, downloaded from https://www.ccgm.org) with 0.5° by 0.5° resolution was used to calculate the proportion of rock types within each watershed. The 1 km by 1 km resolution map of global soil organic carbon map Version 1 was downloaded from Food and Agriculture Organization of the United Nations (FAO) (http://www.fao.org/global-soil-partnership/pillars-action/4-information-and-data-new/global-soil-organic-carbon-gsoc-map/en/). The six global NEE models were downloaded and used to analyze the relationships between the DOC yield and NEP in the river basins in Asia. The detail information of the six NEE models is provided in Table 5.

2.3. Estimation of riverine carbon loads in Asia

Carbon loads in at the lowest point of each river (independent watershed) except nested watershed were used to estimate total riverine carbon loads in Asia. When there were multiple data of carbon loads for a river, the most recent data, measured for at least one year including dry and wet seasons, were used to estimate carbon loads. When the C load was not reported but the data of C concentration and the Q were provided, the C load was calculated by multiplying the flow weighted mean concentration by the Q.

Carbon load of each COSCAT watershed in Asia was estimated using the linear regression between log-transformed carbon loads and log-transformed Q.

Riverine C load was correlated with Q regardless of the carbon form in the independent rivers ($R=0.81–0.91$, $p<0.01$, Figure 1).

2.4. Data analysis

Correlations between riverine carbon yields and the environmental factors were analyzed using SPSS Statistics v20 program (IBM, New York, USA). Normality of data such as carbon loads, yields, and environmental variables were tested using Kolmogorov-Smirnov and Shapiro-Wilk methods (Alvarez-Cobelas *et al.*, 2012). However, most of data failed the normality test, and thus spearman correlation was used instead which does not require the normality of data (Alvarez-Cobelas *et al.*, 2012). Correlation analysis was conducted excluding outliers with the value that are at least three standard deviation apart from mean. DIC yield at the middle of Yangtze River basin, DOC yield of the Siak River basin, POC yields in the watersheds of Lanyang Hsi and the Tanshui rivers, and PIC yield of the Heping River basin were removed, and data of the Yangtze and the Brahmaputra rivers for DIC load, the Lena and Ob' rivers for DOC load, and the Ayeyarwady and the Salween and the Mekong rivers for POC load, and the Huanghe River for PIC eliminated before statistical analysis.

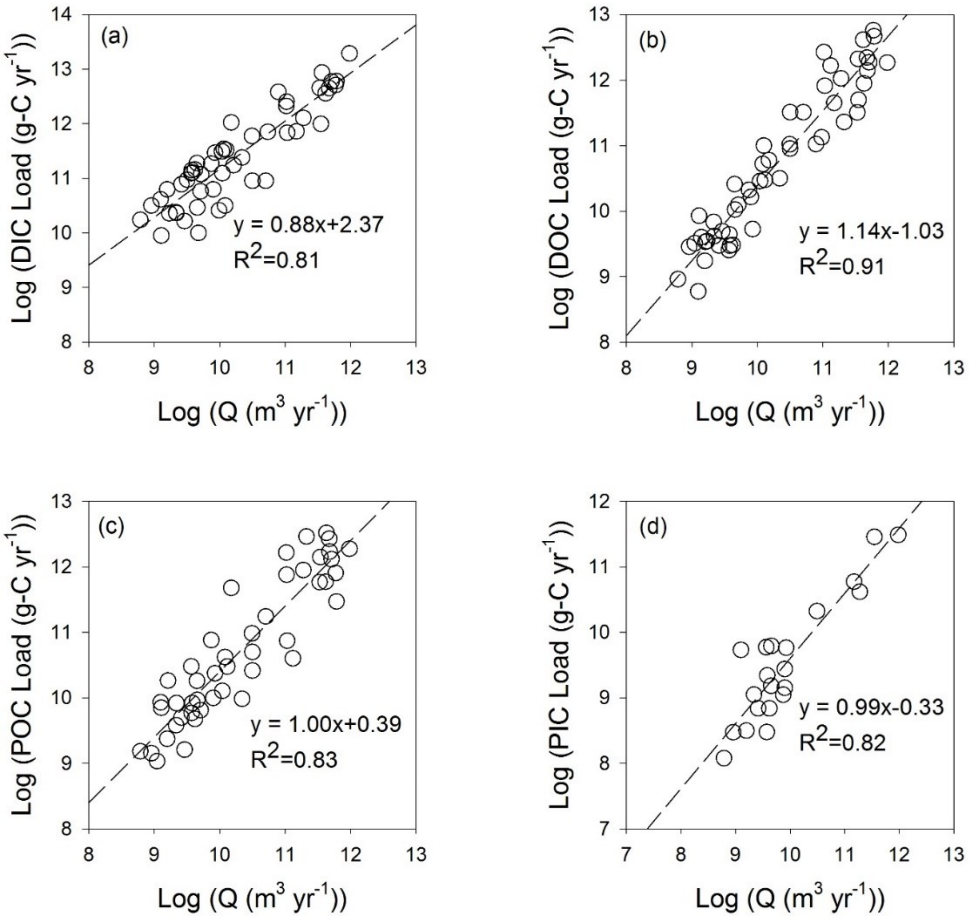

Figure 1. Relationships between Log (Q (m^3 yr^{-1})) and (a) Log (DIC load (g-C yr^{-1})), (b) Log (DOC load (g-C yr^{-1})), (c) Log (POC load (g-C yr^{-1})), and (d) Log (PIC load (g-C yr^{-1})). Only rivers from independent watersheds were used.

3. Results

3.1. Measured concentration, loads, and yields of river carbon

Annual mean [DIC], [DOC], [POC], and [PIC] of rivers in Asia ranged 1.9–58.9 mg L^{-1} (n=110), 0.5–35.9 mg L^{-1} (n=63), 0.3–18.4 mg L^{-1} (n=65), and 0.1–4.3 mg L^{-1} (n=21, excluding an outlier: 113.3 mg L^{-1} of the Huanghe River), respectively (Figure A2a). Annual DIC, DOC, POC, and PIC loads were -1.2–10.1 Tg-C yr^{-1}, -0.05–5.8 Tg-C yr^{-1}, -0.2–3.3 Tg-C yr^{-1}, and 0.0001–1.5 Tg-C yr^{-1}, respectively (Figure A2b). The largest riverine DIC load was 10.1 Tg-C yr^{-1} at the lower reach of the Yangtze River, followed by those of the Brahmaputra River (5.9 Tg-C yr^{-1}) and the Lena River (5.1 Tg-C yr^{-1}). The largest riverine DOC load was observed from the Lena River (5.9 Tg-C yr^{-1}), followed by 4.1 Tg-C yr^{-1} of the Ob' River and 2.7 Tg-C yr^{-1} of the Indus River. The riverine POC load was the highest in the Ayeyarwady River, 3.3 Tg-C yr^{-1}, followed by the Salween River (2.9 Tg-C yr^{-1}) and the lower Mekong River (2.7 Tg-C yr^{-1}). Most riverine PIC loads were below 6.2 Gg-C yr^{-1}, about three orders of magnitude lower than the other carbon types. Relatively high PIC loads were observed from rivers in China; 1.5, 0.3, and 0.3 Tg-C yr^{-1} in the Pearl River, the Yangtze River, and the Huanghe River, respectively.

The annual DIC yield ranged from -68.0 to 79.9 g-C m^{-2} yr^{-1}, DOC yield from -0.2 to 39.8 g-C m^{-2} yr^{-1}, POC yield from -8.2 to 29.0 g-C m^{-2} yr^{-1}, and PIC from

0.1 to 8.0 g-C m^{-2} yr^{-1} (Figure A2c). Negative DIC yields were observed in the Godavari and the Yangtze river basins (Table A1) and negative POC yields in the Godavari and the Pearl river basins (Table A3). The highest carbon yield was observed in the watersheds of small rivers of Southeast Asia, especially in Taiwan regardless carbon species (Figure 2). Annual DIC yield was higher in the small river watersheds in Taiwan and the Ganges River (>70 g-C m^{-2} yr^{-1}) basin than the other river basins (Table A1). The DOC yield was the highest in the watersheds of tributaries of the Siak River, Indonesia (23.0–39.8 g-C m^{-2} yr^{-1}) (Table A2). The POC yield was the largest at the Tanshui River watershed, followed by 22.2 g-C m^{-2} yr^{-1} at the Lanyang Hsi River watershed of Taiwan (Table A3). The PIC yield was the highest in the Heping River watershed in Taiwan (8.0 g-C m^{-2} yr^{-1}) (Table A4).

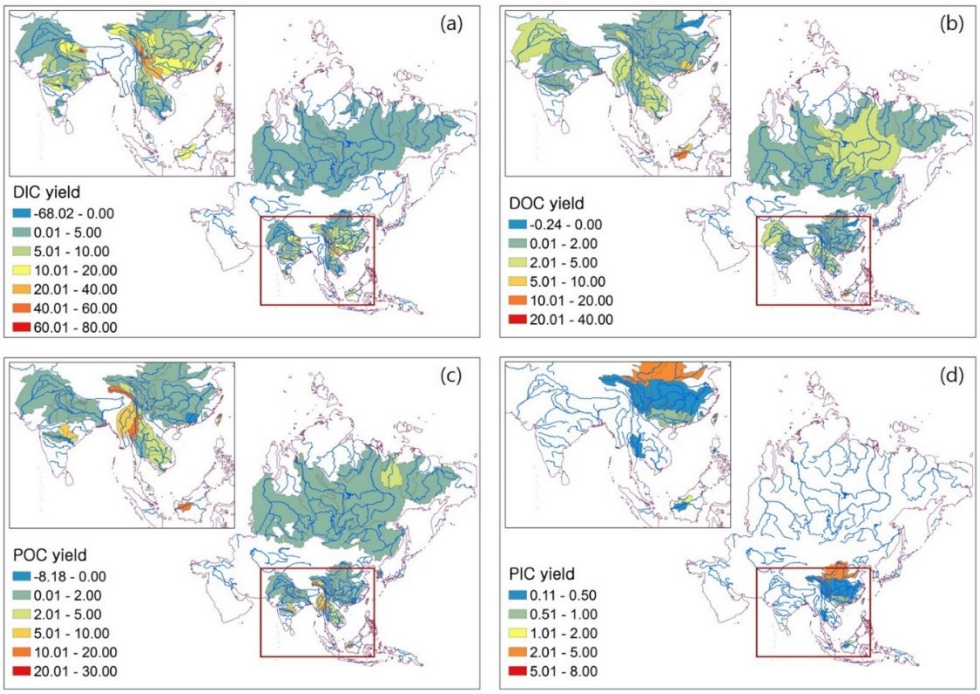

Figure 2. Measured (a) DIC, (b) DOC, (c) POC, and (d) PIC yields in watersheds in Asia. The blue lines are major rivers in Asia. The small boxes in red color are the regions of South Asia and the boxes in upper left corner are an enlargement of this section. The units are in g-C m^{-2} yr^{-1}. Negative values were due to the larger carbon loads upstream than downstream.

3.2. Estimated loads and yields of river carbon

The riverine TC load in Asia was estimated to be about 240 Tg-C yr^{-1}, accounting for ~25% of global TC load (Table 3). Riverine DIC load was the dominant component (57%) of the TC load, followed by DOC (26%), POC (15%), and PIC (2%). The TC yield in Asia was estimated to be 4.8 g-C m^{-2} yr^{-1}. The DIC yield was 2.7 g-C m^{-2} yr^{-1}, followed by DOC of 1.2 g-C m^{-2} yr^{-1}, POC of 0.7 g-C m^{-2} yr^{-1}, and PIC of 0.1 g-C m^{-2} yr^{-1}.

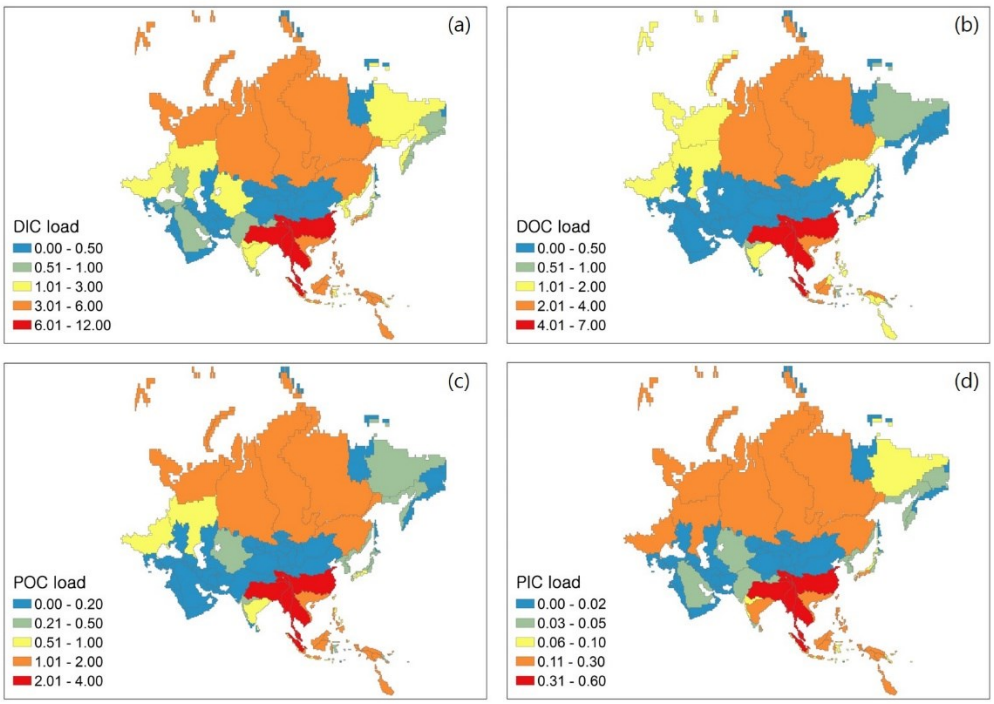

Figure 3. Estimated (a) DIC, (b) DOC, (c) POC, and (d) PIC loads from watersheds in Asia. The units are in Tg-C yr^{-1}.

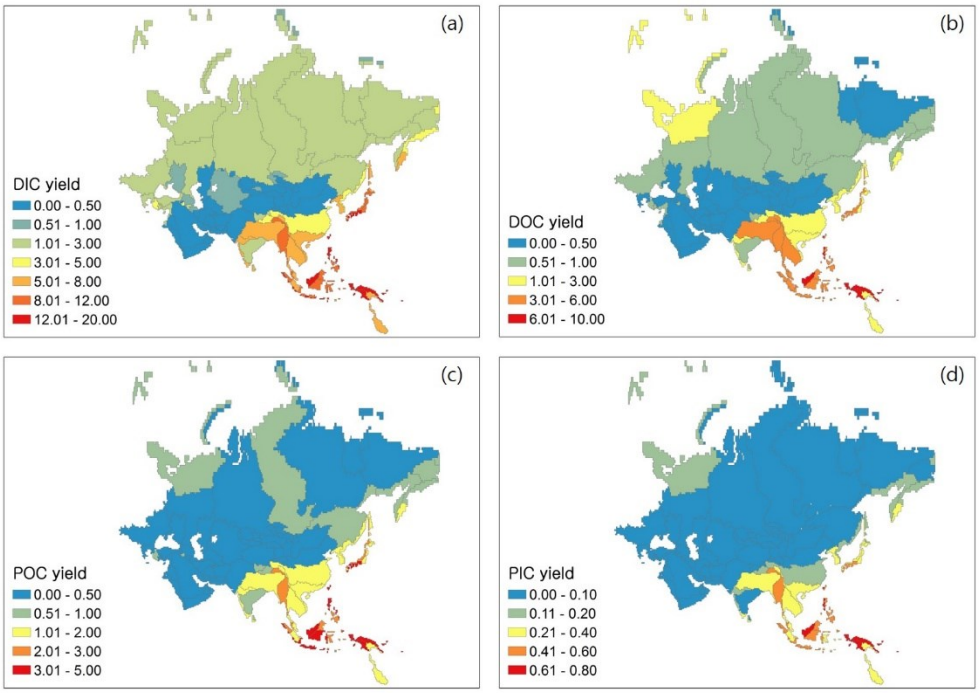

Figure 4. Estimated (a) DIC, (b) DOC, (c) POC, and (d) PIC yields of watersheds in Asia. The units are in g-C m^{-2} yr^{-1}.

3.3. Effects of environmental factors on riverine carbon yields

Carbon loads were positively correlated with Q regardless of carbon species ($R=0.73–0.91$, $p<0.01$) when all the rivers of database were used in analysis including nested rivers. Positive correlations were also observed between carbon yields and water yields ($R=0.32–0.68$, $p<0.01–0.05$). Watershed area was positively correlated with carbon loads of all the carbon species ($R= 0.63–0.83$, $p<0.01$), and had negative

relationships with carbon yields (R= -0.49 to -0.13) because the carbon yield is defined as the carbon load per the watershed area.

3.3.1. DIC

Two types of carbonate distribution maps were used in the analysis; the carbonate outcrop map and GLiM map. The DIC yield had no statistically significant relationship with the ratio of carbonate outcrop area to total watershed area (%carbonate) nor the proportion of carbonate sedimentary rocks of GLiM map (Table 2). The DIC yield of the watersheds was not significantly correlated with any rock type.

The DIC yield was positively correlated with proportion of areas under temperate or subtropical climates (%temperate and %subtropics) (R=0.26–0.46, $p<0.01$), while it was negatively correlated with %boreal and %desert (R= -0.27 to -0.25, $p<0.01$) (Table 2). The DIC yield decreased as the proportion of area (%area) with <16 degree of slope increased (R=-0.54 to -0.31, $p<0.01$) whereas it increased as that with >45 degree of slope increased (R=0.41–0.57, $p<0.01$) (Table 2).

There was no significant relationship between the DIC yield and the proportion of agricultural area (%agriculture) or urban area (%urban), and a negative correlation was observed between the proportion of wetland (%wetland) and DIC yield (R=-0.41, $p<0.01$). The DIC yield decreased as %area with no population

increased (R=-0.50, p<0.01), and slightly increased as population density increased (R=0.26, p<0.01) (Table 2).

3.3.2. DOC

Proportion of areas under temperate climates was negatively correlated to DOC yields (R=-0.27, p<0.01; Table 2). Rock types had no significant relationship with DOC yield. The DOC yield had a positive relationship with SOC content (R=0.34, p<0.01).

There was a negative correlation between the DOC yield as %area with 0–0.5 degree of slope (R=-0.41, p<0.01), whereas the DOC load was positively correlated with as %area with 0–0.5 degree of slope (R=0.42, p<0.01) (Table 2). DOC yield had a positive correlation with %forest (R=0.29, p<0.05) whereas negative relationships were observed between DOC yield and %grasslands and %shrubs (R=-0.49 to -0.34, p<0.01). There was no significant relationship between DOC yield and anthropogenic variables such as population density and %TS (Table 2).

3.3.3. POC

Significant correlations between the POC yield and other natural factors such as SOC content and slope were observed. A positive relationship between the

POC yield and SOC content was observed ($R=0.42$, $p<0.01$). The POC yield was positively correlated with %area with >45 degree of slope ($R=0.44$, $p<0.01$; Table 2). POC yield had a positive correlation with %forest of the watershed ($R=0.28$, $p<0.05$) while it was negatively correlated with %shrubs ($R=-0.31$, $p<0.05$; Table 2). However, the POC yield had no significant relationship with climates and any rock type (Table 2).

A negative relationship was observed between the POC yield and population density, but, that was not statistically significant. The POC yield had weak negative correlation with %TS ($R=-0.28$, $p<0.05$).

3.3.4. PIC

The PIC yield had no significant relationships with all the environmental variables (Table 2). In contrast, the PIC load had significant relationships with rock types including %carbonate- and %mixed-sedimentary rocks ($R=0.57–0.69$, $p<0.05$), LULC types of %crop, %agriculture, and %wetland ($R=0.44–0.67$, $p<0.01$), %area with less than 50 persons km^{-2} of population density ($R=0.56–0.62$, $p<0.01$), and %area with over than 250 persons km^{-2} of population density ($R=-0.51$, $p<0.05$).

Table 2. Correlation coefficient of correlation analysis between major variables and riverine carbon loads or yields (*: p-value<0.05, **: p-value <0.01).

Variables	DIC		DOC		POC		PIC	
(units)	Load	Yield	Load	Yield	Load	Yield	Load	Yield
Area (km^2)	0.74**	-0.49**	0.83**	-0.28	0.63**	-0.24	0.73**	-0.13
Water yield (m yr^{-1})	-0.20	0.68**	-0.32*	0.55**	-0.17	0.60**	0.03	0.44
LULC (%)								
Forest	-0.04	0.13	-0.09	0.29*	0.07	0.28**	-0.01	0.14
Grasslands	0.12	0.10	0.30*	-0.49**	0.43**	-0.06	0.37	0.19
Scrubs	0.29**	-0.34**	0.30*	-0.34**	-0.18	-0.31*	0.38	-0.18
Crop	0.14	-0.15	0.21	-0.04	-0.04	-0.19	0.57**	-0.21
Agriculture	0.18	0.05	0.25	-0.25	0.18	-0.05	0.44*	-0.34
Urban	0.11	0.17	-0.49**	0.02	-0.36**	0.12	-0.68**	-0.12
Wetlands	0.25*	-0.41**	0.53**	-0.00	0.45**	-0.21	0.67**	0.25
Sparsely vegetated	0.24*	-0.45**	0.44**	-0.25	0.47**	-0.19	0.37	0.10

Variables	DIC		DOC		POC		PIC	
(units)	Load	Yield	Load	Yield	Load	Yield	Load	Yield
areas								
Bare areas	0.26**	-0.32**	0.56**	-0.20	0.42**	-0.12	0.37	0.10
Climates (%)								
Polar	0.14	-0.14	0.48**	-0.22	0.42**	-0.08	0.37	0.06
Boreal	0.23*	-0.27**	0.56**	-0.06	0.48**	-0.15	0.37	0.1
Temperate	0.09	0.26**	-0.02	-0.27*	0.15	-0.06	0.08	0.08
Mediterran	0.12	-0.16	0.31*	0.13	0.21	0.13	ND[†]	ND
Subtropics	0.01	0.46**	-0.25*	0.05	-0.11	0.25	-0.44*	-0.38
Tropics	0.06	0.00	0.08	0.14	-0.09	0.15	0.45*	0.35
Deserts	0.29**	-0.25**	0.34**	-0.18	0.37**	-0.15	ND	0.30
Carbonate outcrop area (%)	-0.02	0.24	ND	ND	ND	ND	-0.03	-0.02
Rock types (%)	0.24–0.47*	-0.34–0.05	0.33–0.65*	-0.37**–0.11	0.33–0.61*	-0.30–0.18	0.47–0.70*	-0.43–0.31
Population density								

Variables	DIC		DOC		POC		PIC	
(units)	Load	Yield	Load	Yield	Load	Yield	Load	Yield
(persons km^{-2})								
0	0.33**	-0.50**	0.58**	-0.05	0.52**	-0.05	0.62**	0.04
0 to 2	0.32**	-0.14	0.54**	-0.09	0.51**	0.06	0.56**	0.17
2 to 10	0.34**	-0.05	0.46**	-0.07	0.53**	0.07	0.57**	-0.03
10 to 50	0.34**	-0.04	0.14	-0.12	0.25*	0.19	0.61**	0.08
50 to 250	0.04	0.26**	-0.17	-0.19	-0.27*	-0.09	0.26	-0.21
above 250	-0.03	0.15	-0.32*	0.00	-0.23	0.01	-0.51*	-0.11
Slope (degree)								
0 to 0.5	0.33**	-0.43**	0.43**	-0.41**	0.46**	-0.21	0.42*	-0.20
0.5 to 2	0.32**	-0.31**	0.14	-0.18	0.05	-0.19	0.17	-0.29
2 to 5	0.08	-0.43**	0.20	0.07	-0.02	-0.14	0.08	-0.04
5 to 8	0.01	-0.54**	0.29*	0.05	0.14	-0.15	0.40	-0.07
8 to 16	0.01	-0.43**	0.20	0.07	0.04	-0.16	0.11	-0.2
16 to 30	0.11	-0.13	0.03	-0.07	0.01	-0.07	0.17	-0.23

Variables	DIC		DOC		POC		PIC	
(units)	Load	Yield	Load	Yield	Load	Yield	Load	Yield
30 to 45	0.09	0.41**	-0.15	-0.16	0.05	0.23*	0.17	0.05
above 45	0.02	0.57**	-0.26*	-0.15	0.10	0.44**	-0.36	-0.03
%TS	ND	ND	0.21	-0.14	0.00	-0.28*	ND	ND
SOC content (ton ha^{-1} at 0–30cm depth)	ND	ND	-0.34**	0.34**	0.12	0.42**	ND	ND

† ND: No data

4. Discussion

4.1. Riverine carbon loads in Asia

Estimated riverine TC load in Asia was similar with the results of previous studies (Table 3). However, the proportion of each carbon form to the TC load was different. The DIC load accounted for 57% in this study whereas 37–48% of TC loads in previous studies (Table 3). High DIC loads were observed in low latitudes (30°S–30°N) possibly due to high proportion of carbonate outcrop area (Huang *et al.*, 2012). The proportion of DIC load to the TC load in this study was estimated to be up to 20% higher than that in previous research, which was due to the difference of estimation method and input data. The method of estimating the loads was different for each research. For example, flow weighted mean concentration of river DIC was calculated and then the total Q was multiplied to estimate the total DIC load in Asia (Huang *et al.*, 2012), or CO_2 consumption by rock weathering in the watershed was estimated and then the DIC load was calculated using CO_2 consumption and Q in the previous studies (Li *et al.*, 2015). In addition, while carbon load was estimated using data of the rivers in other continents as well as in Asia in previous studies, only data from the Asian rivers were used to calculated carbon load in this study.

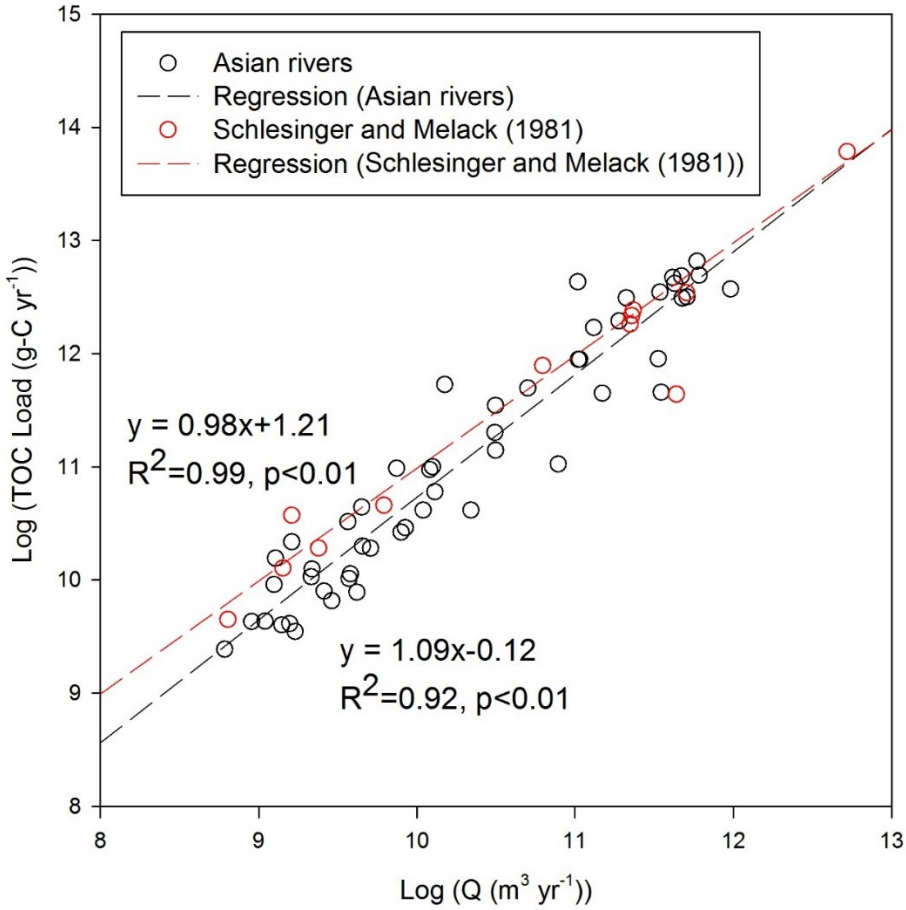

Figure 5. Relationships between Log (Q (m3 yr^{-1})) and Log (TOC load (g-C yr^{-1})) of 12 major rivers of the globe (Schlesinger and Melack, 1981) and 52 rivers in Asia (this study).

There is a statistically significant difference between the relationship used in Schlesinger and Melack (1981) and that derived from 52 Asian rivers in this study ($p<0.01$, Figure 5). The TOC load estimates in this study can be underestimated than TOC load estimates in Schlesinger and Melack (1981) in most Asian rivers. If riverine TOC load in Asia were calculated using the equation in Schlesinger and Melack (1981), it would be ~123Tg-C yr^{-1} which is about 25% higher than the estimates in this study.

The DIC and the DOC yields in the watersheds of Asian rivers were similar with the results of previous studies, whereas the POC and PIC yields were only a half of, and one-tenth of those in previous studies (Ludwig *et al.*, 1998; Meybeck and Vörösmarty, 1999; Huang *et al.*, 2012). The estimated POC yield in recent research tends to be lower than in previous studies, from 2.9 g-C m^{-2} yr^{-1} to 0.7 g-C m^{-2} yr^{-1} (Table 3). This may be due to the effects of construction of dams or reservoirs by water quality management policies. The number of dams increased by more than 70% over the world during 1970–2000, and dam building was concentrated in South America and Asia (Zarfl *et al.*, 2015; Maavara *et al.*, 2017). Although the PIC yield estimates can be inaccurate due to insufficient data and may have large deviations, the effects on total riverine carbon yield can be negligible because the PIC load is 40 times smaller than TC load (Table 3).

Relatively high riverine carbon yields and loads were obtained from the watersheds in Southeast Asia regardless of carbon species (Figure 3 and Figure 4). Measured carbon yields in especially the river watersheds of Southeast Asia were significantly higher than the estimated carbon yields (Figure 6). The estimates of DIC yield were approximately up to10 times lower than measured the DIC yields in Southeast Asia, which was due to high water yield and [DIC] of the watersheds in Southeast Asia. The mean [DIC] in the rivers of Southeast Asia was about 28 mg L^{-1}, 30% higher than that of the other rivers (22 mg L^{-1}) in Asia. The water yield of the watersheds in Southeast Asia with the mean of 3.0 m yr^{-1} was 4 times higher than that of the other rivers in Asia. Thus, estimates on loads and yields of total riverine carbon in Asia are conservative.

Table 3. Water discharge and carbon loads from rivers in Asia

(units: Q (km^3 yr^{-1}), load (10^{12} g-C yr^{-1})).

Q	DIC Load	DOC Load	POC Load	PIC Load	TC Load	Reference
14,460	136	62	37	6	241	This study
12,205	158	94	128		380	Degens et al. (1991)
8,694	111	45	60	15	232	Huang et al. (2012)*
14,070	97	87	77		261	Li et al. (2017)

* Only rivers with more than 60% of the watershed within 30°S–30°N were included.

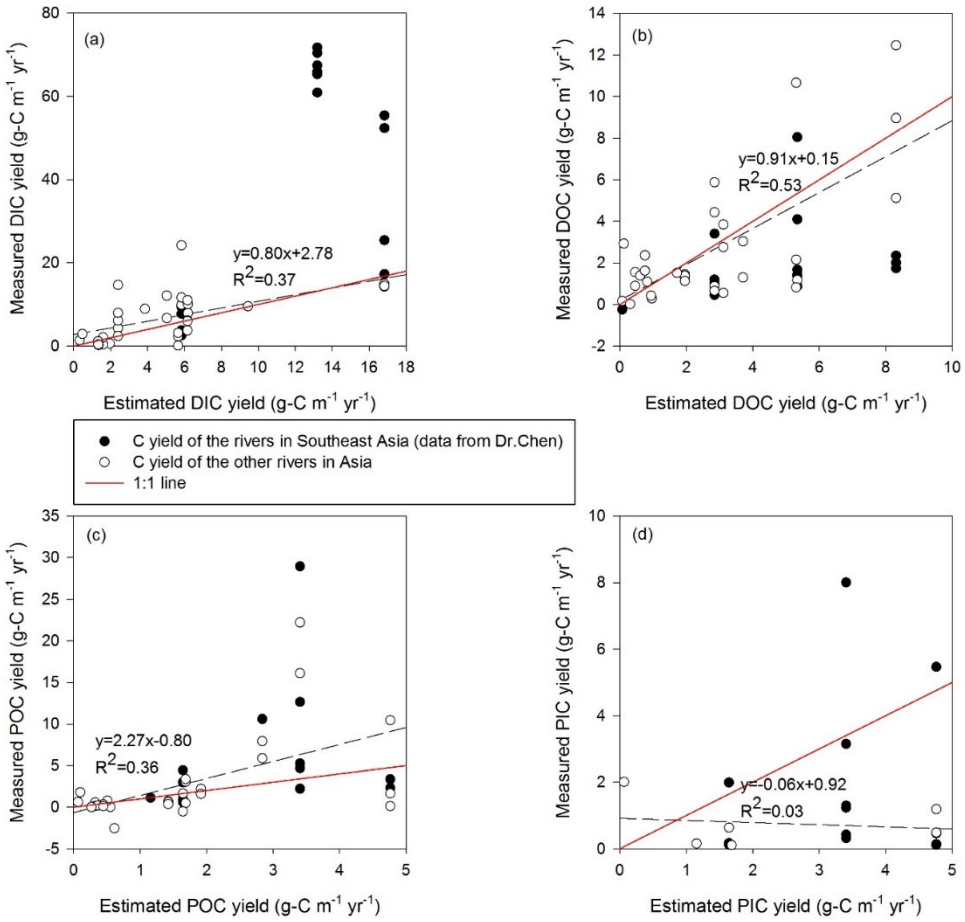

Figure 6. Measured vs. estimated carbon yields of (a) DIC, (b) DOC, (c) POC, and (d) PIC of watersheds in Asia. Closed circles are watersheds in Southeast Asia and open circles are the other Asian river watersheds. The dotted lines are the linear regression line between estimated and measured carbon yields, and the red lines are 1:1 lines. The equations are from the linear regression.

4.2. Hotspots of riverine carbon yields in Asia

Based on measured data, the highest TC load except PIC load was observed in the Yangtze River as 2.3 Tg-C yr^{-1}, which might due to the highest Q (960 km^3 yr^{-1}), because [DIC], [DOC], and [POC] in the Yangtze River were similar or lower than the average of the other Asian rivers. The rivers in polar regions and Southeast Asia had the highest carbon loads among the rivers except the Yangtze River. The three large arctic rivers (the Yenisei, the Lena, and the Ob' rivers) also have the highest Q (608, 591, and 415 km^3 yr^{-1}) except the Yangtze River, which was up to 7 times higher than the other rivers in Asia with the mean of 91 km^3 yr^{-1}. The TC loads except PIC in the three arctic rivers were 8.3–11.6 Tg-C yr^{-1}, and sum of TC loads in these three rivers was ~30Tg-C yr^{-1}, corresponding to about one eighth of TC load estimates in the Asian rivers (Table 3). In particular, the DOC loads of the three arctic rivers ranged from 4.1 to 5.8 Tg-C yr^{-1}, which were more than 10 times higher than the other rivers of Asia with the mean of 399 Gg-C yr^{-1}. However, water yields of the three arctic river basins ranged from 0.08–0.24 m yr^{-1}, which were three to ten times lower than the mean water yield in the other Asian rivers of 0.7 m yr^{-1} due to large watershed area. Thus, 2.8–4.8 g-C m^{-2} yr^{-1} of the TC yields except PIC of arctic rivers were obtained, which were > 10 times lower than the average of the other Asian rivers.

The small rivers of Southeast Asia emerged as hotspot of riverine carbon regardless of carbon species (Figure 2). Based on measured data, the TC loads including PIC loads of the rivers in Southeast Asia ranged from 1.4 to 3,260 Gg-C yr^{-}

^{1}, corresponding to the TC yields of 3.4 to 123.8 g-C m^{-2} yr^{-1}, which correlated with high water yields, soils with high OM content, and human effects. The small river watersheds in Southeast Asia had four times larger water yields (3.0 m yr^{-1}) than the mean of the other Asian rivers, which resulted in about 5 times higher TC yields than that of mean TC yields in the other Asian river watersheds ($p<0.01$). In particular, the DIC and POC yields in the Southeast Asian river basins were two to four times higher than those of the other rivers in Asia. For example, the Hualien and Tanshui rivers in Taiwan had 70–72 g-C m^{-2} yr^{-1} of DIC yields and 2.1–2.8 m yr^{-1} of water yields, which were up to six times and four times higher than the average of the other Asian river watersheds, respectively (Table A1). Abnormally high POC yields of the Lanyang Hsi and Tanshui river basins can be caused by agricultural activities, and a typhoon (Kao and Liu, 1997). The [POC] in the Lanyang Hsi River increased up to 30 times during a typhoon (Kao and Liu, 1997). The proportion of agriculture or urban area increased from the upper to the lower watersheds of the Tanshui River, and the water yield and population density were 2.8 m yr^{-1} and ~2000 persons km^{-2} in the Tanshui River watershed, which four and sixteen times higher than the other Asian rivers, suggesting that POC yield can increase by human impacts.

4.3. Factors affecting riverine carbon exports in Asia

Multivariate stepwise regression was conducted to determine the dominant variables on carbon yields in Asia except PIC due to insufficient data. The DIC yield was mainly correlated with slope. Water yields and slope and climates were related with the DOC yield of the watersheds in Asian rivers. Water yield, slope, and population density were dominantly correlated with the POC yield.

Considering the results of correlation and multivariate stepwise regression analysis (Table 2), the proportion of area with >30 degrees of slope to total watershed area was positively correlated with the DIC yield ($R=0.41–0.57$, $p<0.01$). The high DIC yield in the watersheds indicates enhanced chemical weathering in a watershed. Steep slope can increase surface area by physical weathering which may accelerate chemical weathering (Lloret *et al.*, 2013; Li and Bush, 2015), releasing DIC. The watersheds of several Asian major rivers (e.g. the Yangtze, the Salween, the Brahmaputra, and the Pearl river) and some rivers in Southeast Asia have steep slope (>50% of total watershed area is covered by >30 degrees of slope) (Figure A5), thus, leading to high DIC yield with the mean of 35.4 g-C m^{-2} yr^{-1}. This is more than four times higher than the mean of the other rivers ($p<0.01$). The proportion of carbonate area to total watershed area is considered to be a dominant factor to increase DIC yield (Shin *et al.*, 2011a; Huang *et al.*, 2012), however; there was no significant relationship between DIC yield and % carbonate area in this study, suggesting that

the link between % carbonate area and riverine DIC yield may not be universal. In addition, significant correlations between the DIC yield and %area of urban or agriculture were also not observed in this study. Although the DIC yield can increase due to agricultural activities and urban area expansion, for example, liming or cement usage (Oh and Raymond, 2006; Lu *et al.*, 2014), suggesting that human impacts of urban or agriculture area may not be affected to the DIC yield in Asia.

Water yield had a significant positive correlation with the DOC and POC yields because the carbon yield was calculated by multiplying water yield and carbon concentration. Storm events can increase OC yield of a watershed since not only facilitated soil erosion but also increased water yield (Baum *et al.*, 2007; Bird *et al.*, 2008). Up to ten times of DOC and POC yields were observed during monsoon season compared to that of dry season in the watersheds of the Huanghe, Ayeyarwady and Salween rivers (Zhang *et al.*, 1992; Bird *et al.*, 2008). Soil characteristics can affect riverine OC exports such as water retention capacity, depth of organic layer, and content of water soluble carbon (Amiotte Suchet *et al.*, 2003; Möller *et al.*, 2005; Barnes and Raymond, 2009; Alvarez-Cobelas *et al.*, 2012). In particular, SOC content can directly influence the OC yield because the river DOC can be derived from solubilization of SOC and because river POC from erosion of SOC (Deb and Shukla, 2011). The SOC content (ton ha^{-1} at 0–30cm depth) was positively correlated with both the DOC and POC yields in the Asian river basins (Table 2), suggesting that it can be a dominant factor to affect the OC yield in Asia. Generally the DOC yield can

increase as %wetland increases due to peat dominant soils with high [OC] (Moore *et al.*, 2013), however; there was no significant correlation between %wetland and the DOC yield in this study. There was no wetland in 36 river basins and only 14 river basins had >1% of proportion of wetland to the total watershed area, suggesting that the effect of wetland on the DOC yield may not be observed due to low proportion of wetland in the watersheds in this study.

The POC yield can be mainly controlled by slope as well as water yield in the watersheds. The POC yield tended to increase as %area with >30 degrees of slope increases in the watersheds (Table 2), suggesting that erosion could easily increase OM inputs into the river (Ludwig *et al.*, 1996). Population density had no significant correlation with the POC yield (Table 2), although it was selected as a significant variable in the multivariate stepwise regression model.

To sum up, natural factors such as water yield and slope can predominantly influence carbon yields of the watersheds in Asia, while the effects of anthropogenic variables such as %area of urban or agriculture, and population density on carbon yield in the Asian river basins were low regardless of carbon species (Table 2). There were significant correlations between population density and DIC yield (Table 2). The proportion of land area where no one lives to total watershed area was negatively related to DIC yield (Table 2). In contrast, the DIC yield increased as %land area with >50 persons km^{-2} increased (Table 2). Most of the watersheds in Asia have high population density. About 22% of the watershed area in the Asian rivers had >250

persons km^{-2} of population density and the mean proportion of area with >50 persons km^{-2} of population density to the watershed area in the Asian rivers was ~61% (Figure A4), suggesting that human impacts on the DIC yields in the Asian rivers can be high.

4.4. Trends and possible causes of riverine carbon exports in Asia

Riverine [DOC] and DOC loads have increased in several rivers over the world (Evans *et al.*, 2005; Findlay, 2005; Monteith *et al.*, 2007; Hruška *et al.*, 2009; Shi *et al.*, 2016). Increment of carbon accumulation in the river basin can be one of reasons of the temporally upward variation (Shi *et al.*, 2016). The NEP is the result of a variety of biogeochemical reaction in terrestrial ecosystems, which can be compared to riverine carbon load in the watershed to determine whether the watershed is a carbon sink or a source (Oh, 2016), thus, correlation between gross primary production (GPP), NEP and riverine DOC yields were analyzed. Weak positive correlation was observed between the DOC yields and GPP ($R=0.32$, $p<0.05$), while the relationship between NEP and the DOC yields differed depending on the NEP model (Table 4 and Figure A5). Positive relationships between NEP and the DOC yield in the watersheds were observed in three NEP models, whereas NEP from CarbonTracker was negatively correlated with the DOC yield. In addition, there was no significant correlation between the DOC yield and NEP in the other two models. In other words, there was no clear relationship between NEP and the DOC yields,

thus, DOC yields in Asia might not be significantly related to NEP as the indicator of carbon accumulation within the watersheds.

Table 4. Correlation between DOC yield and NEP downloaded from 6 different NEE models.

Model	Spatial Resolution	Temporal Resolution	Study Duration	Global NEP (Pg-C yr-1)	Relationships with DOC yield	Reference
Upscaled diurnal cycles of land–atmosphere fluxes	0.5° X 0.5°	Monthly	2001-2014	21.42	Positive	Bodesheim *et al.* (2018)
CarbonTracker	1°X1°	Monthly	2000-2016	3.73	Negative	CarbonTracker [a]
VISIT	0.5° X 0.5°	Monthly	2005-2011	4.28	Positive	Fisher *et al.* (2016)
CLASS-CTEM-N	0.5° X 0.5°	Monthly	2005-2011	7.98	not significant	Fisher *et al.* (2016)
SIB3	0.5° X 0.5°	Monthly	2005-2011	-0.19	not significant	Fisher *et al.* (2016)
TRIPLEX-GHG	0.5° X 0.5°	Monthly	2005-2011	16.72	Positive	Fisher *et al.* (2016)

a data was downloaded from https://www.esrl.noaa.gov/gmd/ccgg/carbontracker/

The estimated POC yield in Asia was up to ten times smaller than those of the other studies, which might be caused by temporal variation of the POC yield by constructions of dams or reservoirs. Construction of dams and reservoirs has increased since 1970s over the world and the number of large hydropower dams is expected to increase to about twice (~20,000 large dams over 15 m in height) in the next few decades (Zarfl *et al.*, 2015; Maavara *et al.*, 2017). Construction of new dams is concentrated in Asia, especially in China and India including Yantze, Ganges, and Brahmaputra rivers (Zarfl *et al.*, 2015). About 50,000 dams have been built on the Yangtze River Basin over the past 50 years, which has resulted in an 81% reduction of POC load compared to before dam building (Li *et al.*, 2015). The POC load also decreased with time in Xijiang River during 1954–2005 due to dams and reservoir constructions and reforestations, about 100 Gg-C yr^{-1} of POC had been reduced for 50 years in Xijiang River based on regression equation (Sun *et al.*, 2010). About 13% of riverine TOC load was reduced due to burial and mineralization in the reservoir by damming in the global scale in 2000, and TOC load was predicted to decrease by 19% in 2030 as the dam construction continued (Maavara *et al.*, 2017). The POC yield had a negative relationship with %TS, suggesting that the POC yield can decrease by trapped TS by dams and reservoirs within a watershed (Table 2). Thus, the POC yield in the Asian river basins could decrease over time if water quality management policy using dams and reservoirs continues.

5. Conclusions

Asia is the largest continent with a variety of climate zones, soil types, topography, and high population density, which includes 'hot spots' of global riverine carbon exports. New riverine carbon database of Asia was constructed based on 128 previous research, and 135 watersheds were delineated, which covers 70% of Asia. A total of 241 Tg-C yr^{-1} was released from the rivers in Asia. DIC, DOC, POC, and PIC accounted for 57%, 26%, 15%, and 2% of the total riverine carbon load, respectively. The DIC, DOC, POC, and PIC yields were -68–78 g-C m^{-2} yr^{-1}, -0.2–40 g-C m^{-2} yr^{-1}, -8.2–29 g-C m^{-2} yr^{-1}, and 0.1–8.0 g-C m^{-2} yr^{-1}. More than 30 Tg-C yr^{-1} was released by the three Arctic rivers (the Yenisei, the Lena, and the Ob' rivers) due to high discharge, which corresponds to 13% of the total carbon load estimates in the rivers in Asia. Up to 123.8 g-C m^{-2} yr^{-1} of high carbon yield was observed in the rivers of Southeast Asia. Natural factors such as water yield and slope were mainly correlated with carbon yields in Asia regardless of carbon species. The estimated POC load in Asia has decreased which might be caused by concentrated dam building. Although natural factors can dominantly influence riverine carbon yield, the load or yield of riverine carbon in the future may change by anthropogenic activities since Asia is still undergoing rapid environmental changes by economic development. Studies on long-term variation of riverine carbon in Asia can help us understand biogeochemical fates of riverine carbon due to rapid changes of the environment and climate.

Appendix

Table A1. Concentrations, loads, and yields of riverine DIC in Asia. The units are in parenthesis. The units of carbon loads are 10^{10} g-C yr^{-1}, and the units of carbon yields are g-C m^{-2} yr^{-1}.

River	Location	Q (km^3 yr^{-1})	[DIC] (mg L^{-1})	DIC Load	DIC yield	References
Ganges (Ganga)	Kali 1	1.6	21.9	3.4	9.9	1
Ganges (Ganga)	Kali 2	2.3	21.9	1.7	33.0	1
Ganges (Ganga)	Kali 3	2.4	22.2	0.2	60.2	1
Ganges (Ganga)	Kali 4	5.7	17.6	4.7	24.0	1
Ganges (Ganga)	Kali 5	16.0	21.0	22.0	51.0	1
Ganges (Ganga)	Seti	3.3	24.2	7.9	79.9	1
Ganges (Ganga)	Chepe	0.3	1.9	0.1	4.4	1
Ganges (Ganga)	Darondi	0.8	9.7	0.8	21.4	1
Ganges (Ganga)	Marsyandi	7.3	15.3	11.2	28.0	1
Ganges (Ganga)	Trisuli 1	5.7	9.5	5.4	11.7	1
Ganges	Trisuli 2	8.1	11.5	3.9	25.7	1

River	Location	Q (km^3 yr^{-1})	[DIC] (mg L^{-1})	DIC Load	DIC yield	References
(Ganga)						
Ganges (Ganga)	Andi kohla	1.1	14.1	1.5	61.7	1
Ganges (Ganga)	Narayani	50.5	19.3	34.5	35.9	1
Ganges (Ganga)	Chambal	30.0	31.6	94.9	5.5	2
Ganges (Ganga)	Ganga(before confluence with the Yamuna)	59.0	21.0	123.7	10.2	2
Ganges (Ganga)	Yamuna	93.0	26.2	120.1	4.8	2
Ganges (Ganga)	Ghaghara	94.0	21.3	201.8	17.1	2
Ganges (Ganga)	Son	32.0	18.1	57.7	6.6	2
Ganges (Ganga)	Ganga(after confluence with the Ghaghara, Son and Gandak)	364.0	23.6	164.4	7.9	2
Cauvery	6	8.0	25.4	20.3	10.1	3
Cauvery	7	9.2	26.6	4.1	1.7	3
Cauvery	8	9.6	28.5	2.8	1.8	3
Cauvery	9	11.5	29.9	7.2	4.3	3
Godavari	Pravara	1.4	25.7	3.6	5.1	4
Godavari	Purna	2.8	47.3	13.3	7.4	4
Godavari	Nanded	15.0	40.3	48.8	13.9	4
Godavari	Manjara	7.6	49.0	35.9	10.8	4

River	Location	Q (km^3 yr^{-1})	[DIC] (mg L^{-1})	DIC Load	DIC yield	References
Godavari	Basar	27.2	37.7	-4.9	-6.2	4
Godavari	Mancherial	23.0	45.3	15.3	13.0	4
Godavari	Manair	2.8	30.0	8.5	10.4	4
Godavari	Wardha	11.9	42.0	24.0	7.5	4
Godavari	Penganga	5.1	44.7	23.4	11.4	4
Godavari	Pranahita	36.8	30.7	35.0	4.9	4
Godavari	Indravati	32.9	10.0	24.4	5.4	4
Godavari	Sabari	13.6	8.7	12.5	5.4	4
Godavari	Bhadrachalam	95.3	31.0	-4.8	-2.1	4
Godavari	Rajahmundry	105.0	24.5	17.0	14.7	4
Heping		1.3	32.8	4.1	61.0	a
Houlung		0.9	34.9	3.2	48.2	a
Hsiukuluan		4.2	34.6	14.5	67.5	a
Hualien		3.8	33.5	12.7	71.8	a
Jian Jiang		4.5	6.4	2.9	9.4	a
Jiulong Jiang		7.9	7.9	6.3	3.8	a
Kaoping		8.5	34.7	29.3	65.4	a
Kelantan	Tanah Merah	12.1	5.2	3.2	2.3	5
Langat	Kajang	0.3	8.4	0.2	4.5	5, 6
Langat	Dengkil	1.3	6.6	0.7	9.6	6
Lian Jiang		2.2	10.6	2.3	2.6	a

River	Location	Q (km^3 yr^{-1})	[DIC] (mg L^{-1})	DIC Load	DIC yield	References
Marikina		3.2	29.5	9.4	25.5	a
Mekong		470.0	9.5	3.1	0.1	7
Mekong	Chiang Saen	80.0	21.2	158.5	6.4	8
Mekong	Pakse	310.0	16.4	285.2	7.2	8
Nethravati	Nethravati at Bantwala	9.8	2.7	0.1	14.3	9
Nethravati	Kumaradhara	4.9	2.5	1.2	6.6	9
Nethravati	Nethravati at Uppinangadi	4.9	2.6	1.3	7.2	9
PamPanga		4.5	42.3	18.9	17.3	a
Peinan		3.7	33.7	12.4	65.9	a
Qin Jiang		1.7	13.3	2.3	7.8	a
Taan		1.6	35.7	6.3	67.6	a
Tachia		2.6	29.3	7.8	52.4	a
Tanshui		7.4	24.8	18.5	70.4	a
Touchien		0.6	28.4	1.7	17.5	a
Wu		3.7	37.6	14.0	55.4	a
Yangtze	Tuotuo He	1.3	55.4	7.4	4.6	10
Yangtze	Chumaer He	0.2	38.0	0.9	1.0	10
Yangtze	Tongtian He	33.5	58.9	188.7	16.8	10
Yangtze	Mainstream of the Jinsha Jiang	39.4	37.4	-49.5	-22.5	10

River	Location	Q (km^3 yr^{-1})	[DIC] (mg L^{-1})	DIC Load	DIC yield	References
	(JSJ-7)					
Yangtze	Mainstream of the Jinsha Jiang (JSJ-9)	67.5	38.5	112.3	20.4	10
Yangtze	Mainstream of the Jinsha Jiang (JSJ-11a)	38.0	36.2	-122.4	-68.0	10
Yangtze	Mainstream of the Jinsha Jiang (JSJ-12)		37.4			10
Yangtze	Tributaries of the Jinsha Jiang (JSJ-14a)	34.5	35.3	121.8	9.4	10
Yangtze	Mainstream of the Jinsha Jiang (JSJ-13a)	143.6	36.2	261.0	50.2	10
Yangtze	Tributaries of the Jinsha Jiang (JSJ-16)	2.2	38.7	8.7	27.9	10
Yangtze	Mainstream of the Jinsha Jiang (JSJ-15)	150.4	41.4	103.1	27.9	10
Yangtze	Mainstream of the Jinsha Jiang (JSJ-17)	167.8	40.8	52.5	17.0	10
Yangtze	Minjiang	14.9	37.5	55.8	15.1	10
Yangtze	Daduhe	61.6	27.9	171.7	19.3	10

River	Location	Q (km^3 yr^{-1})	[DIC] (mg L^{-1})	DIC Load	DIC yield	References
Yangtze (Chang jiang)		960.0	21.5	1012.7	8.9	11, 12, 13
Yenisey	Tembenchi (f. Tembenchi)	10.3	2.6	2.5	1.0	14
Yenisey	Kochechum (Tura)	36.5	3.5	12.0	1.3	14
Yenisey	Nidym	3.3	6.8	2.1	1.5	14
Yenisey	Nizhnyaya Tunguska (Tura)	65.2	9.2	70.2	2.8	14
Yenisey	Podkamennaya Tunguska (Baikit)	30.0	9.3	27.8	1.8	14
Yenisey		608.0	10.8	485.4	0.6	15
Xijiang	Wuzhou Station	238.0	19.6	427.0	12.9	16
Xijiang		214.7	21.0	23.0	9.9	17
Anabar		4.7	4.3	1.0	0.4	18
Brahmani (Bhahmani)		16.3	10.6	17.3	6.1	19
Brahmaputra		510.0	11.5	586.1	10.1	15
Chao phraya		31.2	19.0	59.3	3.1	a
Geum		5.1	10.1	5.8	6.2	b
Han		22.0	11.4	24.0	11.0	b
Hong		78.5	48.6	381.2	24.2	a
Huanghe		15.0	41.7	105.0	1.4	20

River	Location	Q (km^3 yr^{-1})	[DIC] (mg L^{-1})	DIC Load	DIC yield	References
(Yellow)						
Indigirka		50.4	1.9	9.0	0.3	15
Indus		104.0	20.2	210.0	2.9	20
Kapuas		189.6	6.7	127.3	15.0	a
Kolyma		107.0	5.7	68.0	1.0	15
Lena		591.0	9.6	507.9	2.1	21
Mahanadi (Mahahadi)		54.4	13.0	70.7	8.0	19
Mahi		10.8	28.5	30.9	12.1	19
Nakdong		11.0	9.9	12.4	6.0	b
Ob’		414.5	8.2	357.0	1.2	15
Pearl		350.0	19.4	99.3	11.7	21, 22
Penner		5.2	22.8	11.8	2.4	19
Rajang		148.7	4.9	72.2	14.5	a
Sumjin		2.9	5.8	1.6	3.8	b
Tapti		12.6	34.1	33.1	6.7	19
Yana		31.5	3.3	9.0	0.4	15
Youngsan		2.2	9.1	2.4	11.0	b

a. data was provided by Dr. Chen-Tung Arthur Chen

b. data from Chapter two

Table A2. Concentrations, loads, and yields of riverine DOC in Asia. The units are in parenthesis. The units of carbon loads are 10^{10} g-C yr^{-1}, and the units of carbon yields are g-C m^{-2} yr^{-1}.

River	Location	Q (km^3 yr^{-1})	[DOC] (mg L^{-1})	DOC Load	DOC yield	References
Ayeyarwady	Seiktha	426.6	2.1	89.0	2.2	23
Heping		1.3	0.5	0.1	0.9	a
Houlung		0.9	0.9	3.2	0.3	a
Hsiukuluan		4.2	4.2	0.7	0.3	a
Hualien		3.8	0.8	0.3	1.7	a
Huanghe (Yellow)		15.0	15.0	3.3	-5.0	20
Huanghe	Toudaoguai	17.4	3.6	6.0	0.1	20
Huanghe	Tongguan	27.1	4.1	5.0	0.1	20
Jian Jiang		4.5	2.3	1.1	3.4	a
Jiulong Jiang		7.9	7.9	2.1	1.6	a
Kaoping		8.5	8.5	0.6	0.5	a
Kelantan	Tanah Merah	12.1	4.5	5.3	3.8	5
Langat	Kajang	0.3	3.9	0.1	2.1	5, 6
Langat	Dengkil	1.3	4.1	0.7	10.7	6
Lanyang Hsi		1.6	1.6	2.1	0.3	24

River	Location	Q (km^3 yr^{-1})	[DOC] (mg L^{-1})	DOC Load	DOC yield	References
Lian Jiang		2.2	1.9	0.4	0.5	a
PamPanga		4.5	4.5	5.8	2.6	a
Pearl delta	Yamen	13.0	2.1	3.0	4.4	25
Peinan		3.7	0.7	0.3	1.4	a
Qin Jiang		1.7	2.1	0.3	1.2	a
Salween	Hpa-an	211.0	1.1	23.0	0.8	23
Siak	S. Tapung Kanan	2.6	21.1	5.4	23.0	26
Siak	S. Tapung Kiri	2.8	7.2	2.1	8.3	26
Siak	Mandau	3.4	35.9	11.9	39.8	26
Taan		1.6	1.1	0.2	1.9	a
Tachia		2.6	1.2	0.3	2.0	a
Tanshui		7.4	2.8	2.1	8.1	a
Touchien		0.6	0.6	1.5	0.1	a
Wu		3.7	1.2	0.4	1.7	a
Yenisey	Tembenchi (f. Tembenchi)	10.3	9.8	8.6	4.7	14
Yenisey	Kochechum (Tura)	36.5	11.3	43.2	3.5	14
Yenisey	Nidym	3.3	12.6	4.2	2.8	14
Yenisey	Nizhnyaya Tunguska (Tura)	65.2	18.7	124.0	4.6	14

River	Location	Q (km^3 yr^{-1})	[DOC] (mg L^{-1})	DOC Load	DOC yield	References
Yenisey	Podkamennaya Tunguska (Baikit)	30.0	17.4	52.1	3.3	14
Yenisei		608.0	7.3	232.4	0.3	27
Xijiang		214.7	1.4	32.0	0.9	28
Amur		344.0	6.1	210.0	1.1	23
Brahmaputra		510.0	3.3	186.8	3.0	23, 29, 15
Chao Phraya		31.2	3.4	10.5	0.6	a
Dalinghe		1.4	2.9	0.4	0.2	29
Ganges		476.0	2.8	140.0	1.3	23
Geum		5.1	2.4	1.3	1.3	b
Godavari		95.9	1.4	13.4	0.4	29, 30
Han		22.0	1.5	3.2	1.5	b
Hong		78.5	1.3	10.6	0.7	a
Indigirka		50.4	6.4	32.3	0.9	29
Indus		104.0	25.7	267.0	2.9	31, 20
Kapuas		189.6	5.6	105.8	12.5	a
Kolyma		107.0	7.4	81.8	1.6	27
Lena		591.0	9.6	575.6	2.4	32, 27

River	Location	Q (km^3 yr^{-1})	[DOC] (mg L^{-1})	DOC Load	DOC yield	References
Mekong		470.0	4.7	219.8	2.8	7
Nakdong		11.0	2.7	2.9	1.4	b
Ob’		414.5	9.6	411.9	1.4	27
Olenek		31.5	10.2	32.3	1.6	33
Omoloy		1.1	2.8	0.3	0.0	33
Pearl		350.0	1.5	50.0	5.9	28
Pechora		131.0	12.3	166.0	5.1	34
Rajang		148.7	3.0	44.8	9.0	a
Sumjin		2.9	1.8	0.5	1.1	b
Tapti		12.6	6.5	10.0	1.5	29
Yana		31.5	2.9	9.0	0.4	35
Yangtze (Chang jiang)		960.0	2.2	184.9	1.0	12
Youngsan		2.2	3.2	0.7	3.2	b

a. data was provided by Dr. Chen-Tung Arthur Chen

b. data from Chapter two

Table A3. Concentrations, loads, and yields of riverine POC in Asia. The units are in parenthesis. The units of carbon loads are 10^{10} g-C yr^{-1}, and the units of carbon yields are g-C m^{-2} yr^{-1}.

River	Location	Q (km^3 yr^{-1})	[POC] (mg L^{-1})	POC Load	POC yield	References
Ayeyarwady	Seiktha	426.6	7.7	328.5	7.9	23
Godavari	Pravara	1.4	3.0	0.4	0.6	4
Godavari	Purna	2.8	0.9	0.3	0.1	4
Godavari	Nanded	15.0	0.8	0.5	0.2	4
Godavari	Manjara	7.6	0.4	0.3	0.1	4
Godavari	Basar	27.2	0.4	-0.4	-0.6	4
Godavari	Mancherial	23.0	0.3	-0.3	-0.3	4
Godavari	Manair	2.8	0.4	0.1	0.1	4
Godavari	Wardha	11.9	12.3	14.1	4.4	4
Godavari	Penganga	5.1	1.1	0.6	0.3	4
Godavari	Pranahita	36.8	16.8	47.3	6.6	4
Godavari	Indravati	32.9	9.0	29.7	6.5	4
Godavari	Sabari	13.6	3.6	4.9	2.1	4
Godavari	Bhadrachalam	95.3	7.7	-19.0	-8.2	4
Godavari	Rajahmundry	105.0	7.2	-2.9	-2.5	4, 31, 20
Heping		1.3	6.8	0.9	12.7	a
Houlung		0.9	1.6	0.1	2.2	a
Hsiukuluan		4.2	1.1	0.5	2.2	a
Hualien		3.8	2.2	0.8	4.7	a

River	Location	Q (km^3 yr^{-1})	[POC] (mg L^{-1})	POC Load	POC yield	References
Huanghe	Toudaoguai	17.4	9.7	16.0	0.2	20
Huanghe	Tongguan	27.1	18.4	43.0	0.8	20
Jian Jiang		4.5	2.0	0.9	3.0	a
Jiulong Jiang		7.9	1.3	1.0	0.6	a
Kaoping		8.5	2.8	2.4	5.3	a
Kelantan	Tanah Merah	12.1	3.5	4.2	3.1	5
Langat	Dengkil	1.3	5.5	0.7	5.9	6
Lanyang Hsi		1.6	11.1	1.8	22.2	24
Lian Jiang		2.2	3.8	0.8	0.9	a
PamPanga		4.5	4.1	1.8	1.7	a
Pearl Delta	Yamen	13.0	2.2	3.0	4.4	25
Peinan		3.7	8.2	3.0	16.1	a
Salween	Hpa-an	211.0	13.7	288.5	10.6	23
Taan		1.6	1.5	0.2	2.6	a
Tachia		2.6	1.9	0.5	3.4	a
Tanshui		7.4	10.2	7.6	29.0	a
Touchien		0.6	2.5	0.2	1.5	a
Wu		3.7	1.6	0.6	2.3	a
Yangtze	Wujiang	37.6	0.6	3.1	0.5	36
Yangtze	Yuanjiang (Wuyanghe)	3.6	0.5	0.1	0.1	36
Yangtze	Yuanjiang (Qingshuijiang)	11.1	0.3	0.4	0.2	36

River	Location	Q (km^3 yr^{-1})	[POC] (mg L^{-1})	POC Load	POC yield	References
Yangtze		960.0	2.9	184.4	1.1	12
Yenisei		608.0	0.5	29.5	0.0	37
Xijiang		214.7	2.7	58.3	1.7	17
Amur		344.0	4.1	140.0	0.8	23
Brahmaputra		510.0	2.6	130.0	2.2	23
Chao Phraya		31.2	3.1	9.6	0.5	a
Ganges		476.0	3.5	170.0	1.6	23
Geum		5.1	1.1	0.6	0.7	b
Han		22.0	0.6	1.0	0.4	b
Huanghe (Yellow)		15.0	15.5	47.4	0.6	20, 38
Indigirka		50.4	3.4	17.4	0.6	35
Indus		104.0	15.8	164.0	1.8	31, 20
Kapuas		189.6	4.7	88.8	10.5	a
Kolyma		107.0	0.7	7.4	0.1	37
Lena		591.0	1.5	80.2	0.3	37
Mekong		470.0	5.7	266.6	3.4	7
Nakdong		11.0	1.9	1.3	0.6	b
Ob’		414.5	1.5	58.9	0.2	37

River	Location	Q (km^3 yr^{-1})	[POC] (mg L^{-1})	POC Load	POC yield	References
Olenek		31.5	0.8	2.6	0.1	33
Omoloy		1.1	0.3	0.1	0.0	33
Pearl		350.0	1.5	-4.3	-0.5	25
Pechora		131.0	0.3	4.0	0.1	34
Sumjin		2.9	0.7	0.2	0.4	b
Yana		31.5	1.6	5.0	2.2	35
Youngsan		2.2	1.6	0.4	1.8	b

a. data was provided by Dr. Chen-Tung Arthur Chen

b. data from Chapter two

Table A4. Concentrations, loads, and yields of riverine PIC in Asia. The units are in parenthesis. The units of carbon loads are 10^{10} g-C yr^{-1}, and the units of carbon yields are g-C m^{-2} yr^{-1}.

River	Location	Q (km^3 yr^{-1})	[PIC] (mg L^{-1})	PIC Load	PIC yield	References
Heping		1.3	4.3	0.5	8.0	a
Houlung		0.9	0.3	0.0	0.5	a
Hsiukuluan		4.2	0.2	0.1	0.3	a
Hualien		3.8	0.6	0.2	1.2	a
Jian Jiang		4.5	1.4	0.6	2.0	a
Jiulong Jiang		7.9	0.3	0.3	0.2	a
Kaoping		8.5	0.7	0.6	1.3	a
Lian Jiang		2.2	0.5	0.1	0.1	a
PamPanga		4.5	0.3	0.2	0.1	a
Peinan		3.7	1.6	0.6	3.1	a
Sarawak		7.9	0.2	0.1	5.5	a
Taan		1.6	0.2	0.03	0.3	a
Tachia		2.6	0.3	0.1	0.5	a
Tanshui		7.4	0.1	0.1	0.4	a
Touchien		0.6	0.2	0.03	0.1	a
Wu		3.7	0.1	0.0	0.1	a
Chao Phraya		31.2	0.7	2.1	0.1	a

River	Location	Q (km^3 yr^{-1})	[PIC] (mg L^{-1})	PIC Load	PIC yield	References
Huanghe (Yellow)		15.0	113.3	151.0	2.0	39
Kapuas		189.6	0.2	4.1	0.5	a
Pearl		350.0	0.8	28.5	0.6	40
Rajang		148.7	0.4	5.9	1.2	a
Yangtze (Chang jiang)		960.0	0.4	30.6	0.2	39

a. data was provided by Dr. Chen-Tung Arthur Chen

b. data from Chapter two

References of Appedix Tables and Figures

1. France-Lanord, C., Evans, M., Hurtrez, J.-E., Riotte, J., 2003. Annual dissolved fluxes from Central Nepal rivers: budget of chemical erosion in the Himalayas. *Comptes Rendus Geoscience* 335, 1131-1140.
2. Sarin, M.M., Krishnaswami, S., 1984. Major ion chemistry of the Ganga–Brahmaputra river systems, India. *Nature* 312, 538-541.
3. Ramanathan, A.L., Vaithiyanathan, P., Subramanian, V., Das, B.K., 1994. Nature and transport of solute load in the cauvery river basin, India. *Water Research* 28, 1585-1593.
4. Balakrishna, K., Probst, J.L., 2005. Organic carbon transport and C/N ratio variations in a large tropical river: Godavari as a case study, India. *Biogeochemistry* 73, 457-473.
5. Lee, K., 2014. Carbon Cycling in Tropical Rivers: A Carbon Isotope Reconnaissance Study of the Langat and Kelantan Basins, Malaysia. ProQuest Dissertations Publishing.
6. Lee, K.Y., Syakir, M.I., Clark, I.D., Veizer, J., 2013. Isotope Constraints on the Aquatic Carbon Budget: Langat Watershed, Malaysia. *Aquatic Geochemistry* 19, 443-475.
7. Li, S., Lu, X.X., Bush, R.T., 2013. CO2 partial pressure and CO2 emission in the Lower Mekong River. *Journal of Hydrology* 504, 40-56.

8. Li, S., Lu, X.X., Bush, R.T., 2014. Chemical weathering and CO2 consumption in the Lower Mekong River. *Science of The Total Environment* 472, 162-177.
9. Gurumurthy, G.P., Balakrishna, K., Riotte, J., Braun, J.-J., Audry, S., Shankar, H.N.U., Manjunatha, B.R., 2012. Controls on intense silicate weathering in a tropical river, southwestern India. *Chemical Geology* 300-301, 61-69.
10. Wu, W., Yang, J., Xu, S., Yin, H., 2008. Geochemistry of the headwaters of the Yangtze River, Tongtian He and Jinsha Jiang: Silicate weathering and CO2 consumption. *Applied Geochemistry* 23, 3712-3727.
11. Prokushkin, A.S., Pokrovsky, O.S., Shirokova, L.S., Korets, M.A., Viers, J., Prokushkin, S.G., Amon, R.M.W., Guggenberger, G., McDowell, W.H., 2011. Sources and the flux pattern of dissolved carbon in rivers of the Yenisey basin draining the Central Siberian Plateau. *Environmental Research Letters* 6.
12. Degens, E., Kempe, S., Richey, J.E., 1991. Biogeochemistry of major world rivers. SCOPE 42. Scientific Committee on Problems of the Environment (SCOPE), p. 356.
13. Gao, Q.Z., Wang, Z.G., 2015. Dissolved inorganic carbon in the Xijiang River: concentration and stable isotopic composition. *Environ Earth Sci* 73, 253-266.
14. Sun, H.G., Han, J., Lu, X.X., Zhang, S.R., Li, D., 2010. An assessment of the riverine carbon flux of the Xijiang River during the past 50 years.

Quaternary International 226, 38-43.

15. Huh, Y., Edmond, J.M., 1999. The fluvial geochemistry of the rivers of Eastern Siberia: III. Tributaries of the Lena and Anabar draining the basement terrain of the Siberian Craton and the Trans-Baikal Highlands. *Geochimica Et Cosmochimica Acta* 63, 967-987.
16. Ramesh, R., Subramanian, V., 1993. Geochemical characteristics of the major tropical rivers of India. *Hydrology of warm humid regions*. Proc. international symposium, Yokohama 1993, 157-164.
17. Ran, L.S., Lu, X.X., Sun, H.G., Han, J.T., Li, R.H., Zhang, J.M., 2013. Spatial and seasonal variability of organic carbon transport in the Yellow River, China. *Journal of Hydrology* 498, 76-88.
18. Li, S.Y., Lu, X.X., He, M., Zhou, Y., Bei, R.T., Li, L., Ziegler, A.D., 2011. Major element chemistry in the upper Yangtze River: A case study of the Longchuanjiang River. *Geomorphology* 129, 29-42.
19. Zhang, S.R., Lu, X.X., Higgitt, D.L., Chen, C.T.A., Sun, H.G., Han, J.T., 2007. Water chemistry of the Zhujiang (Pearl River): Natural processes and anthropogenic influences. Journal of *Geophysical Research-Earth Surface* 112.
20. Zhang, L., Xue, M., Wang, M., Cai, W.-J., Wang, L., Yu, Z., 2014. The spatiotemporal distribution of dissolved inorganic and organic carbon in the main stem of the Changjiang (Yangtze) River and the effect of the Three Gorges Reservoir. *Journal of Geophysical Research: Biogeosciences* 119,

741-757.

21. Chen, J.S., Wang, F.Y., Xia, X.H., Zhang, L.T., 2002. Major element chemistry of the Changjiang (Yangtze River). *Chemical Geology* 187, 231-255.
22. Wang, F.S., Wang, Y.C., Zhang, J., Xu, H., Wei, X.G., 2007. Human impact on the historical change of CO2 degassing flux in River Changjiang. *Geochemical Transactions* 8.
23. Bird, M.I., Robinson, R.A.J., Oo, N.W., Aye, M.M., Lu, X.X., Higgitt, D.L., Swe, A., Tun, T., Win, S.L., Aye, K.S., Win, K.M.M., Hoey, T.B., 2008. A preliminary estimate of organic carbon transport by the Ayeyarwady (Irrawaddy) and Thanlwin (Salween) Rivers of Myanmar. *Quaternary International* 186, 113-122.
24. Kao, S.J., Liu, K.K., 1997. Fluxes of dissolved and nonfossil particulate organic carbon from an Oceania small river (Lanyang Hsi) in Taiwan. *Biogeochemistry* 39, 255-269.
25. Ni, H.G., Lu, F.H., Luo, X.L., Tian, H.Y., Zeng, E.Y., 2008. Riverine inputs of total organic carbon and suspended particulate matter from the Pearl River Delta to the coastal ocean off South China. *Marine Pollution Bulletin* 56, 1150-1157.
26. Baum, A., Rixen, T., Samiaji, J., 2007. Relevance of peat draining rivers in central Sumatra for the riverine input of dissolved organic carbon into the ocean. Estuarine, *Coastal and Shelf Science* 73, 563-570.

27. Holmes, R.M., McClelland, J.W., Peterson, B.J., Tank, S.E., Bulygina, E., Eglinton, T.I., Gordeev, V.V., Gurtovaya, T.Y., Raymond, P.A., Repeta, D.J., Staples, R., Striegl, R.G., Zhulidov, A.V., Zimov, S.A., 2012. Seasonal and Annual Fluxes of Nutrients and Organic Matter from Large Rivers to the Arctic Ocean and Surrounding Seas. *Estuaries and Coasts* 35, 369-382.

28. Shi, G.H., Peng, C.H., Wang, M., Shi, S.W., Yang, Y.Z., Chu, J.Y., Zhang, J.J., Lin, G.H., Shen, Y., Zhu, Q.A., 2016. The Spatial and Temporal Distribution of Dissolved Organic Carbon Exported from Three Chinese Rivers to the China Sea. *Plos One* 11.

29. Dai, M., Yin, Z., Meng, F., Liu, Q., Cai, W.-J., 2012. Spatial distribution of riverine DOC inputs to the ocean: an updated global synthesis. *Current Opinion in Environmental Sustainability* 4, 170-178.

30. Sarin, M.M., Sudheer, A.K., Balakrishna, K., 2002. Significance of riverine carbon transport: A case study of a large tropical river, Godavari (India). *Science in China Series C-Life Sciences* 45, 97-108.

31. Zhang, S., Lu, X.X., Sun, H.Q., Han, J.T., Higgitt, D.L., 2009. Geochemical characteristics and fluxes of organic carbon in a human-disturbed mountainous river (the Luodingjiang River) of the Zhujiang (Pearl River), China. *Science of the Total Environment* 407, 815-825.

32. Raymond, P.A., McClelland, J., Holmes, R., Zhulidov, A., Mull, K., Peterson, B., Striegl, R., Aiken, G., Gurtovaya, T., 2007. Flux and age of dissolved organic carbon exported to the Arctic Ocean: A carbon isotopic study of the

five largest arctic rivers. *Global Biogeochemical Cycles* 21.

33. Lobbes, J.M., Fitznar, H.P., Kattner, G., 2000. Biogeochemical characteristics of dissolved and particulate organic matter in Russian rivers entering the Arctic Ocean. *Geochimica Et Cosmochimica Acta* 64, 2973-2983.
34. Gordeev, V.V., Kravchishina, M.D., 2009. River flux of dissolved organic carbon (DOC) and particulate organic carbon (POC) to the Arctic Ocean: what are the consequences of the global changes? *Influence ofClimate Change on the Changing Arctic and Sub-Arctic Conditions*,edited by J. C. J. Nihoul, and A. G. Kostianoy, pp. 145–160, Springer,Dordrecht.
35. Dittmar, T., Kattner, G., 2003. The biogeochemistry of the river and shelf ecosystem of the Arctic Ocean: a review. *Marine Chemistry* 83, 103-120.
36. Tao, F.X., Liu, C.Q., Li, S.L., 2009. Source and flux of POC in two subtropical karstic tributaries with contrasting land use practice in the Yangtze River Basin. *Applied Geochemistry* 24, 2102-2112.
37. Alvarez-Cobelas, M., Angeler, D., Sánchez-Carrillo, S., Almendros, G., 2012. A worldwide view of organic carbon export from catchments. *Biogeochemistry* 107, 275-293.
38. Hu, B., Li, J., Bi, N., Wang, H., Wei, H., Zhao, J., Xie, L., Zou, L., Cui, R., Li, S., Liu, M., Li, G., 2015. Effect of human-controlled hydrological regime on the source, transport, and flux of particulate organic carbon from the lower Huanghe (Yellow River). *Earth Surface Processes and Landforms* 40,

1029-1042.

39. Wang, X., Ma, H., Li, R., Song, Z., Wu, J., 2012. Seasonal fluxes and source variation of organic carbon transported by two major Chinese Rivers: The Yellow River and Changjiang (Yangtze) River. *Global Biogeochemical Cycles* 26, GB2025.
40. Wang, Q.F., Zheng, H., Zhu, X.J., Yu, G.R., 2015. Primary estimation of Chinese terrestrial carbon sequestration during 2001-2010. *Science Bulletin* 60, 577-590.

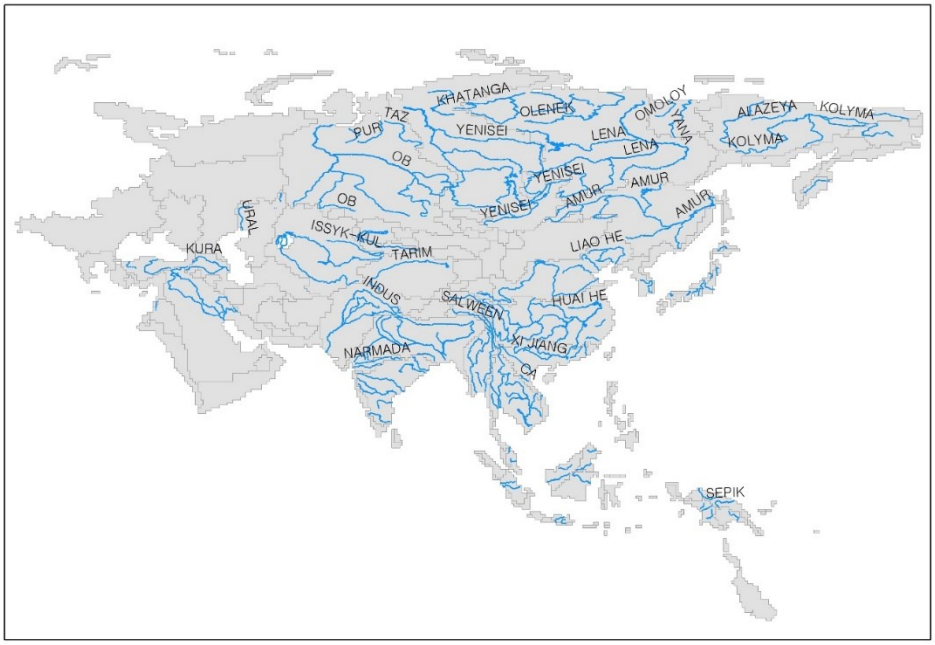

Figure A1. Spatial definition of Asia in this study based on COSCATs watersheds (data from Meybeck *et al.*, 2006). The grey line is the boundary of each COSCAT watershed.

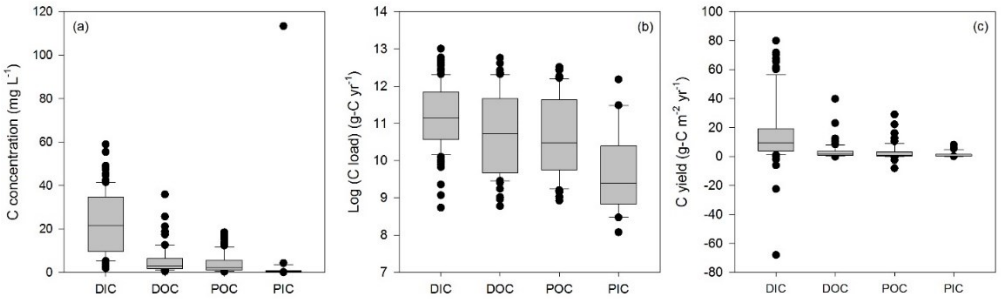

Figure A2. Box plots of (a) concentrations, (b) loads, and (c) yields of riverine carbon in Asia. The number of data are 110 for DIC, 63 for DOC, 65 for POC, and 22 for PIC.

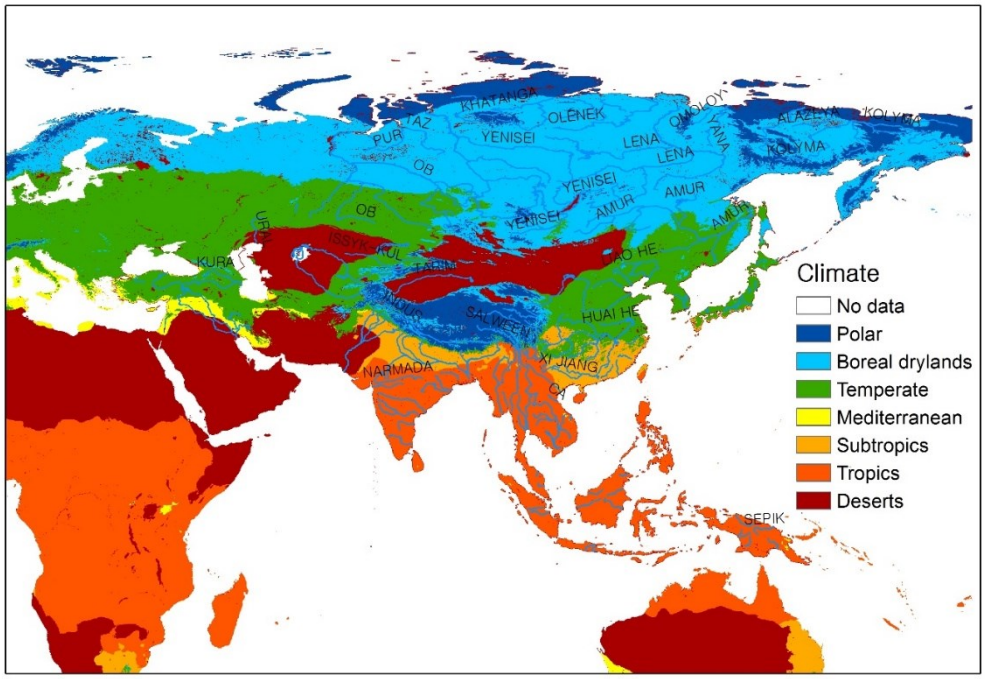

Figure A3. Areas under polar to tropical climates in Asia. Climates map was downloaded from Land Degradation Assessment in Dryland (LADA) project Version 1.1 (http://www.fao.org/land-water/land/land-assessment/assessment-and-monitoring-impacts/en/).

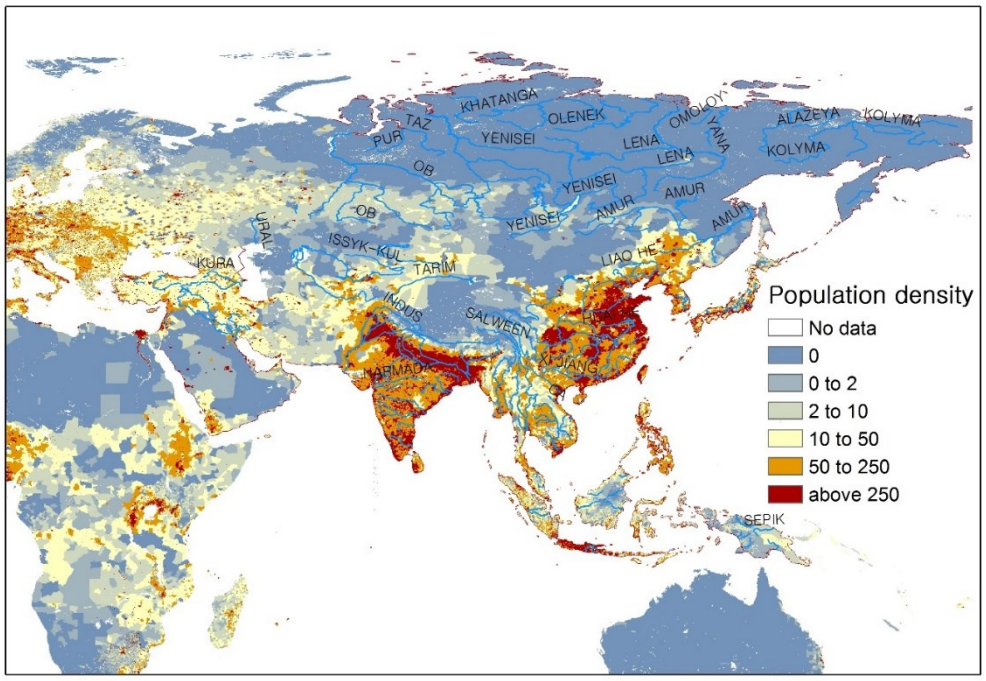

Figure A4. Population density of Asia (unit: persons km^{-2}). Population density map was downloaded from Land Degradation Assessment in Dryland (LADA) project Version 1.1 (http://www.fao.org/land-water/land/land-assessment/assessment-and-monitoring-impacts/en/).

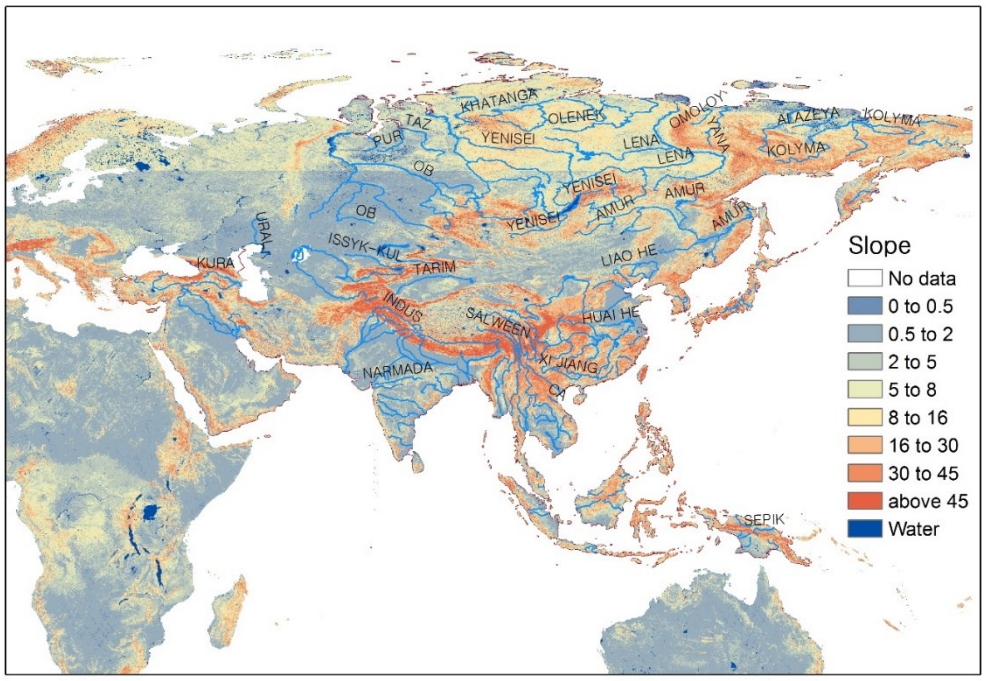

Figure A5. Slope of Asia (unit: degree). Slope map was downloaded from Land Degradation Assessment in Dryland (LADA) project Version 1.1 (http://www.fao.org/land-water/land/land-assessment/assessment-and-monitoring-impacts/en/).

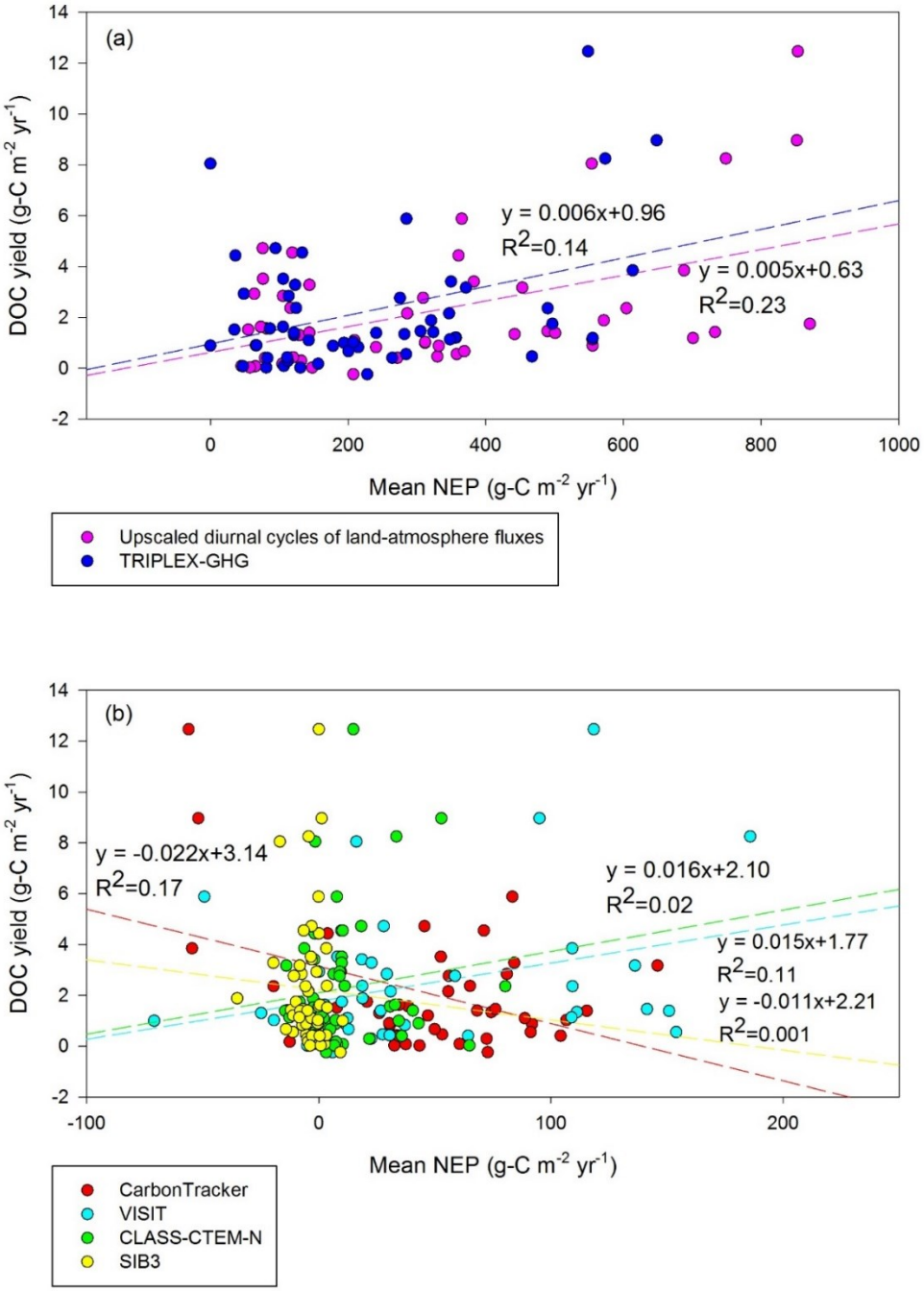

Figure A6. Relationships between the DOC yield and NEP of (a) upscaled diurnal cycles of land-atmosphere fluxes and TRIPLEX-GHG, and (b) Carbon Tracker, VISIT, CLASS-DTEM-N, and SIB3 models of the watershed in Asia.

CHAPTER FIVE

Conclusions

A multiscale approach was applied to watersheds in Asia to analyze the loads and biogeochemical properties of stream and riverine carbon that were influenced by several natural and anthropogenic factors within the watersheds. Hydrological factors such as precipitation (PPT) and discharge (Q) dominantly affected the loads and characteristics of stream and riverine carbon regardless of the carbon species and the size of the watersheds. The DIC was the dominant component in a forest headwater stream of South Korea. Stream [DIC] slightly decreased during storms because of dilution effect, but, the DIC load increased due to increase of Q. The [DOC] and [POC] reached up to 3.8 and 19.1 mg L^{-1} during storms, while the annual mean [DOC] and [POC] of weekly collected samples were 0.9 and 0.4 mg L^{-1}, respectively. The $\Delta^{14}C_{DOC}$ of stream increased during summer monsoon, and reached 45.5‰ at peak of storm indicating inputs of relatively fresh organic materials from vegetation and surface soils.

The DIC was also the main component of carbon in the five largest rivers in South Korea. Loads and yields of riverine carbon in summer accounted for 33–50%

of annual carbon loads in all rivers due to high PPT and Q. The riverine $\Delta^{14}C$ was enriched in summer than the other seasons regardless of carbon species. The $\Delta^{14}C_{DIC}$, $\Delta^{14}C_{DOC}$, and $\Delta^{14}C_{POC}$ decreased down to -88.7, -124.3, and -125.5‰ in the other seasons, respectively, which might be due to anthropogenic impacts such as wastewater treatment plant (WWTP) effluent in urban area and agricultural petrochemical usage in agricultural area in South Korea.

A total of 241 Tg-C was estimated to be released from the rivers in Asia, with DIC accounting for 57%, DOC 26%, POC 15%, and PIC 2% based on the river data collected from 128 studies in Asia. Total carbon loads estimates in the Asian rivers in this study were similar to those of other previous studies (232–380 Tg-C), however; there was a difference in the proportion of loads of each carbon species to total carbon loads. The proportion of DIC loads to total carbon loads is estimated to be 8–19% higher and the proportion of POC loads is estimated to be 11–19% lower compared to those of other studies. The riverine carbon loads were significantly correlated with natural (geomorphological, geological, and meteorological) characteristics in the watersheds such as slopes, rock types, and the distribution of climate zones than anthropogenic factors such as population density, and proportions of agricultural and urban areas.

This study can still be improved with more data on carbon loads and isotopes of rivers. For example, the carbon isotopes of each source such as WWTP effluent and soil organic matter was not included in Chapter three, and the

concentrations and properties of riverine carbon were measured seasonally in Chapter three and many previous studies in Chapter four.

Despite these limitations, the results can be used to predict changes in loads and biogeochemical characteristics of streams and riverine carbon in Asia due to climate change or environmental changes such as urbanization and cropland expansion. Changes in the amount and quality of carbon in the streams and rivers can affect the carbon cycle in the aquatic ecosystem, as well as changes of the metabolism of aquatic organisms in coastal and marine ecosystems. Thus, future studies on biogeochemical fate of carbon in the rivers, estuaries, and the oceans are needed to understand the alteration of global carbon cycle due to climate change and human activities.

References

Aiken, G.R., Spencer, R.G.M., Striegl, R.G., Schuster, P.F., Raymond, P.A., 2014. Influences of glacier melt and permafrost thaw on the age of dissolved organic carbon in the Yukon River basin. *Global Biogeochemical Cycles* 28, 525-537.

Aitkenhead, J., McDowell, W., 2000. Soil C: N ratio as a predictor of annual riverine DOC flux at local and global scales. *Global Biogeochemical Cycles* 14, 127-138.

Alam, M.J., Nagao, S., Aramaki, T., Shibata, Y., Yoneda, M., 2007. Transport of particulate organic matter in the Ishikari River, Japan during spring and summer. *Nuclear Instruments and Methods in Physics Research Section B: Beam Interactions with Materials and Atoms* 259, 513-517.

Aldrian, E., Chen, C.-T.A., Adi, S., Prihartanto, Sudiana, N., Nugroho, S.P., 2008. Spatial and seasonal dynamics of riverine carbon fluxes of the Brantas catchment in East Java. *Journal of Geophysical Research: Biogeosciences* 113

Alvarez-Cobelas, M., Angeler, D., Sánchez-Carrillo, S., Almendros, G., 2012. A worldwide view of organic carbon export from catchments. *Biogeochemistry* 107, 275-293.

Amiotte Suchet, P., Probst, J.-L., Ludwig, W., 2003. Worldwide distribution of continental rock lithology: Implications for the atmospheric/soil CO2 uptake by continental weathering and alkalinity river transport to the oceans. *Global Biogeochemical Cycles* 17.

Aufdenkampe, A.K., Mayorga, E., Raymond, P.A., Melack, J.M., Doney, S.C., Alin, S.R., Aalto, R.E., Yoo, K., 2011. Riverine coupling of biogeochemical cycles between land, oceans, and atmosphere. *Frontiers in Ecology and the Environment* 9, 53-60.

Baker, A., 2001. Fluorescence excitation-emission matrix characterization of some

sewage-impacted rivers. *Environmental Science & Technology* 35, 948-953.

Balakrishna, K., Probst, J.L., 2005. Organic carbon transport and C/N ratio variations in a large tropical river: Godavari as a case study, India. *Biogeochemistry* 73, 457-473.

Barnes, R.T., Butman, D.E., Wilson, H.F., Raymond, P.A., 2018. Riverine export of aged carbon driven by flow path depth and residence time. *Environmental Science & Technology* 52, 1028-1035.

Barnes, R.T., Raymond, P.A., 2009. The contribution of agricultural and urban activities to inorganic carbon fluxes within temperate watersheds. *Chemical Geology* 266, 318-327.

Battin, T.J., Luyssaert, S., Kaplan, L.A., Aufdenkampe, A.K., Richter, A., Tranvik, L.J., 2009. The boundless carbon cycle. *Nature Geoscience* 2, 598.

Baum, A., Rixen, T., Samiaji, J., 2007. Relevance of peat draining rivers in central Sumatra for the riverine input of dissolved organic carbon into the ocean. Estuarine, *Coastal and Shelf Science* 73, 563-570.

Bird, M.I., Robinson, R.A.J., Oo, N.W., Aye, M.M., Lu, X.X., Higgitt, D.L., Swe, A., Tun, T., Win, S.L., Aye, K.S., Win, K.M.M., Hoey, T.B., 2008. A preliminary estimate of organic carbon transport by the Ayeyarwady (Irrawaddy) and Thanlwin (Salween) Rivers of Myanmar. *Quaternary International* 186, 113-122.

Birgand, F., Appelboom, T.W., Chescheir, G.M., Skaggs, R.W., 2011. Estimating Nitrogen, Phosphorus, and Carbon Fluxes in Forested And Mixed-use Watersheds of the Lower Coastal Plain of North Carolina: Uncertainties Associated with Infrequent Sampling. *Transactions of the Asabe* 54, 2099-2110.

Bodesheim, P., Jung, M., Gans, F., Mahecha, M.D., Reichstein, M., 2018. Upscaled diurnal cycles of land-atmosphere fluxes: a new global half-hourly data product.

Earth System Science Data 10, 1327-1365.

Butman, D., Raymond, P.A., Butler, K., Aiken, G., 2012. Relationships between $\Delta^{14}C$ and the molecular quality of dissolved organic carbon in rivers draining to the coast from the conterminous United States. *Global Biogeochemical Cycles* 26, GB4014.

Butman, D.E., Wilson, H.F., Barnes, R.T., Xenopoulos, M.A., Raymond, P.A., 2015. Increased mobilization of aged carbon to rivers by human disturbance. *Nature Geoscience* 8, 112-116.

Cai, W.-J., 2011. Estuarine and coastal ocean carbon paradox: CO2 sinks or sites of terrestrial carbon incineration? *Annual Review of Marine Science* 3, 123-145.

Cho, Y., Driscoll, C.T., Blum, J.D., 2009. The effects of a whole-watershed calcium addition on the chemistry of stream storm events at the Hubbard Brook Experimental Forest in NH, USA. *Science of The Total Environment* 407, 5392-5401.

Cho, Y., Driscoll, C.T., Johnson, C.E., Blum, J.D., Fahey, T.J., 2012. Watershed-Level Responses to Calcium Silicate Treatment in a Northern Hardwood Forest. *Ecosystems* 15, 416-434.

Cho, Y., Driscoll, C.T., Johnson, C.E., Siccama, T.G., 2010. Chemical changes in soil and soil solution after calcium silicate addition to a northern hardwood forest. *Biogeochemistry* 100, 3-20.

Cho, Y.-B., Oh, Y.-K., Shin, D.-C., Park, C.-H., 2014. Distribution of total organic carbon and correlations between organic matters of sewage treatment plants. *Journal of the Korean Society for Environmental Analysis* 17, 207-214 (in Korean with English abstract).

Choi, H., 2001. Developing a rainfall-runoff model for forest watersheds using distributed hydrological concept of TOPMODEL. Seoul National University, pp. 1-199.

Chough, S.K., Kwon, S.T., Ree, J.H., Choi, D.K., 2000. Tectonic and sedimentary evolution of the Korean peninsula: a review and new view. *Earth-Science Reviews* 52, 175-235.

Chow, A.T., Gao, S., Dahlgren, R.A., 2005. Physical and chemical fractionation of dissolved organic matter and trihalomethane precursors: A review. *Journal of Water Supply: Research and Technology-AQUA* 54, 475-507.

Combalicer, E., H. Lee, S., Ahn, S., Kim, D., Im, S., 2008. Comparing groundwater recharge and base flow in the Bukmoongol small-forested watershed, Korea.

Cole, J.J., Prairie, Y.T., Caraco, N.F., McDowell, W.H., Tranvik, L.J., Striegl, R.G., Duarte, C.M., Kortelainen, P., Downing, J.A., Middelburg, J.J., 2007. Plumbing the global carbon cycle: integrating inland waters into the terrestrial carbon budget. *Ecosystems* 10, 172-185.

Dai, M., Yin, Z., Meng, F., Liu, Q., Cai, W.-J., 2012. Spatial distribution of riverine DOC inputs to the ocean: an updated global synthesis. *Current Opinion in Environmental Sustainability* 4, 170-178.

Deb, S., Shukla, M., 2011. A Review of Dissolved Organic Matter Transport Processes Affecting Soil and Environmental Quality. *Journal of Environmental & Analytical Toxicology* 1, p106

Degens, E., Kempe, S., Richey, J.E., 1991. Biogeochemistry of major world rivers. SCOPE 42. Scientific Committee on Problems of the Environment (SCOPE), p. 356.

Dhillon, G.S., Inamdar, S., 2013. Extreme storms and changes in particulate and dissolved organic carbon in runoff: Entering uncharted waters? *Geophysical Research Letters* 40, 1322-1327.

Dhillon, G.S., Inamdar, S., 2014. Storm event patterns of particulate organic carbon (POC) for large storms and differences with dissolved organic carbon (DOC).

Biogeochemistry 118, 61-81.

Downing, J.A., Cole, J.J., Duarte, C.M., Middelburg, J.J., Melack, J.M., Prairie, Y.T., Kortelainen, P., Striegl, R.G., McDowell, W.H., Tranvik, L.J., 2012. Global abundance and size distribution of streams and rivers. *Inland Waters* 2, 229-236.

Druffel, E.R., Williams, P.M., Bauer, J.E., Ertel, J.R., 1992. Cycling of dissolved and particulate organic matter in the open ocean. *Journal of Geophysical Research: Oceans* 97, 15639-15659.

Fellman, J.B., D'Amore, D.V., Hood, E., 2008. An evaluation of freezing as a preservation technique for analyzing dissolved organic C, N and P in surface water samples. *Science of The Total Environment* 392, 305-312.

Gaillardet, J., Dupré, B., Louvat, P., Allègre, C.J., 1999. Global silicate weathering and CO_2 consumption rates deduced from the chemistry of large rivers. *Chemical Geology* 159, 3-30.

Galy, A., France-Lanord, C., 1999. Weathering processes in the Ganges–Brahmaputra basin and the riverine alkalinity budget. *Chemical Geology* 159, 31-60.

Gordeev, V.V., Sidorov, I.S., 1993. Concentrations of major elements and their outflow into the Laptev Sea by the Lena River. *Marine Chemistry* 43, 33-45.

Griffith, D.R., Barnes, R.T., Raymond, P.A., 2009. Inputs of fossil carbon from wastewater treatment plants to U.S. rivers and oceans. *Environmental Science & Technology* 43, 5647-5651.

Gupta, L.P., Subramanian, V., Ittekkot, V., 1997. Biogeochemistry of particulate organic matter transported by the Godavari River, India. *Biogeochemistry* 38, 103-128.

Harrison, J.A., Caraco, N., Seitzinger, S.P., 2005. Global patterns and sources of dissolved organic matter export to the coastal zone: Results from a spatially explicit,

global model. *Global Biogeochemical Cycles* 19.

Hedges, J.I., Stern, J.H., 1984. Carbon and nitrogen determinations of carbonate-containing solids1. *Limnology and Oceanography* 29, 657-663.

Hong, S., Minasny, B., Zhang, Y., Kim, Y., Jung, K., 2010. Digital soil mapping using legacy soil data in Korea. 19th World Congress of Soil Science, *Soil Solutions for a Changing World*, pp. 1-6.

Hood, E., Gooseff, M.N., Johnson, S.L., 2006. Changes in the character of stream water dissolved organic carbon during flushing in three small watersheds, Oregon. *Journal of Geophysical Research: Biogeosciences* 111, n/a-n/a.

Hood, E., Edwards, R.T., D'Amore, D.V., 2009. Changes in the concentration, biodegradability, and fluorescent properties of dissolved organic matter during stormflows in coastal temperate watersheds. *Journal of Geophysical Research: Biogeosciences* 114, G01021.

Hope, D., Billett, M.F., Cresser, M.S., 1994. A review of the export of carbon in river water: Fluxes and processes. *Environmental Pollutio*n 84, 301-324.

Horton, R.E., Murphy, E.C., 1906. Weir experiments, coefficients, and formulas, *Water Supply and Irrigation Paper* 200. U.S. Department of Interior, Government Printing Office, Washington,D.C.

Hossler, K., Bauer, J.E., 2013. Amounts, isotopic character, and ages of organic and inorganic carbon exported from rivers to ocean margins: 2. Assessment of natural and anthropogenic controls. *Global Biogeochemical Cycles* 27, 347-362.

Hu, B., Li, J., Bi, N., Wang, H., Wei, H., Zhao, J., Xie, L., Zou, L., Cui, R., Li, S., Liu, M., Li, G., 2015. Effect of human-controlled hydrological regime on the source, transport, and flux of particulate organic carbon from the lower Huanghe (Yellow River). *Earth Surface Processes and Landforms* 40, 1029-1042

Huang, T.-H., Fu, Y.-H., Pan, P.-Y., Chen, C.-T.A., 2012. Fluvial carbon fluxes in tropical rivers. *Current Opinion in Environmental Sustainability* 4, 162-169.

Hur, J., Nguyen, H.V.-M., Lee, B.-M., 2014. Influence of upstream land use on dissolved organic matter and trihalomethane formation potential in watersheds for two different seasons. Environmental *Science and Pollution Research* 21, 7489-7500.

Inamdar, S., Finger, N., Singh, S., Mitchell, M., Levia, D., Bais, H., Scott, D., McHale, P., 2012. Dissolved organic matter (DOM) concentration and quality in a forested mid-Atlantic watershed, USA. *Biogeochemistry* 108, 55-76.

Ishikawa, N.F., Tayasu, I., Yamane, M., Yokoyama, Y., Sakai, S., Ohkouchi, N., 2016. Sources of Dissolved Inorganic Carbon in Two Small Streams with Different Bedrock Geology: Insights from Carbon Isotopes. *Radiocarbon* 57, 439-448.

Jaffé, R., Boyer, J.N., Lu, X., Maie, N., Yang, C., Scully, N.M., Mock, S., 2004. Source characterization of dissolved organic matter in a subtropical mangrove-dominated estuary by fluorescence analysis. *Marine Chemistry* 84, 195-210.

Jarvie, H.P., King, S.M., Neal, C., 2017. Inorganic carbon dominates total dissolved carbon concentrations and fluxes in British rivers: Application of the THINCARB model – Thermodynamic modelling of inorganic carbon in freshwaters. *Science of The Total Environment* 575, 496-512.

Jeong, D.-H., Cho, Y., Ahn, K., Chung, H.-M., Park, H., Shin, H., Hur, J., Han, D., 2016. A study on the determination method of TOC effluent limitation for public sewage treatment plants. *Journal of Korean Society of Water and Wastewater* 30, 241-251 (in Korean with English abstract).

Jeong, J.H., Kim, C., Goo, K.S., Lee, C.H., Won, H.K., Byun, J.G., 2003. Physico-chemical properties of Korean forest soils by parent rocks. *Journal of Korean Forest Society* 92, 254-262 (in Korean).

Jeong, J.-J., Bartsch, S., Fleckenstein, J.H., Matzner, E., Tenhunen, J.D., Lee, S.D.,

Park, S.K., Park, J.-H., 2012. Differential storm responses of dissolved and particulate organic carbon in a mountainous headwater stream, investigated by high-frequency, in situ optical measurements. Journal of *Geophysical Research: Biogeosciences* 117, G03013.

Ji, U., Hwang, M.-H., Lim, G.-S., Kang, S.-U., 2012. Analysis on land-use and the four rivers' watershed characteristics using GIS. *Magazine of Korea Water Resources Association* 45, 26-33 (in Korean).

Jin, H., Yoon, T.K., Begum, M.S., Lee, E.J., Oh, N.H., Kang, N., Park, J.H., 2018. Longitudinal discontinuities in riverine greenhouse gas dynamics generated by dams and urban wastewater. *Biogeosciences* 15, 6349-6369.

Jobbágy, E.G., Jackson, R.B., 2000. The Vertical Distribution of Soil Organic Carbon and Its Relation to Climate and Vegetation. *Ecological Applications* 10, 423-436.

Johnson, M.S., Lehmann, J., Riha, S.J., Krusche, A.V., Richey, J.E., Ometto, J.P.H., Couto, E.G., 2008. CO2 efflux from Amazonian headwater streams represents a significant fate for deep soil respiration. *Geophysical Research Letters* 35.

Jung, B.-J., Lee, H.-J., Jeong, J.-J., Owen, J., Kim, B., Meusburger, K., Alewell, C., Gebauer, G., Shope, C., Park, J.-H., 2012. Storm pulses and varying sources of hydrologic carbon export from a mountainous watershed. *Journal of hydrology* 440, 90-101.

Jung, B.-J., Lee, J.-K., Kim, H., Park, J.-H., 2014. Export, biodegradation, and disinfection byproduct formation of dissolved and particulate organic carbon in a forested headwater stream during extreme rainfall events. *Biogeosciences* 11, 6119-6129.

Kao, S.J., Liu, K.K., 1996. Particulate organic carbon export from a subtropical mountainous river (Lanyang Hsi) in Taiwan. *Limnology and Oceanography* 41, 1749-1757.

Kao, S.J., Liu, K.K., 1997. Fluxes of dissolved and nonfossil particulate organic carbon from an Oceania small river (Lanyang Hsi) in Taiwan. *Biogeochemistry* 39, 255-269.

Keller, V.D.J., Williams, R.J., Lofthouse, C., Johnson, A.C., 2014. Worldwide estimation of river concentrations of any chemical originating from sewage-treatment plants using dilution factors. *Environmental Toxicology and Chemistry* 33, 447-452.

Kim, B., Park, J.-H., Hwang, G., Jun, M.-S., Choi, K., 2001. Eutrophication of reservoirs in South Korea. *Limnology* 2, 223-229.

Kim, J.-K., Jung, S., Eom, J.-s., Jang, C., Lee, Y., Owen, J.S., Jung, M.-S., Kim, B., 2013. Dissolved and particulate organic carbon concentrations in stream water and relationships with land use in multiple-use watersheds of the Han River (Korea). *Water International* 38, 326-339.

Kim, M.-S., Hwang, J.-Y., Kim, B.-K., Cho, H.-S., Youn, S.J., Hong, S.-y., Lee, W.-S., Kwon, O.-S., Kim, J.-M., 2014. Determination of the origin of particulate organic matter at the Lake Paldang using stable isotope ratios $\delta^{13}C$, $\delta^{15}N$. *Korean Journal of Ecology and Environment* 47, 127-134 (in Korean with English abstract).

KMA, 2012. Korean Peninsula Climate Change Outlook Report. 1-152 (in Korean).

Kohn, M.J., 2010. Carbon isotope compositions of terrestrial C3 plants as indicators of (paleo) ecology and (paleo) climate. *Proceedings of the National Academy of Sciences* 107, 19691-19695.

Komada, T., Anderson, M.R., Dorfmeier, C.L., 2008. Carbonate removal from coastal sediments for the determination of organic carbon and its isotopic signatures, $\delta^{13}C$ and $\Delta^{14}C$: comparison of fumigation and direct acidification by hydrochloric acid. *Limnology and Oceanography: Methods* 6, 254-262.

Kwon, K.Y., Moon, C.H., Kang, C.K., Kim, Y.N., 2002. Distribution of particulate organic matters along the salinity gradients in the Seomjin River estuary. *Journal of*

the Korean Fisheries Society 35, 86-96 (in Korean with English abstract).

Lee, K.-S., Ryu, J.-S., Ahn, K.-H., Chang, H.-W., Lee, D., 2007. Factors controlling carbon isotope ratios of dissolved inorganic carbon in two major tributaries of the Han River, Korea. *Hydrological Processes* 21, 500-509.

Lee, S.-H., Kim, Y.-H., Shin, D.-R., 2003. Characteristics of dissolved organic matters in Nakdong River. *Journal Korean Society of Environmental Engineers* 25, 701-708 (in Korean with English abstract).

Lee, Y.-J., Jeong, B.-K., Shin, Y.-S., Kim, S.-H., Shin, K.-H., 2013. Determination of the origin of particulate organic matter at the estuary of Youngsan River using stable isotope ratios ($\delta^{13}C$, $\delta^{15}N$). *Korean Journal of Ecology and Environment* 46, 175-184 (in Korean with English abstract).

Li, G., Wang, X.T., Yang, Z., Mao, C., West, A.J., Ji, J., 2015. Dam-triggered organic carbon sequestration makes the Changjiang (Yangtze) river basin (China) a significant carbon sink. *Journal of Geophysical Research: Biogeosciences* 120, 39-53.

Li, M., Peng, C., Wang, M., Xue, W., Zhang, K., Wang, K., Shi, G., Zhu, Q., 2017. The carbon flux of global rivers: A re-evaluation of amount and spatial patterns. *Ecological Indicators* 80, 40-51.

Li, S., Bush, R.T., 2015. Changing fluxes of carbon and other solutes from the Mekong River. *Scientific Reports* 5, 16005.

Lloret, E., Dessert, C., Pastor, L., Lajeunesse, E., Crispi, O., Gaillardet, J., Benedetti, M.F., 2013. Dynamic of particulate and dissolved organic carbon in small volcanic mountainous tropical watersheds. *Chemical Geology* 351, 229-244.

Lu, Y., Bauer, J., Canuel, E., Chambers, R.M., Yamashita, Y., Jaffé, R., Barrett, A., 2014. Effects of land use on sources and ages of inorganic and organic carbon in

temperate headwater streams. *Biogeochemistry* 119, 275-292.

Ludwig, W., Amiotte-Suchet, P., Munhoven, G., Probst, J.-L., 1998. Atmospheric CO_2 consumption by continental erosion: present-day controls and implications for the last glacial maximum. *Global and Planetary Change* 16-17, 107-120.

Ludwig, W., Probst, J.-L., Kempe, S., 1996. Predicting the oceanic input of organic carbon by continental erosion. *Global Biogeochemical Cycles* 10, 23-41.

Ma, J., Shugart, H.H., Yan, X., Cao, C., Wu, S., Fang, J., 2017. Evaluating carbon fluxes of global forest ecosystems by using an individual tree-based model FORCCHN. *Science of The Total Environment* 586, 939-951.

Maavara, T., Lauerwald, R., Regnier, P., Van Cappellen, P., 2017. Global perturbation of organic carbon cycling by river damming. *Nature Communications* 8, 15347.

Martin, E.E., Ingalls, A.E., Richey, J.E., Keil, R.G., Santos, G.M., Truxal, L.T., Alin, S.R., Druffel, E.R., 2013. Age of riverine carbon suggests rapid export of terrestrial primary production in tropics. *Geophysical Research Letters* 40, 5687-5691.

Marwick, T.R., Tamooh, F., Teodoru, C.R., Borges, A.V., Darchambeau, F., Bouillon, S., 2015. The age of river-transported carbon: A global perspective. *Global Biogeochemical Cycles* 29, 122-137.

Mayorga, E., Aufdenkampe, A.K., Masiello, C.A., Krusche, A.V., Hedges, J.I., Quay, P.D., Richey, J.E., Brown, T.A., 2005. Young organic matter as a source of carbon dioxide outgassing from Amazonian rivers. *Nature* 436, 538-541.

Möller, A., Kaiser, K., Guggenberger, G., 2005. Dissolved organic carbon and nitrogen in precipitation, throughfall, soil solution, and stream water of the tropical highlands in northern Thailand. *Journal of Plant Nutrition and Soil Science* 168, 649-659.

Meybeck, M., 1993. Riverine transport of atmospheric carbon: Sources, global

typology and budget. *Water, Air, and Soil Pollution* 70, 443-463.

Meybeck, M., Dürr, H.H., Vörösmarty, C.J., 2006. Global coastal segmentation and its river catchment contributors: A new look at land-ocean linkage. *Global Biogeochemical Cycles* 20.

Meybeck, M., Vörösmarty, C., 1999. Global transfer of carbon by rivers. *Global Change Newsletter* 37, 18-19

Meybeck, M., 2003. Global occurrence of major elements in rivers. In: Drever JI, Holland HD, Turekian KK (eds). *Treatise on Geochemistry: Biogeochemistry* (Vol 5, pp 207–223). New York, Elsevier.

Min, H., Woo, B., 1995. Throughfall, stemflow and interception loss at Pinus taeda and Pinus densiflora stands. *Journal of Korean Forestry Society* (Korea Republic).

Moon, J.-W., Choi, S.-J., Kang, S.-K., Lee, D.-R., 2010. *Contribution degree analysis of discharge from sewage treatment plants at streamflow in river*. Paper presented at the Korea Water Resources Association Conference, 2010. Korea Water Resources Association, Daejeon, South Korea (in Korean).

Moore, S., Evans, C.D., Page, S.E., Garnett, M.H., Jones, T.G., Freeman, C., Hooijer, A., Wiltshire, A.J., Limin, S.H., Gauci, V., 2013. Deep instability of deforested tropical peatlands revealed by fluvial organic carbon fluxes. *Nature* 493, 660-663.

Nguyen, H.V.-M., Lee, M.-H., Hur, J., Schlautman, M.A., 2013. Variations in spectroscopic characteristics and disinfection byproduct formation potentials of dissolved organic matter for two contrasting storm events. *Journal of hydrology* 481, 132-142

O'Brien, B.J., 1986. The use of natural and anthropogenic ^{14}C to investigate the dynamics of soil organic carbon. *Radiocarbon* 28, 358-362.

Oh, N.-H., 2016. The Loads and Biogeochemical Properties of Riverine Carbon.

Korean Journal of Ecology and Environment 49, 245-257 (in Korean with English abstract).

Oh, N.-H., Raymond, P.A., 2006. Contribution of agricultural liming to riverine bicarbonate export and CO_2 sequestration in the Ohio River basin. *Global Biogeochemical Cycles* 20, GB3012.

Park, H.-G., Jang, B.-S., Kwak, M.S., 2005. Introduction to large dams in Korea. *Journal of the Korean Society of Civil Engineers* 53, 206-218 (in Korean).

Park, H.-K., Byeon, M.-S., Shin, Y.-N., Jung, D.-I., 2009. Sources and spatial and temporal characteristics of organic carbon in two large reservoirs with contrasting hydrologic characteristics. *Water Resources Research* 45, W11418.

Patra, P.K., Canadell, J.G., Houghton, R.A., Piao, S.L., Oh, N.H., Ciais, P., Manjunath, K.R., Chhabra, A., Wang, T., Bhattacharya, T., Bousquet, P., Hartman, J., Ito, A., Mayorga, E., Niwa, Y., Raymond, P.A., Sarma, V.V.S.S., Lasco, R., 2013. The carbon budget of South Asia. *Biogeosciences* 10, 513-527..

Pereira, R., Bovolo, C.I., Spencer, R.G.M., Hernes, P.J., Tipping, E., Vieth-Hillebrand, A., Pedentchouk, N., Chappell, N.A., Parkin, G., Wagner, T., 2014. Mobilization of optically invisible dissolved organic matter in response to rainstorm events in a tropical forest headwater river. *Geophysical Research Letters* 41, 1202-1208.

Qu, B., Sillanpää, M., li, C., Kang, S., Stubbins, A., Yan, F., Sue Aho, K., Zhou, F., A. Raymond, P., 2017. Aged dissolved organic carbon exported from rivers of the Tibetan Plateau. *PLOS ONE* 12, e0178166.

Raymond, P.A., Bauer, J.E., 2001. DOC cycling in a temperate estuary: a mass balance approach using natural 14C and 13C isotopes. *Limnology and Oceanography* 46, 655-667.

Raymond, P.A., Bauer, J.E., 2001. Use of ^{14}C and ^{13}C natural abundances for evaluating riverine, estuarine, and coastal DOC and POC sources and cycling: a

review and synthesis. *Organic Geochemistry* 32, 469-485.

Raymond, P.A., Hartmann, J., Lauerwald, R., Sobek, S., McDonald, C., Hoover, M., Butman, D., Striegl, R., Mayorga, E., Humborg, C., Kortelainen, P., Dürr, H., Meybeck, M., Ciais, P., Guth, P., 2013. Global carbon dioxide emissions from inland waters. *Nature* 503, 355-359.

Raymond, P.A., McClelland, J., Holmes, R., Zhulidov, A., Mull, K., Peterson, B., Striegl, R., Aiken, G., Gurtovaya, T., 2007. Flux and age of dissolved organic carbon exported to the Arctic Ocean: A carbon isotopic study of the five largest arctic rivers. *Global Biogeochemical Cycles* 21.

Raymond, P.A., Oh, N.H., 2007. An empirical study of climatic controls on riverine C export from three major U.S. watersheds. *Global Biogeochemical Cycles* 21, GB2022.

Raymond, P.A., Saiers, J.E., 2010. Event controlled DOC export from forested watersheds. *Biogeochemistry* 100, 197-209.

Ren, W., Tian, H., Cai, W.-J., Lohrenz, S.E., Hopkinson, C.S., Huang, W.-J., Yang, J., Tao, B., Pan, S., He, R., 2016. Century-long increasing trend and variability of dissolved organic carbon export from the Mississippi River basin driven by natural and anthropogenic forcing. *Global Biogeochemical Cycles* 30, 1288-1299.

Runkel, R.L., Crawford, C.G., Cohn, T.A., 2004. Load estimator (LOADEST): A FORTRAN program for estimating constituent loads in streams and rivers. U.S. *GeologicalSurvey Techniques and Methods Book 4*, Chapter A5. 69 pp., U.S. Geological Survey, Denver, Colorado.

Sanderman, J., Baldock, J.A., Amundson, R., 2008. Dissolved organic carbon chemistry and dynamics in contrasting forest and grassland soils. *Biogeochemistry* 89, 181-198.

Sanderman, J., Lohse, K.A., Baldock, J.A., Amundson, R., 2009. Linking soils and

streams: Sources and chemistry of dissolved organic matter in a small coastal watershed. *Water Resources Research* 45, W03418.

Schiff, S., Aravena, R., Trumbore, S.E., Dillon, P., 1990. Dissolved organic carbon cycling in forested watersheds: a carbon isotope approach. *Water Resources Research* 26, 2949-2957.

Schiff, S., Aravena, R., Trumbore, S.E., Hinton, M., Elgood, R., Dillon, P., 1997. Export of DOC from forested catchments on the Precambrian Shield of Central Ontario: clues from 13C and 14C. *Biogeochemistry* 36, 43-65.

Schlünz, B., Schneider, R., 2000. Transport of terrestrial organic carbon to the oceans by rivers: re-estimating flux-and burial rates. *International Journal of Earth Sciences* 88, 599-606.

Schlesinger, W.H., Bernhardt, E.S., 2013. Chapter 11 - The Global Carbon Cycle. *Biogeochemistry (Third Edition)*. Academic Press, Boston, pp. 419-444.

Schlesinger, W.H., Melack, J.M., 1981. Transport of organic carbon in the world's rivers. *Tellus* 33, 172-187.

Seitzinger, S.P., Harrison, J.A., Dumont, E., Beusen, A.H.W., Bouwman, A.F., 2005. Sources and delivery of carbon, nitrogen, and phosphorus to the coastal zone: An overview of Global Nutrient Export from Watersheds (NEWS) models and their application. *Global Biogeochemical Cycles* 19.

Shi, G.H., Peng, C.H., Wang, M., Shi, S.W., Yang, Y.Z., Chu, J.Y., Zhang, J.J., Lin, G.H., Shen, Y., Zhu, Q.A., 2016. The Spatial and Temporal Distribution of Dissolved Organic Carbon Exported from Three Chinese Rivers to the China Sea. *Plos One* 11.

Shibata, H., Mitsuhashi, H., Miyake, Y., Nakano, S., 2001. Dissolved and particulate carbon dynamics in a cool-temperate forested basin in northern Japan. *Hydrological Processes* 15, 1817-1828.

Shin, W.-J., Lee, K.-S., Park, Y., Lee, D., Yu, E.-J., 2015. Tracing anthropogenic DIC in urban streams based on isotopic and geochemical tracers. *Environmental Earth Sciences* 74, 2707-2717.

Shin, W.-J., Ryu, J.-S., Park, Y., Lee, K.-S., 2011a. Chemical weathering and associated CO_2 consumption in six major river basins, South Korea. *Geomorphology* 129, 334-341.

Shin, W.J., Chung, G.S., Lee, D., Lee, K.S., 2011b. Dissolved inorganic carbon export from carbonate and silicate catchments estimated from carbonate chemistry and $\delta^{13}C_{DIC}$. *Hydrology and Earth System Sciences* 15, 2551-2560.

Shin, Y., Lee, E.-J., Jeon, Y.-J., Hur, J., Oh, N.-H., 2016. Hydrological changes of DOM composition and biodegradability of rivers in temperate monsoon climates. Journal of *Hydrology* 540, 538-548.

Sickman, J.O., DiGiorgio, C.L., Davisson, M.L., Lucero, D.M., Bergamaschi, B., 2010. Identifying sources of dissolved organic carbon in agriculturally dominated rivers using radiocarbon age dating: Sacramento–San Joaquin River Basin, California. *Biogeochemistry* 99, 79-96.

Spencer, R.G.M., Bolton, L., Baker, A., 2007. Freeze/thaw and pH effects on freshwater dissolved organic matter fluorescence and absorbance properties from a number of UK locations. *Water Research* 41, 2941-2950.

Stedmon, C.A., Bro, R., 2008. Characterizing dissolved organic matter fluorescence with parallel factor analysis: a tutorial. *Limnology and Oceanography: Methods* 6, 572-579.

Stedmon, C.A., Markager, S., 2005. Resolving the variability in dissolved organic matter fluorescence in a temperate estuary and its catchment using PARAFAC analysis. *Limnology and Oceanography* 50, 686-697.

Stets, E.G., Kelly, V.J., Crawford, C.G., 2014. Long-term trends in alkalinity in large

rivers of the conterminous US in relation to acidification, agriculture, and hydrologic modification. *Science of The Total Environment* 488–489, 280-289.

Sun, H., Han, J., Zhang, S., Lu, X., 2007. The impacts of '05.6'extreme flood event on riverine carbon fluxes in Xijiang River. *Chinese Science Bulletin* 52, 805-812.

Sun, H.G., Han, J., Lu, X.X., Zhang, S.R., Li, D., 2010. An assessment of the riverine carbon flux of the Xijiang River during the past 50 years. *Quaternary International* 226, 38-43.

Tranvik, L.J., Downing, J.A., Cotner, J.B., Loiselle, S.A., Striegl, R.G., Ballatore, T.J., Dillon, P., Finlay, K., Fortino, K., Knoll, L.B., Kortelainen, P.L., Kutser, T., Larsen, S., Laurion, I., Leech, D.M., McCallister, S.L., McKnight, D.M., Melack, J.M., Overholt, E., Porter, J.A., Prairie, Y., Renwick, W.H., Roland, F., Sherman, B.S., Schindler, D.W., Sobek, S., Tremblay, A., Vanni, M.J., Verschoor, A.M., von Wachenfeldt, E., Weyhenmeyer, G.A., 2009. Lakes and reservoirs as regulators of carbon cycling and climate. *Limnology and Oceanography* 54, 2298-2314.

Trumbore, S.E., Schiff, S., Aravena, R., Elgood, R., 1992. Sources and transformation of dissolved organic carbon in the Harp Lake forested catchment: the role of soils. *Radiocarbon* 34, 626-635.

Ushie, H., Kawahata, H., Suzuki, A., Murayama, S., Inoue, M., 2010. Enhanced riverine carbon flux from carbonate catchment to the ocean: A comparative hydrogeochemical study on Ishigaki and Iriomote islands, southwestern Japan. *Journal of Geophysical Research: Biogeosciences* 115.

Wang, X., Luo, C., Ge, T., Xu, C., Xue, Y., 2016. Controls on the sources and cycling of dissolved inorganic carbon in the Changjiang and Huanghe River estuaries, China: ^{14}C and ^{13}C studies. *Limnology and Oceanography* 61, 1358-1374.

Wang, X., Ma, H., Li, R., Song, Z., Wu, J., 2012. Seasonal fluxes and source variation of organic carbon transported by two major Chinese Rivers: The Yellow River and

Changjiang (Yangtze) River. *Global Biogeochemical Cycles* 26, GB2025.

Wei, X., Shen, C., Li, N., Wang, F., Ding, P., Wang, N., Guo, Z., Liu, K., 2010. Apparent ages of suspended sediment and soil erosion of the Pearl River (Zhujiang) drainage basin. *Chinese Science Bulletin* 55, 1547-1553.

Westerhoff, P., Chen, W., Esparza, M., 2001. Fluorescence analysis of a standard fulvic acid and tertiary treated wastewater. *Journal of Environmental Quality* 30, 2037-2046.Xia, B., Zhang, L., 2011. Carbon distribution and fluxes of 16 rivers discharging into the Bohai Sea in summer. *Acta Oceanologica Sinica* 30, 43-54.

Yang, L., Chang, S.W., Shin, H.S., Hur, J., 2015a. Tracking the evolution of stream DOM source during storm events using end member mixing analysis based on DOM quality. *Journal of Hydrology* 523, 333-341.

Yang, L., Hur, J., Lee, S., Chang, S.W., Shin, H.S., 2015b. Dynamics of dissolved organic matter during four storm events in two forest streams: source, export, and implications for harmful disinfection byproduct formation. *Environmental Science and Pollution Research* 22, 9173-9183.

Yoon, B., Raymond, P.A., 2012. Dissolved organic matter export from a forested watershed during Hurricane Irene. *Geophysical Research Letters* 39, L18402.

Zamanian, K., Pustovoytov, K., Kuzyakov, Y., 2016. Pedogenic carbonates: Forms and formation processes. *Earth-Science Reviews* 157, 1-17.

Zarfl, C., Lumsdon, A.E., Berlekamp, J., Tydecks, L., Tockner, K., 2015. A global boom in hydropower dam construction. *Aquatic Sciences* 77, 161-170.

Zhang, S., Gan, W.-B., Ittekkot, V., 1992. Organic matter in large turbid rivers: the Huanghe and its estuary. *Marine Chemistry* 38, 53-68.

Zeng, F.-W., Masiello, C., Hockaday, W., 2011. Controls on the origin and cycling of riverine dissolved inorganic carbon in the Brazos River, Texas. *Biogeochemistry* 104,

275-291.

Zeng, F.-W., Masiello, C.A., 2010. Sources of CO_2 evasion from two subtropical rivers in North America. *Biogeochemistry* 100, 211-225.

요약 (국문초록)

하천탄소의 유출량과 생지화학적 특성:

산림시냇물, 우리나라 5대강, 아시아 하천을 대상으로

서울대학교 환경대학원

환경계획학과 환경관리전공

이은주

하천은 전 지구적 탄소순환에서 탄소의 주요 저장고인 육지와 바다를 연결하는 매개체로서, 비록 그 절대량은 연간 약 1.0 Pg-C로 광합성이나 호흡 같은 탄소 이동량에 비해 매우 작지만, 이는 생태계 총 생산량(NEP: Net Ecosystem Production)과 비교할만한 양이다. 따라서 하천탄소 유출량이 계산되어야 육생생태계가 탄소 흡수원인지 배출원인지를 판정할 수 있다. 하천을 통해 유출된 탄소를 정량하고, 하천탄소의 유출량과 생지화학적 특성에 영향을 미치는 요인을 분석하는 연구가 다양한 규모의 유역에서 활발히 이루어지고 있다.

소유역 하천 연구는 하나의 영향요인에 따른 하천탄소의 유출량이나 특성의 변화를 독립적으로 연구하기에 적합하다. 반면에 중규모, 대규모 유역 연구는 유역 내 여러 요인이 탄소 유출량과 성질에 미치는 영향을 종합적으로 분석하기 쉽다. 아시아 하천탄소의 유출량과 생지화학적 특성을 이해하기 위해, 우리나라 산림 소유역 하천, 우리나라 주요 5대강(한강, 금강, 영산강, 섬진강, 낙동강), 아시아 전지역의 강을 대상으로 유출되는 탄소의 양과 특성에 대한 다중 규모 유역 연구를 수행하였다.

전라남도 광양시 백운산 남부학술림 산림 소유역 하천에서 2012년 1월부터 2015년 4월까지 매 주 하천수 시료를 채취하여 하천탄소의 농도를 측정하고 계절별 동위원소 분석(^{13}C, ^{14}C)을 실행하였다. 총 8번의 강우사상에 대해서는 매 2-24시간마다 하천수 시료를 채취하였다. 산림 소유역의 단위면적당 연평균 총 탄소 (용존무기탄소(DIC), 용존유기탄소(DOC), 입자성유기탄소(POC)의 합) 유출량은 약 1.7 g-C m^{-2} yr^{-1} 이었으며 이중 약 83%가 DIC 형태로 유출되었다. 여름(6월–8월)에는 연평균 하천탄소 유출량의 50% 이상이 유출되었다. $\Delta^{14}C_{DOC}$는 -81.5‰에서 45.5‰, $\delta^{13}C_{DOC}$는 -29.4‰에서 -13.4‰의 범위를 가졌는데, 이 결과를 바탕으로 여름철 강우 사상시에는 표층유기물질이, 그 외 계절에는 깊은 지하수가 하천 DOC에 주로 영향을 미치는 것으로 추정된다.

우리나라 주요 5대강 유역에서는 2012년부터 2013년 동안 연간 약 580 Gg-C의 탄소가 유출되었는데, 단위면적당 연평균 유출량은 약 10 g-C m^{-2} yr^{-1}로, 전 지구적 평균의 약 2배였다. DIC가 총 탄소 유출량의 80%을 차지하며 우리나라 강 탄소의 주요 구성성분이었고, 여름에 연간 유출량의 약 34–46%가 빠져나가는 것으로 추정되었다. 우리나라 강 탄소의 $\Delta^{14}C_{DIC}$는 -88.7‰에서 26.9‰, $\Delta^{14}C_{DOC}$는 -124.3‰에서 0.8‰, $\Delta^{14}C_{POC}$는 125.5‰에서 35.1‰의 범위를 가졌으며, 여름철에 모든 탄소 성상(DIC, DOC, POC)에서 높은 값을 나타내었다. 비록 여름을 제외한 계절에는 상대적으로 오래된 탄소가 주로 강을 통해 유출되었지만, 여름철에는 상대적으로 최근에 생성된 탄소가 하천을 통해 빠져나갔다.

전 지구적 강 탄소 유출량의 25%인 약 241 Tg-C의 탄소가 아시아 강을 통해 바다로 유출될 것으로 추정되었다. DIC가 아시아 총 하천탄소 유출량의 57%를 차지하는 주요 구성 성분이었으며, DOC는 26%, POC는 15%, PIC는 2%를 차지했다. 아시아 강의 총 탄소 유출량은 기존 연구들과 비슷하였으나, 탄소 성상별 비율에는 차이가 있었는데, DIC의 비율은 다른 선행연구들보다 19%까지 높게, POC의 비율은 11–19% 낮게 추정

되었다. 이는 기존 연구들과는 달리 많은 아시아 강의 측정치만을 대상으로 만든 강 탄소 유출량과 유량의 새로운 추정식을 사용하여 총 유출량을 계산하였기 때문이다. 단위면적당 유량과 유역의 경사도와 같은 자연적 요인이 농업, 도시 지역의 비율이나 인구밀도와 같은 인위적 요인보다 탄소 유출량과 유의미한 상관관계를 보였다. 이러한 결과는 강 탄소의 기원이 계절에 따라, 특히 여름철에 변화할 수 있음을 시사한다. 아시아 지역의 하천 탄소의 양과 생지화학적 특성은 여름철 강우사상에 의해 강한 영향을 받으며, 이에 따라 더 많은 양의 최근에 생성된 탄소가 육상생태계에서 하구, 해양생태계로 유출되어 영향을 미칠 수 있다.

주요어: 탄소, 동위원소, 유출량, 용존유기탄소, 용존무기탄소, 입자성유기탄소, 입자성무기탄소, 하천, 유역, 아시아

학번: 2013-30709